2004

Predicting spatial distributions of sediments in fluvial environments using kriging and flowline based distances.

Jason S. Wintermute
University of Windsor

Follow this and additional works at: https://scholar.uwindsor.ca/etd

PREDICTING SPATIAL DISTRIBUTIONS OF SEDIMENTS IN FLUVIAL ENVIRONMENTS USING KRIGING AND FLOWLINE BASED DISTANCES

by

Jason S. Wintermute

A Thesis
Submitted to the Faculty of Graduate Studies and Research
through the Department of Civil and Environmental Engineering
in Partial Fulfillment of the Requirements for
the Degree of Masters of Applied Science at the
University of Windsor

Windsor, Ontario, Canada

2004

© 2004, Jason S. Wintermute

Abstract

The process of predicting reasonable spatial distributions of surficial sediments in fluvial environments using interpolation techniques can be quite challenging. The process of sediment transport creates anisotropy in the spatial distributions that follow the direction of flow. Standard geostatistical software only allow for the incorporation of one anisotropy direction for the entire problem domain. This is problematic for fluvial environments because an average direction usually misrepresents the local changes in anisotropy throughout the river.

A distance transformation technique based on flowlines was applied in an attempt to improve the way geostatistical algorithms deal with anisotropy. The standard geostatistical method of ordinary kriging was modified so that distances measured along, and perpendicular to, flowlines are substituted for the Cartesian coordinate system distances typically used. Five simple test cases were generated using the CH3D hydrodynamic model with sediment transport to examine how the method performs in idealized environments. Two test cases were used to determine whether the modified kriging algorithm was performing as expected. The other three test cases; a 90-degree bend, a channel with an island and a diverging channel were used to examine the effectiveness of the flowline method compared to standard kriging. Sediment sampling conducted on the Detroit River was also examined as a test case to see how the flowline method performs in real environments.

The ability of the flowline method to properly track sediment patterns around bends in the channels allows for predictions of spatial distributions that visually appear more reasonable. The curved channel test case showed consistently better statistical performance using the flowline method. For the diverging channel and island test cases, the flowline method performed equally well or better than standard kriging, however the diverging channel and to a lesser extent the island test case exhibit decreasing effectiveness with larger sample set sizes, apparently due to numerical sensitivity in the

current implementation to the size of the problem. Overall, the results indicate that the flowline method performs well for a variety of flow-dominated environments.

Acknowledgements

I would like to express my appreciation to all those people who have aided me during the course of my research. In particular, I would like to extend special thank to my co-advisors Dr. Stan Reitsma and Dr. Phil Graniero for all the support they provided during this endeavour. Also, thanks go out to Dr. Brian Fryer and Dr. Kerry Mazurek for acting as members of my thesis committee and to Dr. Seth for acting as a chair for my defense. In addition, thanks go out to Dr. Doug Haffner and all the researchers at the Great Lakes Institute for Environmental Research involved in collecting and compiling the data on the Detroit River. Similarly, mention should be made regarding Dr. Edzer Pebesma who originally wrote the GSTAT geostatistical program that I modified as part of my thesis. I would also like to express my sincerest thanks to my wife Renée for all her support and understanding over the years. Finally, thanks should go out to all my family, friends and colleagues for the part they played in making all this work come together.

Table of Contents

List of Tables

List of Figures

x

xii

1.0 Introduction

The surficial sediments in an aquatic ecosystem play an important role in determining the overall health of the ecosystem. These sediments provide habitat for a wide variety of benthic organisms and act as an interface between the water column and the underlying geology. Sediments in contact with the water column may act as either sources or sinks for environmental contaminants depending on their physical and chemical properties and the relative concentrations of contaminants in the sediments to that of the surrounding environment. As a result, environmental assessment studies of aquatic ecosystems often include a sediment sampling survey.

Regardless of the analyses performed on the sediment samples, the objective of a sampling program is usually to use the sediment properties observed at individual sample locations to generate some kind of conclusion about the properties over larger spatial extents. This may involve producing a map of the spatial distribution of the sediment properties as they vary continuously over the entire study area. Various methods are available to produce such spatial distribution maps, each with their own strengths and weaknesses. The hydrodynamics of fluvial environments distinguish them from other aquatic environments and present additional difficulties when trying to produce spatial distribution maps.

Environmental assessment studies are often conducted in phases. The first phase is often to collect sample points with a very sparse spatial distribution to determine if there are any areas of concern. If such areas are found, the next step is to delineate the extent of the problem. In order to delineate the areas, additional samples are taken in locations expected to be near the boundary of the areas of concern. Usually very few samples have been taken at this point so there is often no way to statistically determine an extent for the areas of interest. Instead, it is left up the professional judgment of the researcher involved to determine where those samples should be taken. The construction of a spatial distribution map is one way to help aid in determining where the next round of sampling should be conducted. If a statistical assessment is not feasible, this spatial distribution

1

map needs to produce spatial patterns that intuitively match the expected behaviour of the problem domain to be of any use as a guide. Once the problem areas have been delineated it may be required to quantify the extent of the problem. For example, a volume of sediments or a mass of contamination may need to be determined in order to take remedial action. The construction of a spatial distribution map is often required for this task. In this case, the spatial distributions should be statistically defendable if a reasonable estimate of quantity is to be made. As a result, if a method of spatial interpolation is to be useful for these kinds of studies a method that provides both intuitively match the expected behaviour of the problem domain and provide statistically quantifiable results.

1.1 Determining Spatial Distributions in Fluvial Environments

The peer-reviewed literature contains surprisingly few attempts at producing continuous maps of sediment properties for fluvial environments. In order to obtain a better critical examination of techniques applicable to fluvial environments, those techniques used in non-fluvial aquatic environments also need to be examined, as well as those techniques used in the related fields of hydrology and hydrogeology. Although there are a variety of techniques that could be used to create maps of sediment properties, the literature seems to be dominated by interpolation techniques and by kriging in particular. For a further discussion of interpolation techniques and geostatistics (i.e. kriging) as related to this thesis refer to Section 2.

Many researchers choose not to produce maps of sediment properties that vary continuously over a study area. Instead, they simply discuss any observed trends and areas of concern. The discussion often contains a non-spatial statistical evaluation of the collected data. If a map is used to convey information, it may only have the sample point locations on the map and rely on the reader to make assumptions about the size of the area that the sample represents and its relation to nearby unsampled areas. This approach is fairly common in studies where the objective of the research is something other than

2

quantifying overall sediment properties or where few samples are examined. For some examples of such studies, refer to Marvin et al. (2003), Roth et al. (2001) and Metcalfe et al. (2000).

When producing spatial distribution maps of aquatic sediment properties, Baudo (1990) recommends that if the maps are to be used for any real-world application, then at least two different techniques should be attempted, one moving average technique and one trend surface technique. Kriging is recommended for the moving average technique and if the slope of the bed is significant, a method that accounts for depth is suggested.

Geostatistical techniques have been applied to a wide variety of hydrologic variables. For an overview of such applications, refer to Delhomme (1978), Kitanidis (1993) and Haan (2002). The most relevant techniques are those that have been applied to sediment mapping. Methods for the mapping of sediments on a watershed basis have been examined by several researchers. For example, Zhang and Selinus (1997) examined the concentrations of copper, lead and zinc in the sediments of the Yangtze River basin using ordinary block kriging. Variogram analysis conducted as part of the kriging revealed anisotropy at ranges longer than 500 km. However, since the variogram revealed isotropic behaviour at ranges less than 500 km, the authors chose to ignore the long-scale anisotropy and only model the isotropic behaviour. Anisotropy is a fairly common occurrence in hydrologic data and is further discussed in Sections 2.3.7 and 2.4. Lu et al. (2003) examined sediment yield in the Upper Yangtze basin by measuring sediment load in the river and its tributaries and applying universal kriging techniques across the watershed. The paper provides a good reference for other techniques of sediment yield mapping and attempts to deal with the problem of using hydrologic station point data that represents processes not centred on the data point. The distinguishing factor between sediment mapping across watersheds and sediment mapping in fluvial environments is that the sediments at the bottom of a river are subject to the hydrodynamics of channelized fluid flow. As a result, the distributions of sediments are dominantly influenced by the process of sediment transport.

3

Hydrogeology has also benefited from the use of geostatistical techniques. For an overview of such applications, refer to Delhomme (1978), ASCE (1990), Kitanidis (1997), and their excellent lists of references. Mapping sediments for hydrogeological studies is very similar to mapping surface soil types except that the process is a three-dimensional analysis. As in a fluvial environment, the sediments in hydrogeological studies are subject to fluid flow. However, generally speaking, the sediments in hydrogeological studies are not mobile. The examination of some mobile property, such as a chemical contaminant, is more analogous to the type of analysis needed for mapping sediment distributions in fluvial environments. A few examples of the geostatistical examination of chemical contaminants in groundwater can be found in D'Agostino et al. (1998), Critto et al. (2003) and Gaus et al. (2003). As pointed out in ASCE (1990), Rubin (1991) and D'Agostino et al. (1998), it is very difficult to model the spatial variances in plumes because the concentrations are time dependent. There are also the problems of non-stationarity and the typically sparse data sets to deal with. D'Agostino et al. (1998) attempts to improve upon geostatistical estimations by using cokriging on several data sets collected at different times. Rubin (1991) attempts to deal with these same problems by using the physical principles underlying transport phenomena to generate the model of spatial variability. The use of the underlying theory allows for the modelling of variability in both time and space. Using sample data, the model of spatial and temporal variability can then be conditioned. Once the model is conditioned, predictions can be made just as in ordinary kriging. The application of geostatistical techniques using such methods is known as conditional simulation. The theoretical model of variability points out the model characteristics that should be seen in flow generated plumes. It was shown that the model of spatial variability is non-stationary, non-symmetrical, anisotropic and that the correlation is stronger along the mean-flow direction. It also points out that the model should be bounded. These characteristics should also be observed in the spatial variability models of fluvial environments. However, in real fluvial environments these model characteristics may be moderated or masked by the other processes involved, such as the effects of channelization, erosion and exposure of historical deposition, unsteady flow conditions and biological activity.

4

Geostatistical techniques have been applied to sediment properties in a wide range of aquatic environments. Büttner et al. (1998) used inverse distance weighting (IDW) interpolation, ordinary kriging and principal component analysis (PCA) to examine the geochemistry of surficial sediments in Mining Lake 111, Brandenburg, Germany. This study also addresses the issue of the number of sampling points required to produce an acceptable interpolation. In total 66 samples were taken from 47 locations throughout the lake. However, the authors deemed that this was an insufficient number of points to reduce the variance observed in the analysis to an acceptable level. Geostatistical techniques have also been applied to larger bodies of water and unbounded study areas. Danielsson et al. (1998) used cokriging to examine the distribution of nutrients in the surficial sediments of the Gulf of Riga. The distributions of organic carbon, nitrogen and phosphorus were examined using loss on ignition as a covariable. Poon et al. (1999) used ordinary block kriging to examine the spatial distribution of sewage pollution in a coastal area east of Hong Kong. The slow movement of water and the lack of channelized flow in these aquatic environments create a much different situation than one would expect to observe in a river. As might be expected, no obvious trend or anisotropy was found in the above studies.

There are not nearly as many studies on mapping sediment properties within fluvial environments as there are for the other environments discussed above. However, the studies that do exist use very similar techniques to those already mentioned. The St. Johns River Water Management District, Palatka, Florida (Ouyang et al., 2002), in their studies of the Cedar and Ortega Rivers, used ordinary kriging in three-dimensions on lead, zinc, copper and cadmium concentrations to produce maps of metal concentrations at various depths in their river channels. Another study on the same rivers (Ouyang et al., 2003) examined dichloro-diphenyl-trichloroethane (DDT) and its metabolites using similar techniques. Butcher (1996) used cokriging to estimate polychlorinated biphenyl (PCB) loadings in the Hudson River of the State of New York. In this study, contaminated sediment was screened into qualitative concentration ranges and a subset of each was sent for more accurate laboratory analysis. The more abundant screening data was used as the covariable for the less abundant but more accurate laboratory analyzed

5

data. Given that these studies were conducted in fluvial environments, it could be expected that there would be some trend or anisotropy in the downstream direction. However, no such trend or anisotropy was found in the above studies.

Studies performed in complex coastal and estuarine environments have lead to the recognition that Euclidean distances may not always be appropriate for aquatic studies. The abundance of islands, braided channels and peninsulas lead to situations where a straight line measurement between two sample points would have to cross over land. If the process being modelled only occurs through water, it would make sense that the distances between samples should also be measured only through the water. This recognition has lead to the introduction of alternate distance metrics into kriging analysis. Little et al. (1997) attempted ordinary and universal kriging using only in-water distances to predict several water and sediment quality indicators for Murrells Inlet, South Carolina. The improvement in the results depended on the indicator being examined. In four of the eight indicators being examined a 10-30% improvement in prediction error variance was observed. However, one indicator, the presence of fluoranthene in oyster tissue, showed a 10% larger prediction error variance. Rathbun (1998) attempted the use of in-water distances with universal kriging on dissolved oxygen and salinity for Charleston Harbour, South Carolina. In this study, dissolved oxygen saw only a slight improvement from the use of the alternate distance metric, while salinity saw slightly worse results. The results were not significant enough to recommend one method over the other. The Rathbun study also examined the use of concentration boundary conditions in kriging.

Less complicated fluvial environments can also benefit from the use of alternate distance metrics. Large rivers often contain islands, and even small meandering channels can suffer from the situation where straight line measurements between sample points cross over land. Researchers dealing in river environments have, in effect, created alternate distance metrics through the use of domain transformation techniques. The domain transformation techniques arose from the need to have continuous, regular grids that can be used for hydrodynamic modelling. It is easy to visualize why the lines connecting

6

adjacent nodes in a hydrodynamic modelling mesh must not cross over land. If the nodes in a modelling mesh are thought of as sample points or prediction points for the model, then by analogy, the straight line measurements between samples in a kriging analysis should not cross over land either. Merwade et al. (2003) reviewed and built upon a coordinate transformation technique that converts a Cartesian coordinate system into a curvilinear orthogonal coordinate system similar to those used in road engineering. Any point along a river can be thought of as having a location described by the distance along the centreline of the channel and by a perpendicular offset. One of the most important decisions to make when conducting such transformations is how to define the centreline of the river. Although other concepts of a river centreline are possible, they chose the thalweg as a centreline for their study. The method works quite well for single channels, but runs into conceptual problems when a channels splits, for example, to go around an island. Although the focus of their research was to investigate better methods of generating modelling grids, the potential of using such alternate coordinate systems for interpolation merits further investigation.

At least one researcher has attempted to use a transformed space for geostatistical mapping of fluvial sediments. Barabás et al. (2001) used indicator kriging to quantify the uncertainty in the interpolated estimates of 2, 3, 7, 8-tetrachlorodibenzo-p-dioxin concentrations in the Passaic River, New Jersey. In order to prevent measurement from crossing over land they applied a domain transformation with a different structure than Merwade et al. (2003). The physical boundary of the study area was transformed into a rectangle. The channel banks were treated as opposite sides of the rectangle as were the upstream and downstream boundaries. An equal number of evenly spaced points were placed along each bank. The same was performed for the upstream and downstream boundaries. The problem domain was then 'rubber-sheeted' using linear interpolation into a rectangular domain. After the kriging was performed, the results were then back-transformed into the original problem domain. Using this transformation technique, all possible distance measurements between points within the river stay within the transformed domain. This straightening of the problem domain also aids in the detection of anisotropy in the river. Although the improved ability to detect anisotropy was not

7

discussed in the paper, it is worth mentioning here and is also discussed further in Section 2.4.

Anisotropy in river channels occurs in the 'downstream' direction. However, when a river meanders across the landscape, the geographic bearing of 'downstream' varies. In highly meandering rivers, the bearing of anisotropy can be exact opposites in different parts of the river. If a geographic coordinate system is used, the anisotropy can average out and be missed leading to poor models. The same argument can be made for the detection of trends in the data. Unlike the studies of fluvial environments previously mentioned (Butcher, 1996; Ouyang et al., 2002; and Ouyang et al., 2003) anisotropy was detected in the Barabás et al. (2001) study. It is possible that anisotropy did exist in those previous studies but was missed because of this problem.

1.2   Thesis Objectives and Structure

The objective of this thesis is to build upon the concepts of alternate distance metrics and domain transformations to develop a method of interpolation that improves upon standard techniques and can be applied to surficial sediment properties in a fluvial environment to produce maps of sediment properties that vary continuously over a study area.

Section 2 describes the basic theory underling interpolation methods that are used in the construction of spatial distributions that vary continuously over the study area. Since kriging seems to be the dominant method in the literature, it is also the method used extensively in this study. A brief overview of the kriging technique is presented in Section 2.3. Having established the underlying assumptions and theory behind kriging, Section 2.4 discusses the shortcomings of using standard kriging techniques in fluvial environments.

Section 3 proposes a new distance transformation and flowline based kriging method that is examined throughout the rest of the thesis. The new distance transformation method

8

uses flowlines derived from a hydrodynamic model to substitute the typical Δx and Δy distances measured in Cartesian space for Δx distances measured along the flow direction and Δy distances measured perpendicular to the flow direction. These distances are then used in a kriging algorithm to interpolate spatial distributions. Having outlined the method, the technique is applied to five simple test cases. The test cases are created using sediment transport simulations on simple idealized channel geometries. The intention of using a simulation as a test case is to show how the method performs in environments dominated by the process of sediment transport without having to be concerned with the influence of other geomorphological processes that may exist in real environments. At the same time, these simulations allow for knowledge of an 'actual' value for all locations in the problem space.

Since a method that only works well in idealized environments is of little practical value, the new flowline kriging method is applied to a real-world test case in Section 4. Surficial sediment sampling and hydrodynamic modelling conducted on the Detroit River as part of the Detroit River Modelling and Management Framework (GLIER, 2002) was examined to determine the technique's applicability to real rivers. The section also includes some background information on the larger Detroit River project and a description of the river itself.

Finally, Section 5 discusses the flowline based kriging method's limitations and its applicability to various problem domains. It includes a discussion of the interpolation artefacts produced by the flowline kriging method that are different from those typically produced by standard kriging methods. It also includes discussions of the types of environments where flowline kriging may be applicable and recommends topics that merit further investigation.

9

2.0 Constructing Spatial Distributions

In order to represent spatial distributions, maps can be produced that show how a property varies continuously over the study domain. In order to interpolate a map, the study area is discretized into smaller sub-areas upon which predictions can be made. Then an interpolation algorithm is applied to the sampled data that makes one prediction for each sub-area in the domain. In this way an estimate of the property is obtained for every location in the domain.

Choosing an appropriate size and shape for the sub-areas can greatly affect the accuracy of the final result. Typically these sub-areas are small, regularly shaped and sized grid cells. The most appropriate size of the grid cells is one that roughly corresponds to the sampling support; that is, the area (or volume) over which the sample was collected and therefore actually represents. Predicting on areas different from the sampling support can lead to change-of-support problems as discussed in Cressie (1993) and elsewhere. In practice, the grid size is often chosen for other reasons such as effective communication of the results, computational efficiency or personal preference.

2.1 Interpolation methods

In general, algorithms that interpolate a data value at an unsampled location based on the values at other sampled locations can be broken down into two categories (Baudo et al., 1990). The first category is trend surface analysis. This method uses a regression approach to determine an equation that relates the spatial coordinates to the data values. Examples of these include: polynomial interpolation such as splines, triangular irregular networks (TINs) and other forms of regression analysis. The second category is moving average algorithms. These methods more explicitly use the assumption that samples collected close together should have values that are more similar than those that are spaced further apart. They determine weighting functions to account for the decreasing

10

influence of data as distances increase. Examples of these are inverse distance weighting and kriging. Each interpolation method has its own advantages and disadvantages due to its underlying assumptions and implementation, as discussed below.

2.2   Inverse Distance Weighting

Inverse distance weighting is the moving average method of interpolation that is most commonly used across all applications (Lo and Yeung, 2002). The method determines a set of weights that are explicitly based on a pre-determined, often arbitrarily selected, decay function. An estimate, p, of a property, Z, at an unknown location, s_o, can be estimated using the following formula

$$p(Z; s_o) = \frac{\sum_{i=1}^{n} z(s_n) d_n^{-q}}{\sum_{i=1}^{n} d_n^{-q}}$$

(1)

where d_n is the distance between s_o and a known data point s_n and p is the decay parameter. Typically this decay function is squared ($q=2$), or in other words, the weights are inversely proportional to the squared distance between the prediction location and a data point used in that prediction. While inverse distance weighting is easy to use and implement, it suffers from the use of the predetermined decay function. For any particular application, the influence of nearby points may not decay exponentially with distance and may not decay at the same rate at all distances.

2.3   Kriging

Since kriging was the dominant method of interpolation used in this study, a brief overview is presented here. A more comprehensive review of kriging techniques can be found elsewhere (Matherson, 1963; Journel and Huijbregts, 1978; Clark, 1979; Cressie,

11

1993; Kitanidis, 1997; Deutsch and Journel, 1998; Wackernagel, 1998; and Deutsch, 2002).

Kriging is a moving average method of interpolation. Interpolated values are calculated as a weighted average of the sample data where the weights are established by an analysis of the distribution, variation and spatial structure of the sample points. The implementation of a kriging analysis involves several steps. First, the data must be examined to ensure that it meets the underlying assumptions, as described in Section 2.3.1. A model of variability versus distance between sample points is then determined. Using the model and the sample points, a set of interpolation weights to be applied to the sample points can be determined for any unsampled location. The interpolation weights are then used to predict an expected value at the unsampled location. Since a statistical distribution has been assumed for the data, the interpolation weights can be optimized. Usually, the optimization criterion is the minimization of the mean-squared error of prediction. As long as the statistical assumptions are valid, the interpolation weights produce a best unbiased estimator.

In contrast to inverse distance squared weighting, the kriging weights are not solely functions of the number of samples and their distances. Instead, the weights are based on the expected variability between points as reflected in the variogram model.

2.3.1 Assumptions

There are two essential assumptions underlying kriging. The first is that a sample is a realization of a random process. If the process is a Gaussian random process, the interpolation weights will form a best linear unbiased estimator. If the underlying process is not Guassian, transformations such as log-normalization can be applied to the sample data to make it Gaussian. However, the backtransformed prediction values are not unbiased (Cressie, 1993). There are nonlinear forms of kriging that do not require the Gaussian assumption, such as disjunctive kriging. However, the solutions to such

12

problems will be more mathematically intensive and have additional, and more strict, statistical assumptions (Cressie, 1993).

The second assumption is that of stationarity in the random process. Different types of kriging require different degrees of stationarity. Strong stationarity exists when all realizations of the random process, $Z(x)$, are independent of their locations, x, in the model space. This means that all statistical parameters of the distribution are consistent throughout the model space. Strong stationarity is required for disjunctive kriging and other nonlinear forms of kriging (Cressie, 1993).

A less rigid form of stationarity is known as second-order stationarity. It requires that two conditions be met. First, there must be a constant mean value throughout the model space. Second, there must exist a covariance model that depends only on the distance between points and not on their locations, and that is consistent throughout the model space. Second-order stationarity is required when covariograms and a covariance function are to be used in kriging (Wackernagel, 1998).

Intrinsic stationarity is a weaker form of stationarity than second-order stationarity. Rather than assuming that the data is stationary, it assumes that the differences between pairs of points in the data exhibit stationarity. Therefore, the expected value of the difference between any two realizations is zero. This is mathematically expressed as

$$E(Z(s+h)-Z(s))=0 \tag{2}$$

where E symbolizes the expected value, Z is the attribute in question, s is a location in the problem domain, and h is a separation vector.

There must also exist a variance model that depends only on the distance between points, not on their locations, and is consistent throughout the model space. This is usually expressed as

13

$$\mathrm{var}(Z(s+h) - Z(s)) = 2\gamma(h) \tag{3}$$

where var is the variance and the function 2γ is called the variogram. Most forms of kriging require at least intrinsic stationarity because of the use of the variogram.

In practice, the required assumptions of Gaussian data and the existence of stationarity are often ignored. Kriging has been demonstrated to be exceptionally robust to misspecification of the model and, in many situations, kriging will still produce acceptable results even though the above assumptions have been violated (Journel and Rossi, 1989; Cressie and Zimmerman, 1992; and Cressie, 1993). Kriging owes much of its popularity to this robustness and, for this reason, kriging is the interpolation method used extensively in this study.

2.3.2 The Variogram

The variogram is the model that attempts to quantify the variability between sample data points in relation to the distances between them. From the assumption of intrinsic stationarity,

$$\mathrm{var}(Z(s_1) - Z(s_2)) = 2\gamma(s_1 - s_2) \tag{4}$$

where s_1 and s_2 are any two sample points. This equation is used as the basis for constructing a variogram plot. A variogram plot is essentially a plot of semivariance, $\gamma(h)$, versus separation distance or lag, h, that includes all pairs of points in the sample data set. The semivariance is calculated as

$$\gamma(h) = \frac{1}{2N(h)} \sum_{i=1}^{N(h)} ((Z(x_i) - Z(y_i))^2 \tag{5}$$

14

where $N(h)$ is the number of pairs separated by a vector of length h. When data is sampled on a regular grid, many pairs of points will all have the same separation distance and all those pairs will be averaged into one point on the variogram plot. This plot is often called an experimental variogram. If data is randomly sampled, then very few points will have the same separation distance and there will be many more points plotted. This plot is often called a variogram cloud. When variogram clouds are created, the points are often 'binned' into groups with similar separation distances and an average of the points is used to represent each group. In either case, a mathematical model is fitted to the variogram plot. The selection of an appropriate variogram model is made by examining the variogram plot for a match to some standard family of mathematical functions. Some goodness-of-fit measure is then used to parameterize the function. The selection of an appropriate model may also be tempered by knowledge of the underlying physical processes. For a good discussion of which mathematical functions may be used as variogram models refer to Cressie (1993).

When a mathematical model is fitted to the data, several significant parameters can be observed in the model. The parameters are the nugget, the sill and the range (Figure 1). However, some mathematical models may not have all of these parameters. Any two sample points taken at the same location should have the exact same value and therefore the semivariance should be zero at zero distance. The nugget value is the semivariance at zero distance and represents a combination of microscale processes and measurement error. Since the nugget is predicted from extrapolating data points, nothing can truly be said about the nature of the variogram at distances smaller than the shortest distance measured between sample points. Caution is required when predicting values at distances closer than this.

As the distance between samples increases, the semivariance also increases. Under some mathematical models the semivariance reaches a maximum value known as the sill. The value of the sill represents the semivariance around the mean. The distance where the sill is reached, called the range, can be interpreted as the distance where spatial autocorrelation becomes insignificant. This value is often used as a rough guide in

15

determining a kriging neighbourhood. Neighbourhoods are often used to exclude data from interpolation calculations, thereby decreasing computational requirements, under the assumption that sample points at great distances will have an insignificant influence on the final interpolated result. However, the range should not be blindly used for determining a kriging neighbourhood. As previously mentioned, kriging weights are not solely functions of the number of samples and their distances, but also of the local clustering and variability in the data. If insufficient sample points fall within the range, the interpolation weights will be a complex combination of weights from points beyond the range (Cressie, 1993).
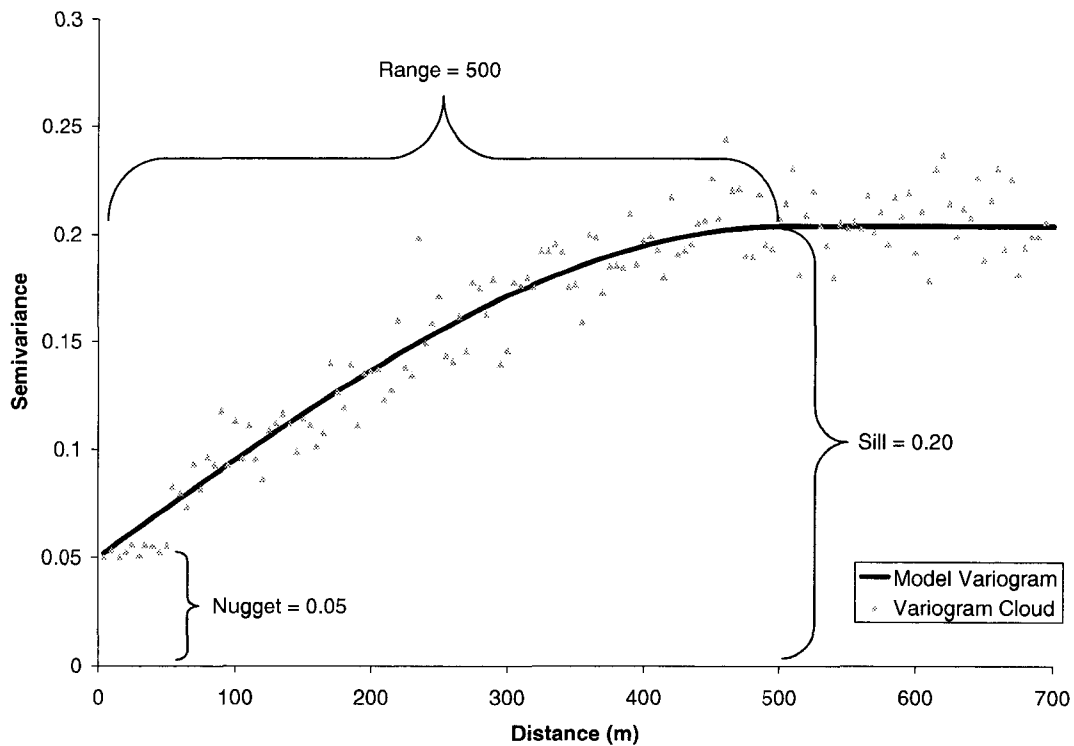
Figure 1: A sample variogram plot and fitted variogram model showing the parameters nugget, sill and range.

16

2.3.3 Predicting Interpolation Weights

In kriging, the interpolation weights are calculated by performing an analysis to determine the best predictor that minimizes the mean-squared error. If the process is Gaussian, then the optimal linear predictor is the optimal overall predictor. For the rest of this discussion, it is assumed that the process is Gaussian and therefore the analysis can be performed with linear predictors.

In the predictor p, we are looking for the best set of linear weights L_i;

$$p(Z;s_0) = \sum_{i=1}^{n} L_i Z(s_i) \tag{6}$$

such that

$$E(Z(s_0) - p(Z;s_0))^2 \tag{7}$$

is minimized.

In matrix notation, the weights, L_n, are solved by,

$$\begin{bmatrix} \gamma(s_1 - s_1) & \gamma(s_1 - s_2) & \cdots & \gamma(s_1 - s_n) & 1 \\ \gamma(s_2 - s_1) & \gamma(s_2 - s_2) & \cdots & \gamma(s_2 - s_n) & 1 \\ \vdots & \vdots & \ddots & \vdots & \vdots \\ \gamma(s_n - s_1) & \gamma(s_n - s_2) & \cdots & \gamma(s_n - s_n) & 1 \\ 1 & 1 & \cdots & 1 & 0 \end{bmatrix} \begin{bmatrix} L_1 \\ L_2 \\ \vdots \\ L_n \\ \mu \end{bmatrix} = \begin{bmatrix} \gamma(s_o - s_1) \\ \gamma(s_o - s_2) \\ \vdots \\ \gamma(s_o - s_n) \\ 1 \end{bmatrix} \tag{8}$$

where μ is a Lagrange multiplier to ensure that the weights sum to 1. When filling the matrices, the (n, n) matrix could be obtained either from the variogram data itself or from the mathematically fitted modelled variogram. Since s_o is an unknown location and not contained in the data set, the right hand vector values must be calculated from the model

17

variogram for every estimated location. Typically, the model variogram is also used for the (n, n) matrix so that should s_o fall on a known data point, and there is no nugget effect, the kriging method is an exact interpolator.

2.3.4 Predicting Values

Once the interpolation weights have been determined, they are used to calculate a value at that location.

$$\begin{bmatrix} Z(s_1) & Z(s_2) & \cdots & Z(s_n) \end{bmatrix} \begin{bmatrix} L_1 \\ L_2 \\ \vdots \\ L_n \end{bmatrix} = \begin{bmatrix} p(Z;s_0) \end{bmatrix} \tag{9}$$

The process of predicting weights and calculating a prediction value is then repeated for all locations where an estimate is desired.

2.3.5 Kriging Variance

As the prediction values are being calculated, the mean squared prediction error, or kriging variance, can also be calculated. This can be extremely valuable in determining areas where uncertainty in the data exists and where more rigorous sampling may be required in the future. The mean squared prediction error, also called the kriging variance, σ^2, is calculated as:

$$\sigma^2(s_0) = \sum_{i=1}^{n} L_i \gamma(s_o - s_i) + \mu \tag{10}$$

It should be noted that actual data values are not required for the calculation of the kriging variance. In effect, it is a variogram-dependent estimate of uncertainty given the relative locations of the data points. This property has allowed the use of the kriging

18

variance for the determination of optimal sampling strategies (Ben-Jemaa et al., 1995 and Lo et al., 1996). Since the kriging variance is variogram-dependent, it should not be used for comparisons between simulations with different variogram models. A misspecification of the variogram model could lead to the false assumption that variability is low and that the model is predicting well.

2.3.6   Other Forms of Kriging

The form of kriging described above is known as ordinary kriging. Other methods of kriging have been developed that allow for departures from the underlying assumptions or that consider the joint variability of more than one attribute. A brief discussion of a few of these methods will be included here as mention is made of them elsewhere in this thesis.

Universal kriging is a variant that allows for the incorporation of an unknown spatial trend into the data. As such, it is sometimes called 'kriging with a trend model'. The trend is usually modelled as a polynomial function on the spatial coordinates. The parameters of this polynomial function are not specified in advance. They are instead incorporated into the kriging equations and are worked out in the solution matrices. As such, universal kriging will not necessarily produce the same results as removing the trend, performing ordinary kriging, and then reapplying the trend.

Cokriging is a variant of kriging that allows for the incorporation of ancillary data into the estimations. It can be based on any of the other forms of kriging since its only mathematical difference is that it incorporates additional information in the form of additional data values and their cross-variability. Any ancillary information that is expected to vary in a similar spatial pattern to the primary variable could be used. Cokriging is most useful when the ancillary data set is larger than the primary data set. For example, cokriging can be used with screening data. If a large number of field tests were conducted with a less accurate instrument and then only a subset of those samples

19

sent in for laboratory analysis, the analyzed samples could be cokriged with the field data to obtain a better spatial distribution from the analyzed data. Similarly, if an extensive sampling program has already been conducted on a particular chemical that is known to occur in conjunction with a chemical to be sampled, a much smaller sampling program could be conducted and then the results cokriged with the larger study.

Block kriging can be applied to any of the above methods of kriging. It is used to find an average prediction value for an area (or volume) larger than the grid discretization. The prediction block uses the average variogram from all the locations contained within that block. This averaging tends to smooth out the map values.

Indicator kriging is not performed to make predictions of a property. Instead it is applied to indicator functions to determine a probability of occurrence. For indicator kriging, a series of indicator functions with various cut-offs are created, kriging is performed with each, and then the results are combined to form a conditional cumulative distribution function that represents the probability of occurrence.

Disjunctive Kriging is a non-linear form of kriging that can be used for sample data which does not fit the required Gaussian distribution. It enables the calculation of a probability of occurrence in addition to the prediction values. This is achieved by examining not only the data values themselves, but also a series of functions of the data. The use of functions with the data requires the use of more rigid assumptions. If the functions examined are indicator functions, then disjunctive kriging can be an alternative to indicator kriging.

2.3.7   Anisotropy

In some situations, the variability between any two points may be a function of direction as well as distance. This property is known as anisotropy. Anisotropy is often described in terms of an anisotropy ellipse. The boundary of the ellipse can be thought of as a

20

contour of equal influence. Figure 2 shows a representation of a plan view, two-dimensional anisotropy ellipse, however the concept is also extendable to three-dimensions. The major axis represents the range in the direction of greatest continuity. Ideally, the minor axis is perpendicular to the major axis and represents the range in the direction of least continuity.
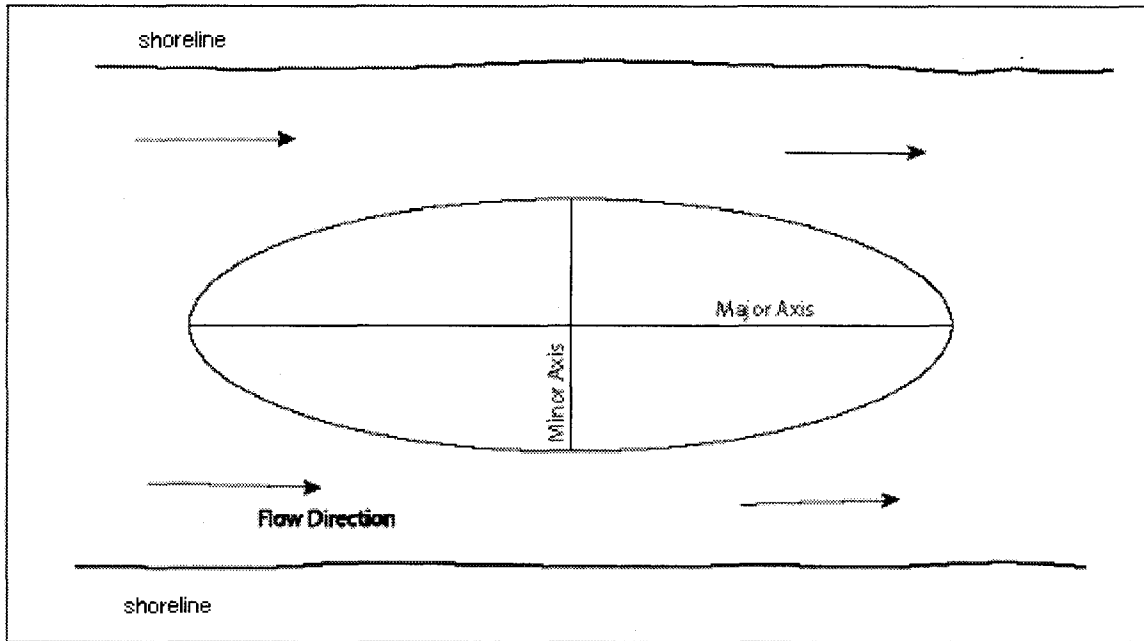
Figure 2: A plan view, two-dimensional anisotropy ellipse in the context of a river.

In order to uncover anisotropy in the data, directional variograms need to be created. In the construction of a directional variogram, rather than using all pairs of points for the variogram plot, only those pairs of points that have a separation vector with the suspected anisotropy direction are used. Many directions may need to be examined before the direction with the maximum continuity (i.e. the longest range) is discovered. The ratio between the range of the major axis and the range of the minor axis is known as the anisotropy ratio and is an indication of how strong the anisotropy is.

If the semivariances along the major and minor axis reach the same value of sill, but at different ranges, the anisotropy is known as geometric anisotropy and can be corrected

21

for by applying a scaling factor to distances along the axes. In effect, this scales the Euclidean space so that the major axis and the minor axis have the same range. The standard isotropic kriging algorithms can then be applied. If the data along the major and minor axis do not reach the same sill, the situation is known as zonal anisotropy. To properly model zonal anisotropy a composite variogram model is required. A composite model is essentially the sum of two standard variogram models with one component representing distances in the major direction and the other representing distances in the minor direction.

Unless the direction of anisotropy is known in advance, and some attempt is made to sample points in pairs along the major and minor directions, it is unlikely that there will be many points with which to construct the directional variograms. In most cases, some tolerance is used so that pairs of points that lie only roughly along the anisotropy direction get included in the directional variogram. Unfortunately, this means that some of the variability from the perpendicular direction is included in the directional variogram. This leads to a situation where the directional variograms almost always indicate an apparent anisotropy that is less that the true anisotropy (Deutsch and Journel, 1998).

2.4   Shortcomings of the Standard Techniques in Fluvial Environments

Since the focus on this thesis is on the surficial sediments that lie on the bed of the river, the following discussions with only treat the issues from a two-dimensional perspective. Since rivers are in fact three-dimensional environments, future work in extending the concepts laid out here may require the application of three-dimensional techniques in order to extend the concept for other applications.

The primary shortcoming with standard interpolation techniques when applied to fluvial environments is in how they deal with the process of sediment transport. The process of sediment transport creates anisotropy in the spatial distributions of sediments and other

22

attributes influenced by the flow of water. The flow of water will tend to draw sediment downstream much faster than it can disperse them across the channel. This creates anisotropy in the distribution of sediments. The major axis of the anisotropy ellipse is in the downstream direction, while the minor axis of anisotropy is cross-stream. The problem arises when a river begins to meander across the landscape. Depending on the location in the river being examined, the angle (geographic bearing) of anisotropy may be different (Figure 3). Since most kriging algorithms allow only one angle of anisotropy for the entire problem domain, the local anisotropy is not properly characterized. When these situations arise, unique solutions need to be created to deal with the issue of anisotropy.
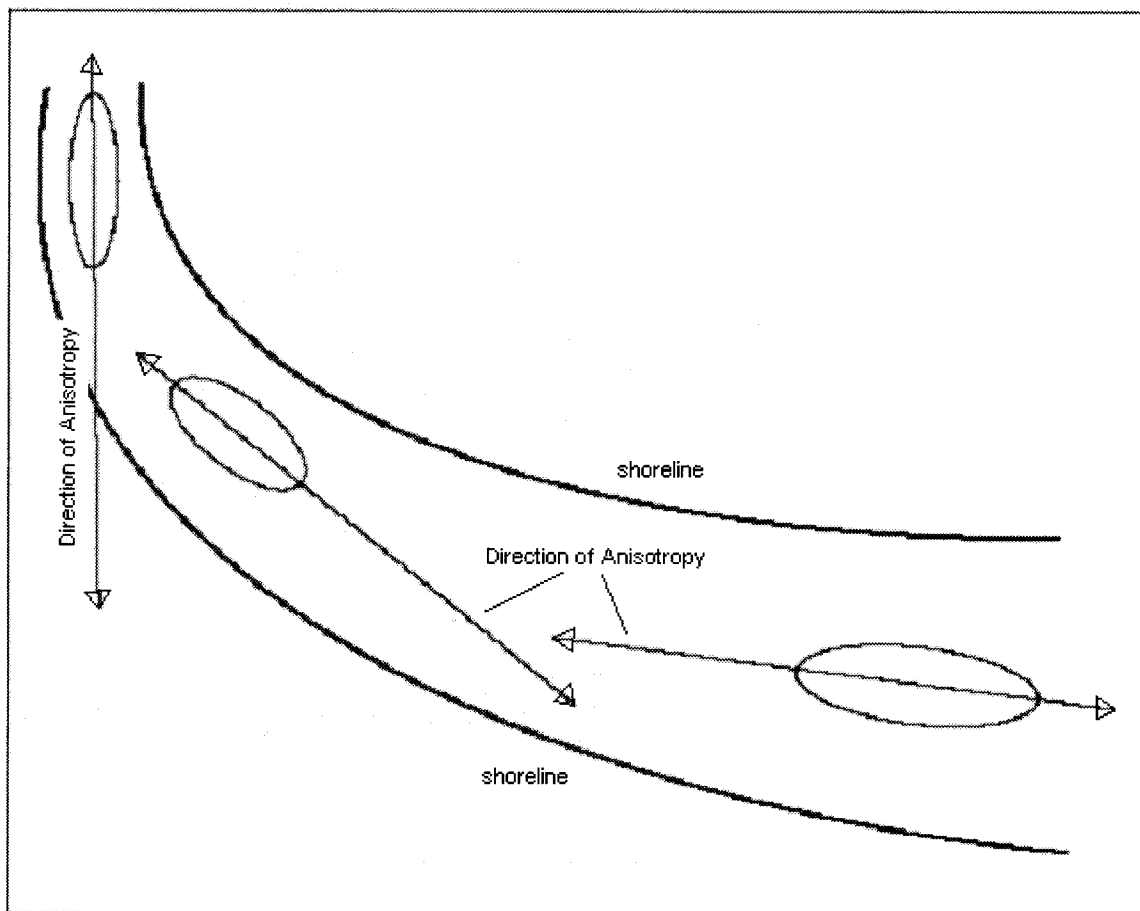
Figure 3: Plan view of anisotropy ellipses and anisotropy direction shown in the context of a meandering river bend.

23

Without an easy method to deal with this anisotropy, it may be tempting to simply try to ignore anisotropy and model the environment as isotropic. With extremely dense sampling, this may produce acceptable results. However, sampling is expensive and in most studies, sample points are sparsely sampled with respect to the study extent and sample variability. The advantage of incorporating anisotropy is to increase the range of the major axis and decrease the range of the minor axis. In this way sample points sparsely sampled downstream are more likely to lie within the range and have their true spatial autocorrelation included in the analysis. At the same time, it will not be incorrectly assumed that points with significant cross-stream separation distances have the same spatial correlation.

If the river does not meander too much, it may be tempting to use an average anisotropy angle for the area. However, this becomes problematic as the meanders become more pronounced. Using a 90 degree bend as an example, the water is flowing at a bearing of 0 degrees at the start of the bend. As the water leaves the bend, it is flowing at a bearing of 90 degrees. The average angle is 45 degrees. The angle of 45 degrees should work well in the middle of the bend, but will work poorly for the start and end. This leads to some areas being predicted more accurately than others and makes it very difficult to judge the accuracy of the overall results. In addition, using an average angle will certainly produce an apparent degree of anisotropy that is much less than the true anisotropy. Using a 180 degree bend as an extreme example, the bearing of anisotropy can be exactly opposite in different parts of the bend. The anisotropy averages out to no apparent anisotropy.

Another common approach is to take the area and break it up into subsections that have roughly the same direction of anisotropy, model each section as being anisotropic and mosaic the results back together. This method can also be used to help overcome violations of the assumption of stationarity. This method has the advantage of being easy to implement. However, it may not always be practical. By breaking up the river into subsections, the number of data points in each section is reduced. With fewer data points

24

in the set, the effectiveness of the interpolation decreases. Another problem that occurs when breaking up the domain is that mapping artefacts can occur where the subsections are pieced back together. Rather than a smooth transition of values between subsections, there is often a jump in values since the estimates on either side of the boundary were constructed with different data sets.

The approach taken by Barabás et al. (2001) was to completely transform the real-world Euclidean space into a linear model space, conduct the kriging and then backtransform the data. To summarize the technique already described in Section 1.1, the channel boundaries were treated as opposite sides of the rectangle. An equal number of evenly spaced points were placed along each bank and along the upstream and downstream boundaries. The problem domain was then 'rubber-sheeted' using linear interpolation into a rectangular domain within which the kriging was conducted. The use of such transformations helps deal with two critical issues. They eliminate the possibility of distances between points being measured across land and aid in the detection of anisotropy by straightening the river. However, the channel examined in their study had a fairly regular width, had no islands (or at least none were mentioned), and therefore had a fairly consistent flow environment. The effects of such domain transformations in complex environments need to be examined. In particular, it is important to consider the effect of the domain transformation on the anisotropy ellipse and prediction areas.

When transforming a channel with diverging width into a linear model space, the cross-stream compression changes along the length of the channel. The effect of this is to distort the anisotropy ellipse (Figure 4). It is then questionable as to whether standard kriging algorithms, which assume a regular ellipse, are valid under this transformation. From a more physically based view, it may seem intuitive that the degree of anisotropy is related to the velocity in the channel. If the velocity in the channel decreases as a channel diverges, it may be that the anisotropy ellipse is already distorted and that the transformation is distorting the ellipse back into a more regular shape. However, an increase in channel width does not necessitate a decrease in the flow velocity and therefore the argument still needs to be considered. The issue of whether the concept of a

25

regular anisotropy ellipse is valid in the physical world or in the transformed world would be an area that requires further examination.

Another issue involving domain transformation deals with gridding the domain. The domain in which the kriging is performed needs to be discretized. Using the example of a diverging channel again, if the real-world grid has regularly sized and shaped cells, it will have distorted grid cells in the transformed domain and vice versa (Figure 4). This may create problems if the values of the sampled data are highly dependent on the sampling support. It may also create problems for block kriging by altering the number points that should be averaged into the block.
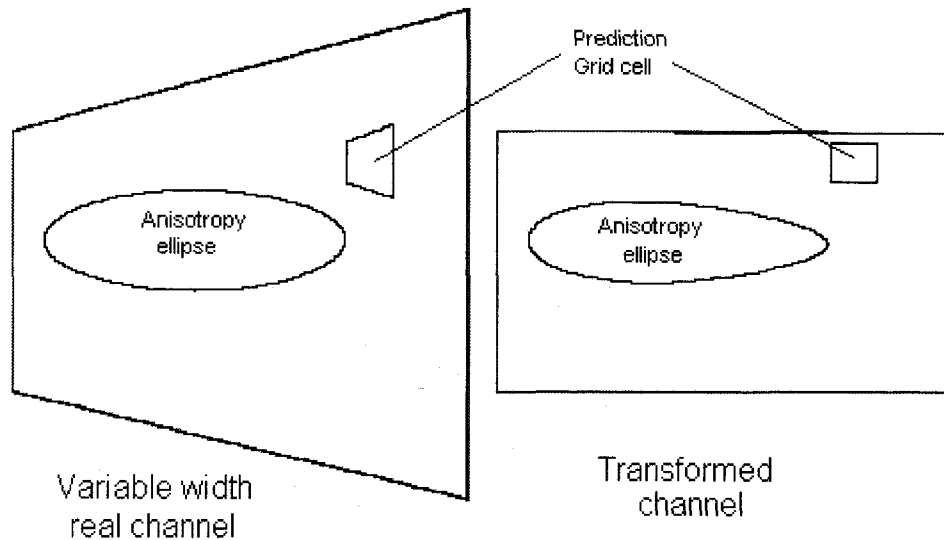
Figure 4: Distortions to grid cells and anisotropy ellipses caused by a variable cross stream compression in a domain transformation.

Islands present several other conceptual problems when interpolation is attempted in aquatic environments. One problem is whether or not to treat the island as a barrier to spatial autocorrelation. Consider two points on opposite sides of an island. If the property being predicted has a different source on opposite sides of the island, there is no reason to suspect correlation and the island could safely be modelled as a barrier.

26

However, if both points are influenced by the same upstream source, there is some argument that the points are correlated. The next problem is modelling the degree of correlation. Using normal distance measures, the width of the island increases the distance between the points and therefore decreases the correlation. If the source process does not distinguish between land and water, it may be appropriate to simply measure across the islands. However, a one metre wide island provides just as effective a barrier to the flow of water as a one kilometre wide island. For another example, it would not take twice the effort to swim around an island 100 m long by 2 m wide than it would to swim around an island 100 m long by 1 m wide. Clearly the process creating the underlying spatial distribution is important when deciding how to deal with islands in an interpolation.

The other problem with islands is that they split the flow of water and send it in different directions. The effect on modelled anisotropy is similar to that caused by meanders in the channel. The geographic bearing of anisotropy is altered. However, in the case of islands, the channel is split and two changes in direction need to be considered. If not for the problem of modelling correlation across islands, this would be fairly easy to deal with in a domain transformation. The distance across the island would simply be left out when scaling across the width of the channel.

3.0 Flowline Transformation Approach

In order to create spatial distribution maps in complex fluvial environments, a method was devised to improve upon the interpolation of sample data. The method was created to allow for more specific modelling of local anisotropy without suffering from the spatial distortions arising from domain transformations.

Given enough information about the flow dynamics of a river and assuming that advection is the only transport process, a theoretical path that a group of particles might follow as it is carried through a river can be constructed. This path can be called a

27

flowline (also known as streamlines or pathlines in other, more specific applications). If the particles move off this path, the assumption is that it they are being influenced by other transport processes such as secondary currents and cross-stream dispersion. For the purposes of this thesis, the perpendicular offset from the flowline that the particles have been moved will be called a cross-line.

When calculating the distance between two points for an anisotropic model, a distance along the major axis is required and a distance along the minor axis is required. The major axis becomes a transformed x-axis and the minor axis a transformed y-axis. In this flowline distance transformation method, the distance between two points along a flowline corresponds to the major axis and the distance along a cross-line from a point to the flowline corresponds to the minor axis (Figure 5).
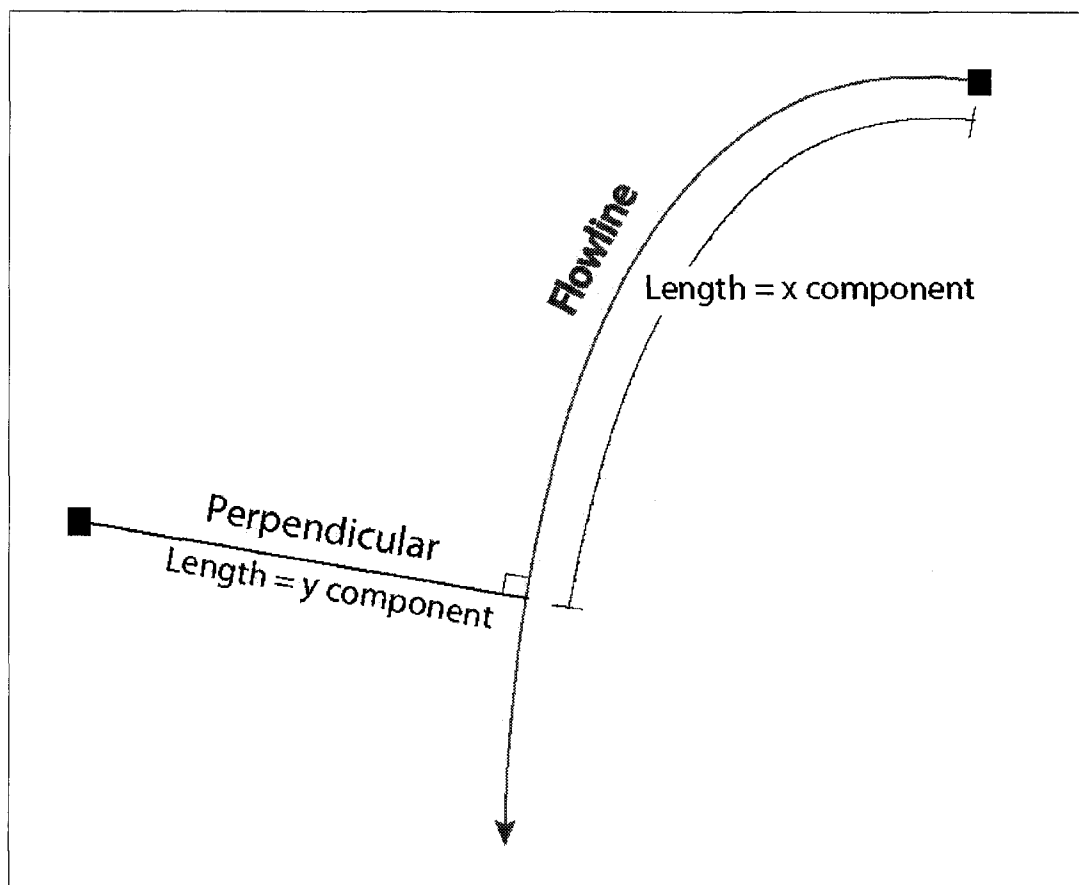
Figure 5: Conceptual diagram of flowline and cross-line distance transformations.

28

Using this new distance measurement technique a variety of interpolation algorithms could be used simply by substituting flowline and cross-line distances for the Euclidean Δx and Δy.

3.1 Algorithm Implementation

In order to perform interpolation using this method, the following general steps need to be performed. First the sample data points are obtained. Flowlines are then generated upstream and downstream from each of the data points (see Appendix A for the algorithm used in this thesis). If kriging is to be used for interpolation, then a variogram plot needs to be created using the new distance system and a variogram model fitted to the data. Interpolation can then be conducted. During interpolation, each time a distance is required between a prediction point and a data point, the cross-line distance from the prediction point to the sample point's flowline is used as Δy and the distance along the flowline from the cross-line to the sample point is used as Δx. The distances are then used as appropriate for the given interpolation method.

In order to generate flowlines, information regarding the channel hydrodynamics is required. Although there may be other means of generating flowlines, in this study flowlines were generated using a velocity vector field. The velocity vector fields were generated with flow simulations using the CH3D hydrodynamic model (Chapman et al., 1996). A small group of software tools was created using Microsoft Visual Basic 6.0 and ESRI's ArcObjects development environment in order to import the CH3D data and to trace flowlines through the velocity vector field. The flowlines were stored as ESRI shapefiles for later use. For a detailed description of the algorithm used in the generation of the flowlines and cross-lines refer to Appendix A.

Kriging was chosen as the preferred method of interpolation because of its widespread usage, robustness, extensibility and error estimation capabilities. Therefore, a variogram model was required. One of the software tools created in this study exports a variogram

29

plot based on the new flowline distance system. The variogram plot was then brought into Microsoft Excel and a spherical variogram model with geometric anisotropy was interactively fitted to the data.

For the actual kriging implementation, the GSTAT (version 2.4.0) geostatistical modelling software (Pebesma, 1999) was modified. Two dynamic link libraries (DLLs) were also created in order to allow GSTAT to use the flowline shapefiles. The primary DLL was created with Visual Basic and ArcObjects and contains all the required numerical processing functionality. The secondary DLL was created with Visual C++ 6.0 and merely provides a data conduit for the otherwise incompatible ANSI C code of GSTAT and the Visual Basic DLL. The GSTAT source code was modified so that when the program is first executed the primary DLL imports the flowline shapefile and stores the information in memory. When the GSTAT algorithm requires distances, a function in the DLL is called that calculates the flowline and cross-line distances and returns them to the main GSTAT code. Otherwise, the kriging algorithm in GSTAT remained unmodified.

3.2   Simple Test Cases

In order to test that the modified GSTAT algorithm works properly and to determine whether the algorithm performs well under ideal cases, a series of five geometrically simple test cases were generated using the CH3D hydrodynamic model with sediment transport. Samples data sets were selected from the model results and used with both standard ordinary kriging with anisotropy and flowline ordinary kriging with anisotropy to determine the effectiveness of the methods.

The CH3D hydrodynamic model is a three-dimensional numerical finite difference model. It has the capability to model a broad range of physical processes such as sediment transport, salinity, temperature, density effects, tidal effects, wind effects,

30

turbulence and the effect of the earth's rotation. For a more detailed description of its capabilities refer to Chapman et al. (1996).

Although the CH3D model is capable of sediment transport simulations, it is not the intention of this thesis to make predictions of spatial distributions using it. It is being used as a tool to aid in the interpolation of sample data points and to investigate the effectiveness of interpolation methods. Large amounts of data are required to produce reasonable spatial distributions of sediments for real world applications with a sediment transport simulation. Often times, sampling and interpolation need to be performed as pre-processing steps in setting up the sediment transport simulation. The true purpose of the CH3D model in this thesis is twofold. First, it is being used to generate reasonable velocity vector fields for the test case channels, which in turn are used to generate flowlines. Second, it is being used to create simple simulation test cases where the spatial distributions are controlled by the processes of advection and dispersion.

The purpose of using a simulation as a surrogate for a real-world test case allows for a test case with much less complexity in its spatial structure. A real-world test case could be influenced by several geomorphological processes. The multiple processes may interact, masking the true effectiveness of the flowline method, and making it difficult to assess the results. Using simulations, the individual processes may be examined separately. In addition, the use of a simulation allows for the complete knowledge of the 'actual' sample values at every location in the problem domain. This provides a true representation of what the spatial distributions should look like. The use of a simulation also allows for complete control of sample sizes, number of samples and sample locations. In this way, the effects of sampling density, sampling patterns and interpolation methods can be compared without the prohibitive cost of actually conducting a real-world sampling program to such a fine degree of detail.

Since the CH3D model is a three-dimensional model, the resulting output is discretized into multiple layers. Since it is the surficial sediments are being interpolated, it is expected that the flow conditions in the bottom layer adjacent to the bed will have the

31

most influence on the resulting distributions. Consequently, it is the steady state velocity vector field for this layer that is used to generate the flowlines. The sediment transport output of a CH3D simulation is a series of files showing suspended sediment concentrations and the bed sediment mass fractions for several grain sizes specified in the model input. For these test cases, only the bed sediment fractions were examined. When conducting the simulations, they were run only as long as was required to generate reasonable looking plumes, not necessarily to steady state. This was done because of the setup and purpose of the simulations. The simulations were simple geometries designed to be depositing sediments on the bed of the channel. Running the simulations for too long would have produced plumes that covered large areas of the channel bed with 100% mass fractions of fine grained sediment. Since such distributions would be inappropriate for testing the interpolation methods, the simulations were terminated when reasonably large plumes and a wide range of mass fractions had been generated in the simulation.

The details for each simulation can be determined from the input files found in Appendices B-E. However, a quick summary of the common elements will be briefly discussed here. Although the geometry of each CH3D simulation is slightly different, the numerical modelling mesh was created so that elements were approximately 5 m^2 in size. Six sediment point sources were placed within the channel so that they would generate sediment plumes on the bed of the channel with a wide range of mass fractions. Seven random samplings with 30, 50, 70, 90, 110, 130 and 150 sample points were selected from the CH3D model results. Flowlines were created for each of the data sets using the algorithm outlined in Appendix A without any manual editing of the resulting flowlines. Variogram plots were then created for the sample data sets using both a standard and a flowline distance system. Although the histograms of sediment distributions are skewed towards lower concentrations, it was decided not to apply any transformations to normalize the data in order to provide a more objective view of the limitations of each method and to ensure that the data transformation was not biasing the results towards one method or the other.

Microsoft Excel was used to fit a spherical model with geometric anisotropy to the sample variogram plots based on the criteria of minimizing the averaged sum of the squared residuals. The spherical model is composed of a combination of a linear section and an exponential section (Deutsch, 2002). Using the spherical model with geometric anisotropy seemed to provide a reasonable fit for all the variogram plots obtained in the study without having to switch model types between trials. Geometric anisotropy was chosen because the directional variograms in the y-direction were insufficient to determine a composite variogram model. To reduce the computational effort of fitting a model, the plot was 'binned' into ranges of 10 m for the 150, 130 and 110 sample sets or 20 m for the 70, 50 and 30 sample sets. The 90 sample sets used whichever binning produced the most reasonable results. Anisotropy ratios between 0.50 and 0.01 were examined in increments of 0.01 and the Solver Add-in tool for Microsoft Excel was used to solve for the nugget, sill and range. In order to provide an objective comparison of the standard and flowline kriging methods, the model parameterization that produce the smallest averaged sum of the squared residuals was used for the kriging, regardless of any visual assessment of the fit.

The problem domain was discretized into 5 m^2 regular sized grid cells upon which kriging predictions were to be made. The results were imported into ESRI's ArcGIS for visualization and the generation of test statistics.

3.2.1   Horizontal and Vertical Straight Channels

The primary purpose of these two test cases was to verify the correctness of the basic algorithm. A perfectly horizontal channel with perfectly horizontal flow will have all its flowlines running straight along the x-axis and all the cross-lines perfectly straight along the y-axis. Consequently, the results of the flowline kriging method should produce exactly the same results as a standard kriging algorithm. A perfectly vertical channel with all the same inputs should produce a rotated version of the horizontal channel.

33

Since the purpose of these simulations was only to determine whether the algorithm produced correct numerical results, the resolution of the computations was decreased and an isotropic variogram model was used in order to decrease the computational effort. The simulation used a 20 m^2 grid cell resolution for the CH3D simulation, 3 random sediment sources, 30 random sample points and a 10 m grid resolution for prediction cells.

The CH3D input files, random samples and variogram equations used for the simulations can be found in Appendix B.

The standard kriging and flowline kriging methods produced nearly identical results for the horizontal and vertical straight channels (Figures 6, 7 and 8). A cell by cell examination of the results from the two methods reveals that the methods produce identical values to an accuracy of 5 decimal places. The results were taken as a demonstration that the newly developed algorithm was working as expected.

34
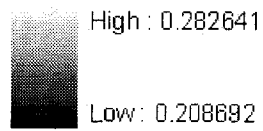
Downstream   Upstream
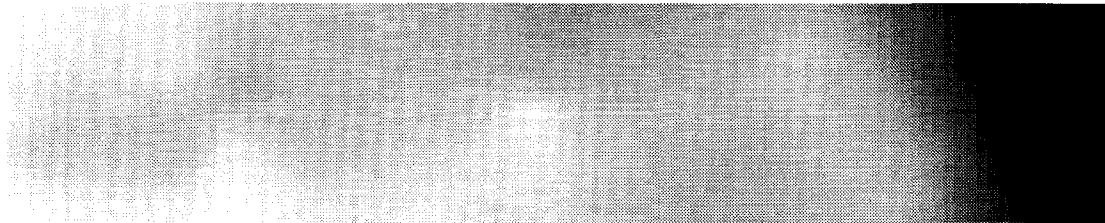
Figure 6: Predicted mass fractions of sediment with grain size diameter of 0.037 mm using isotropic standard kriging on 30 random samples in a straight horizontal channel.
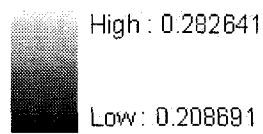
Downstream   Upstream
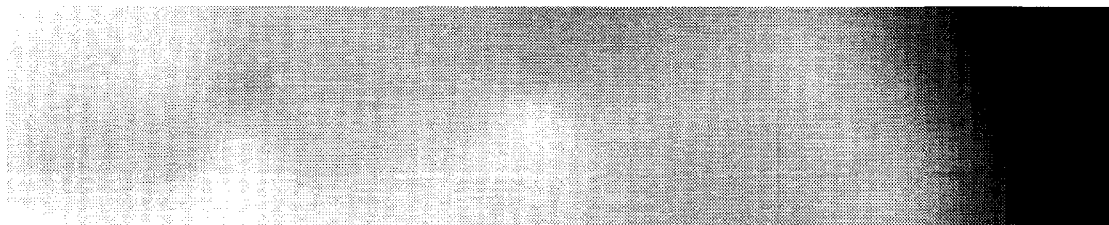
Figure 7: Predicted mass fractions of sediment with grain size diameter of 0.037 mm using isotropic flowline kriging on 30 samples in a straight horizontal channel.
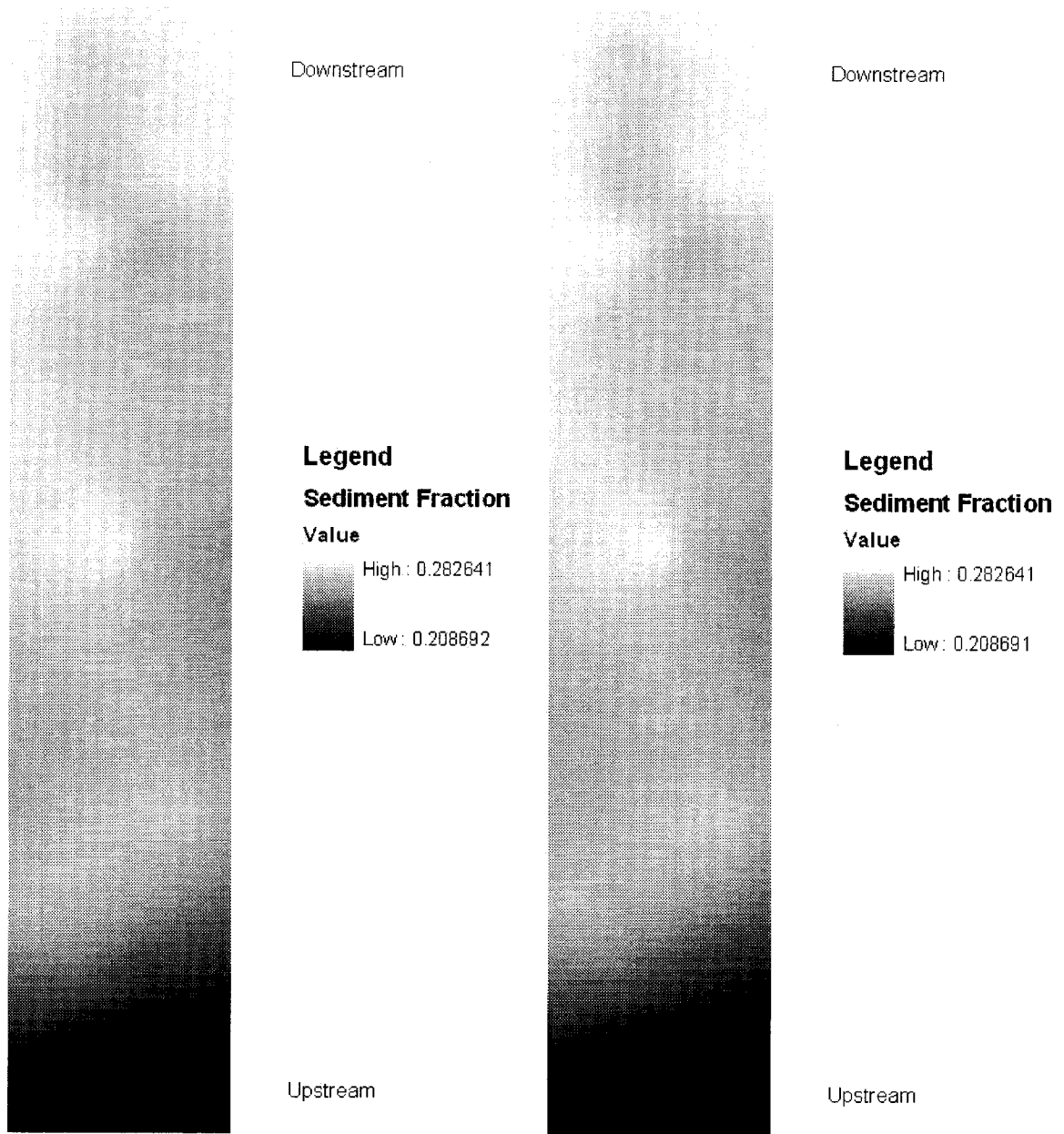
Figure 8: Predicted mass fractions of sediments with grain size diameter of 0.037 mm using isotropic standard kriging (left) and isotropic flowline kriging (right) on 30 samples in a straight vertical channel.

36

3.2.2   Curved Channel

A 90-degree curved channel served as the primary test case to compare how the flowline algorithm performs compared to standard methods. When standard anisotropy algorithms are applied to curving or meandering channels, an average anisotropy angle needs to be applied. It is expected that in areas where the local anisotropy angle is far from the global average angle, the results of the standard prediction techniques would behave poorly. The flowline kriging method, since it does not use a global average angle, should behave better in those areas.

The sediment sources were randomly placed in the channel for these simulations and an average anisotropy angle of 45 degrees was used for the standard variogram model. The CH3D input files, random samples and variogram equations used in this test case can be found in Appendix C.

It can be seen in Figures 9, 10, and 11 that the flowline method does a better job of characterizing the actual shape and extent of the sediment plumes. The plumes generated by both kriging algorithms show lower concentrations than the actual concentrations. This should be expected since a random sample would have to land exactly on a source or extremely close and perfectly downstream of a source to capture the highest concentrations and incorporate them into the interpolation. As was expected, the standard kriging method performed poorly in areas where the average direction of anisotropy was far from the true local direction of anisotropy. Figure 10 shows how, at the ends of the channels, the standard kriging method predicts sediment plumes that extend cross-channel, rather than along the direction of flow. This inability of the standard method to compensate for changes in the direction of anisotropy around curves can even divide a plume into two (or more) separate plumes as seen at the downstream end of Figure 10.

37
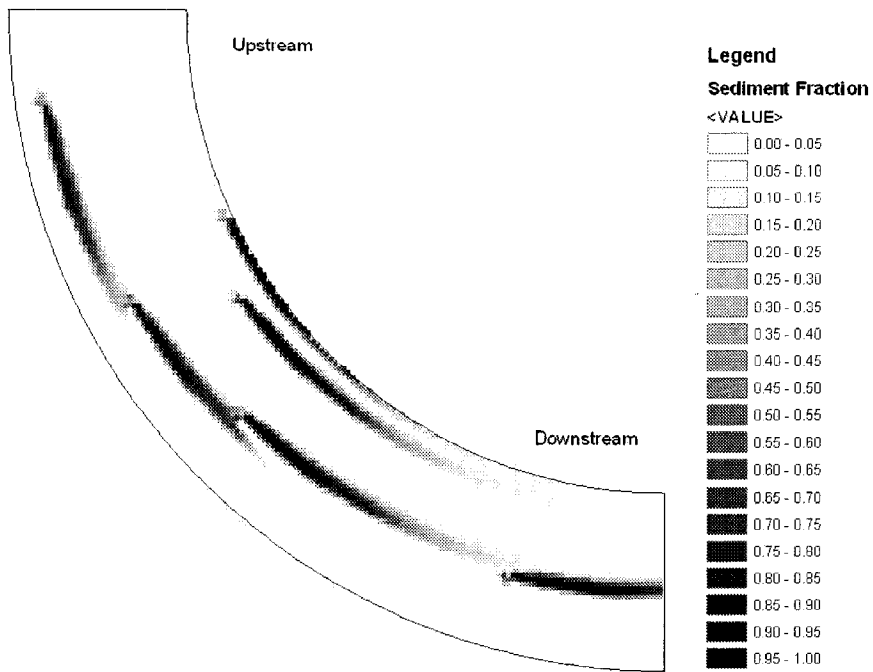
Figure 9: Mass fractions of sediment with grain size diameter of 0.01 mm for a curved channel as output from the CH3D model.
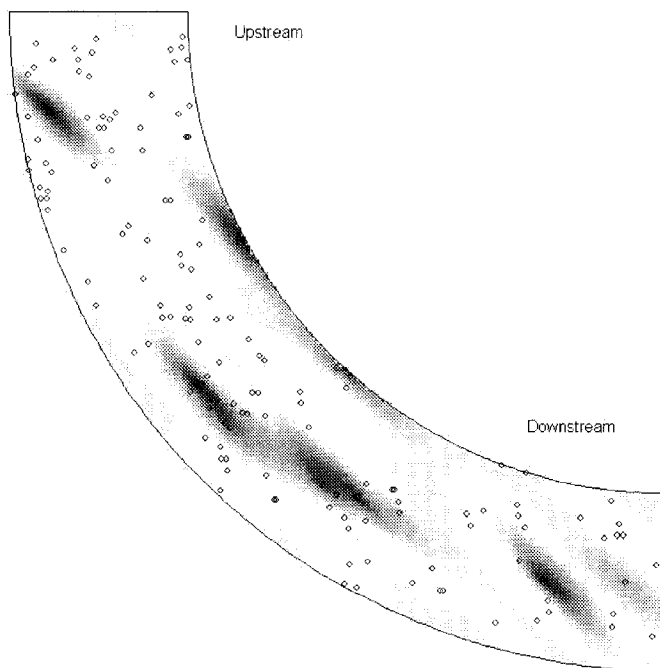
Figure 10: Predicted mass fractions of sediment with grain size diameter of 0.01 mm using standard kriging on 150 samples in a curved channel (Same legend as in Figure 9).

38
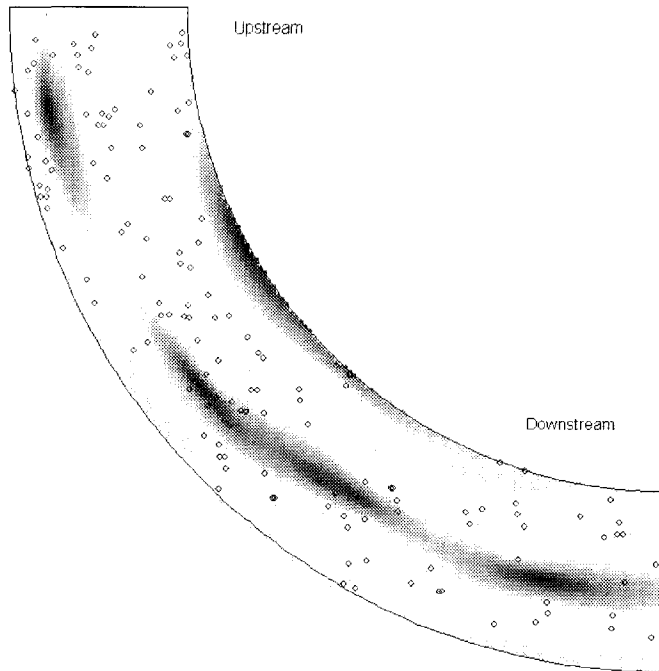
Figure 11: Predicted mass fractions of sediments with grain size diameter of 0.01 mm using flowline kriging on 150 samples in a curved channel (Same legend as Figure 9).

Figures 12 and 13 show the distributions of kriging variances. The variance maps also show the flowline method's ability to track around curves. The standard method shows a narrower range of variances and more area with low variance. As mentioned in Section 2.3.5, the kriging variance is model-dependent and therefore should not be used to directly compare methods. The smaller variability predicted by the standard method may actually be misleading. It may lead to the false assumption that areas are being well-predicted, when in fact, a better model specification would actually reveal that they are being poorly predicted.

39
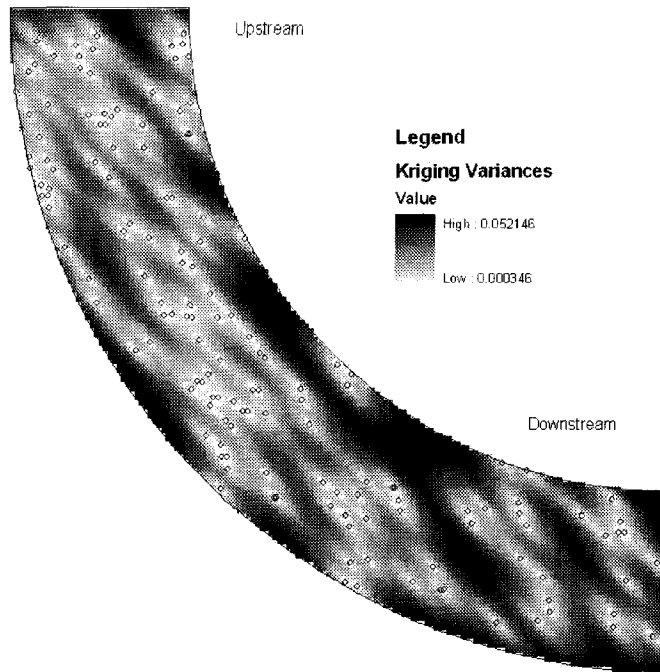
Figure 12: Kriging variances for sediment with grain size diameter of 0.01 mm using standard kriging on 150 samples in a curved channel.
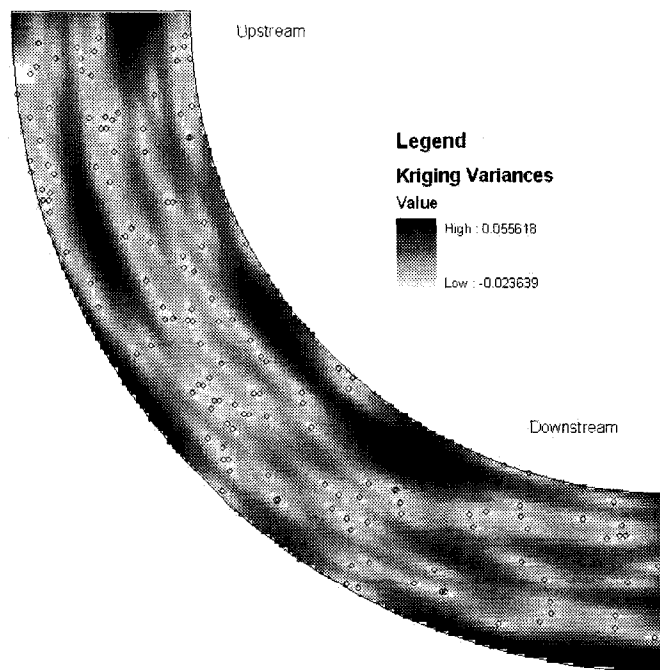
Figure 13: Kriging variances for sediment with grain size diameter of 0.01 mm using flowline kriging on 150 samples in a curved channel.

40

In addition to the visual inspection of the kriging results, two statistical measures were examined to compare the performance of the standard and flowline kriging methods. The correlation coefficient and the root mean squared error of prediction (RMS) were generated for each of the seven simulations by comparing, on a cell by cell basis, all the values predicted by kriging to the actual values output from the CH3D model. The statistics are shown in Figures 14 and 15. The graphs show that the flowline method outperforms the standard method over a wide range of sampling densities. The better predictive capability is indicated by larger correlation coefficients and lower error in predictions, as indicated by the RMS. It should be expected that as the number of sample points is increased, the interpolated results would be better. This is observed in both the standard and flowline kriging methods. However, the flowline method consistently has a higher correlation coefficient and a lower RMS over all seven simulations examined. From a sampling perspective, this would mean that in order to obtain the same predictive accuracy, fewer points would need to be sampled using the flowline method than using the standard kriging method. At a first glance, it also appears that the correlation coefficient for the flowline kriging method approaches 1 (i.e. perfect correlation) more rapidly than for the standard kriging method. However, each of the test simulations uses only one of the many possible random samplings. Consequently the single random sampling may not represent the average behaviour well enough to verify that particular conclusion. In addition, variogram modelling can be very subjective and a poor random sampling combined with poor variogram modelling could lead to differing results. However, the consistent performance improvement of the flowline kriging method over the standard kriging method gives confidence that the flowline method produces better numerical as well as visual results.

41
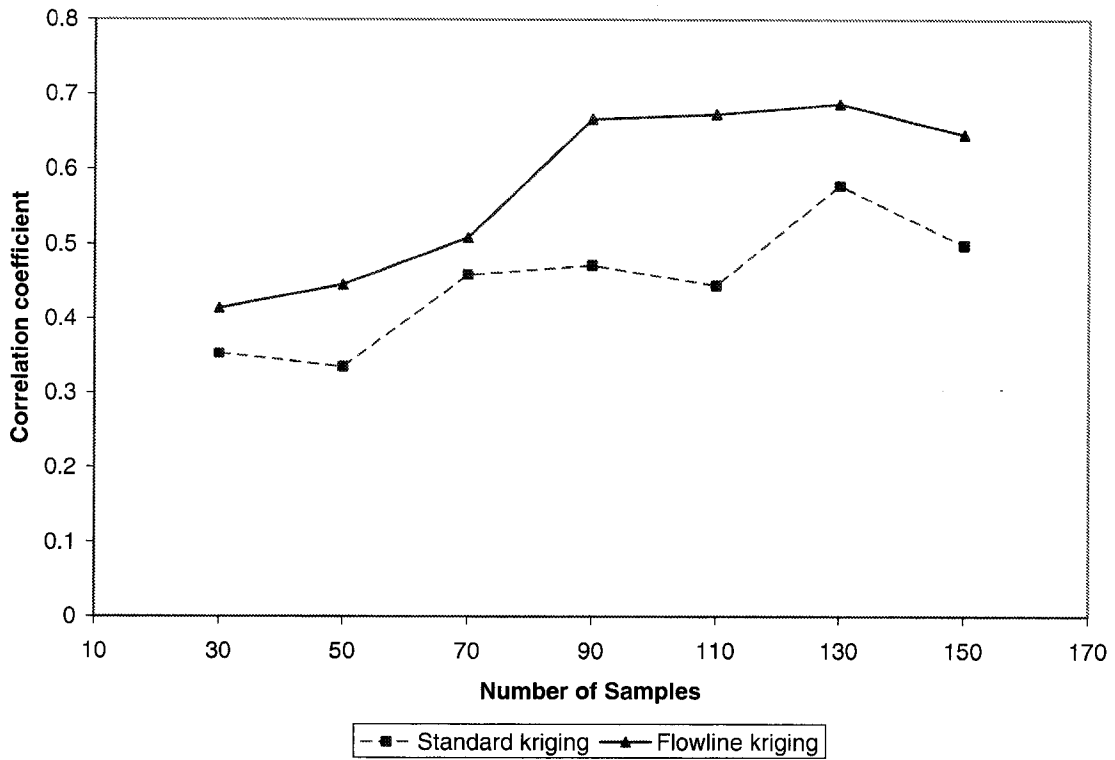
Figure 14: Graph of correlation vs. number of samples for a curved channel.
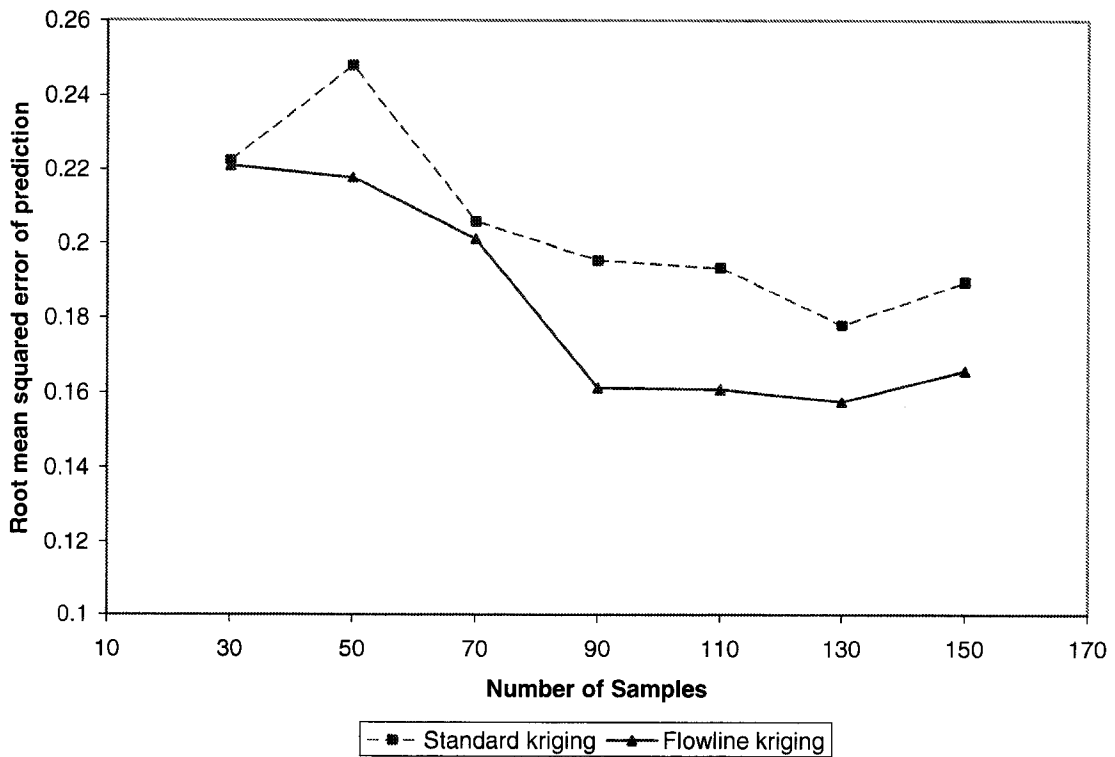
Figure 15: Graph of RMS vs. number of samples for a curved channel.

42

3.2.3 Channel with Island

As discussed in Section 2.4, islands can create a variety of problems in kriging. The current implementation of the flowline kriging algorithm measures across islands and therefore the island's width decreases the correlation between points on either side of the island. Although the issue of modelling spatial correlation across islands requires more thorough study, these test cases were performed as an initial estimation of the effectiveness of the flowline kriging method in such complex environments.

For this simulation (Figure 16), three sediment sources were randomly placed throughout the channel and the other three were placed together just upstream of the island. The flow of water is from left to right so an average anisotropy direction of 90 degrees was used for the standard variogram model. The sediment sources just at the head of the island create plumes that flow around both sides of the island, although dominantly along the top. The other sources flow around corners in the channel. It is these effects that the interpolation methods must capture. The CH3D input files, random samples and kriging equations used in this test case can be found in Appendix D.

43
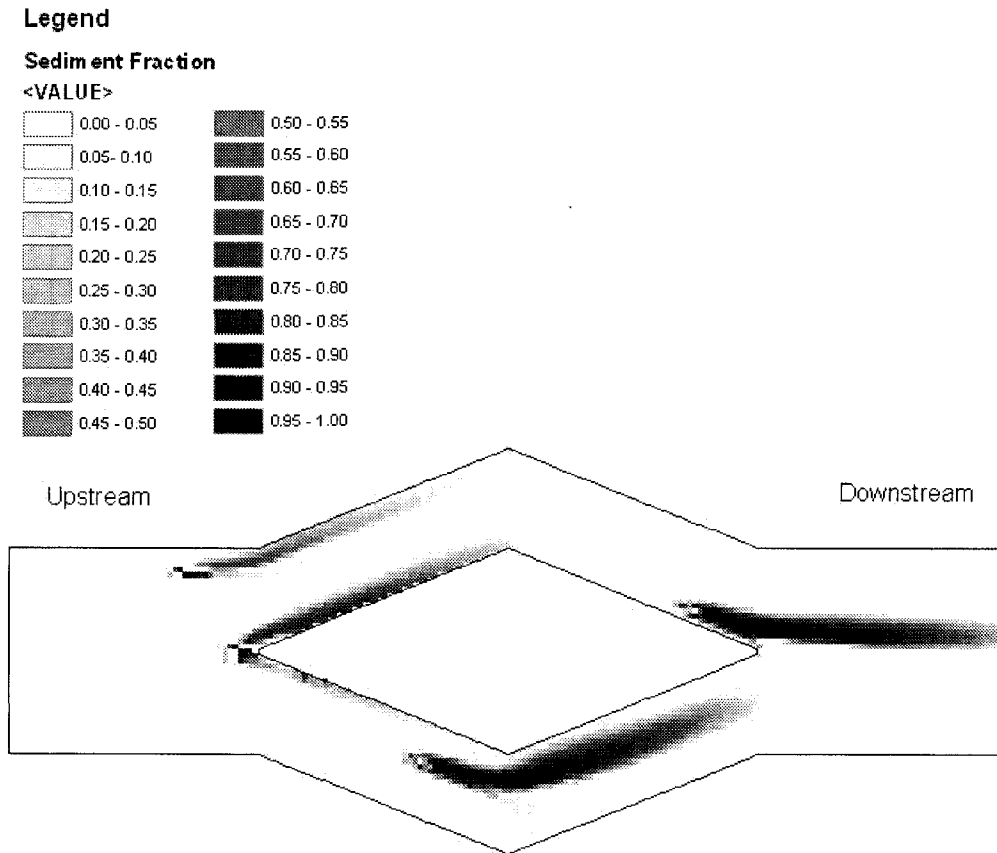
Figure 16: Mass fraction of sediments with grain size diameter of 0.05 mm for a channel with an island as output from the CH3D model.

The two methods produce similar results with respect to the kriging predictions and the kriging variances. There are two primary areas where differences occur. The first is around the head of the island. The standard method (Figure 17) shows a sediment plume stretching horizontally off the upper left side of the island. The method fails to extend the plume up to the head of the island where the source actually occurs. The method also fails to show the sediment plume on the opposite side of the island. The standard method does an acceptable job of capturing the elongated plumes that curve around the corners of the channel simply because of the sampling density. The elongated plumes are created by several small horizontal plumes that blend together. The flowline kriging method (Figure 18) captures the sediment plume on both sides of the island and elongates the plumes up to the head of the island where the source occurs. The flowline method does an equally good job of capturing the other plumes.

44

The other area that differentiates the two methods is just offshore at the bottom of the island. With the flowline kriging method, an area with a larger-than-actual proportion of sediment is predicted. The flowline kriging method produced quite a few values that were either less that 0 or greater than 1. Since it is not possible to have less than a 0% mass fraction or greater than a 100% mass fraction, the values that exceeded these bound were reclassified to the limits of 0% or 100%. This overestimation beyond 100% is the cause of the large area off the bottom of the island with the larger than actual proportion of sediment. The effect of this is also observed in the map of kriging variances for the flowline method (Figure 20) and in the graphs of correlation vs. number of samples (Figure 21) and RMS vs. number of samples (Figure 22). The map of kriging variances shows a large area of low variance (i.e. high predictability) that occurs in the same location as the overestimation. The graphs show less accuracy in the results for the flowline method simulation with 150 samples compared to the standard method because of this overestimation in some areas and the underestimation in other areas. The cause of this is likely a combination of factors. It is possible that the particular geometric arrangement of sediment sources and sample points makes it difficult to determine the variogram structure. It may also be that the flowline method is numerically more sensitive to the underlying assumptions of kriging, the specification of the variogram model and/or the number of samples used in the calculation. This could cause the greater variability in the prediction results. Since this effect was not as prominent for the simulations with other sample sizes, it is likely that a different random sampling and variogram model would produce different (and more likely better) results.

The simulations for 90 sample points also show better performance with the standard method over the flowline method. The cause of this is actually due to the existence of a large kriging artefact. The cause of kriging artefacts is discussed in Section 5.1. For the other 5 simulations with sample sizes 30, 50, 70, 110 and 130, the flowline method performed equally as well as, or better than, the standard kriging method.

45
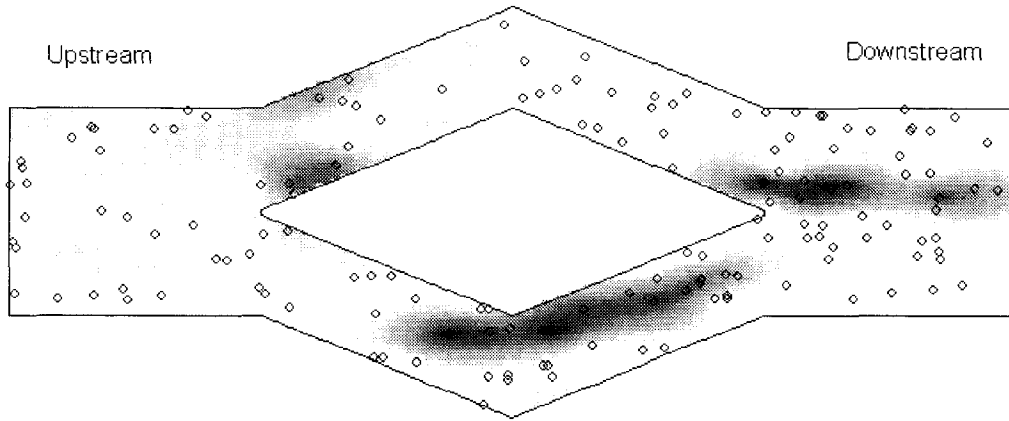
Figure 17: Predicted mass fractions of sediment with grain size diameter of 0.05 mm using standard kriging on 150 samples in a channel with an island (Same legend as Figure 16).
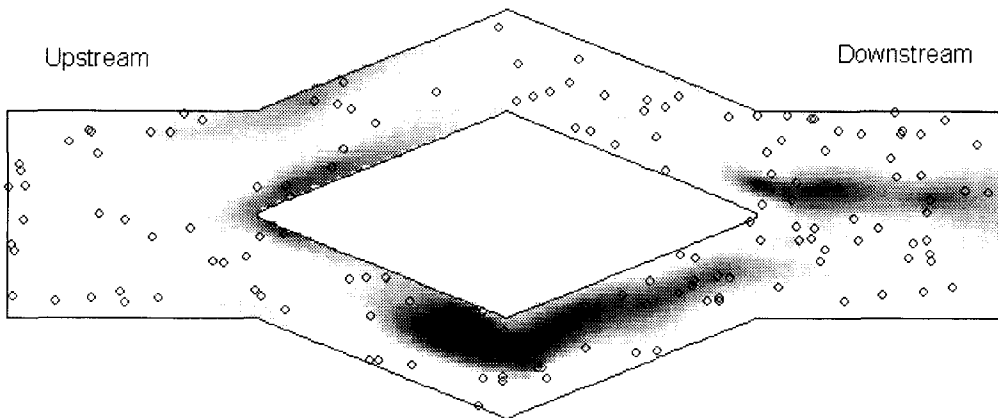
Figure 18: Predicted mass fractions of sediment with grain size diameter of 0.05 mm using flowline kriging on 150 samples in a channel with an island (Same legend as Figure 16).

46

Legend

Kriging Variance
Value

High: 0.061568

Low: 0.000289

Upstream   Downstream
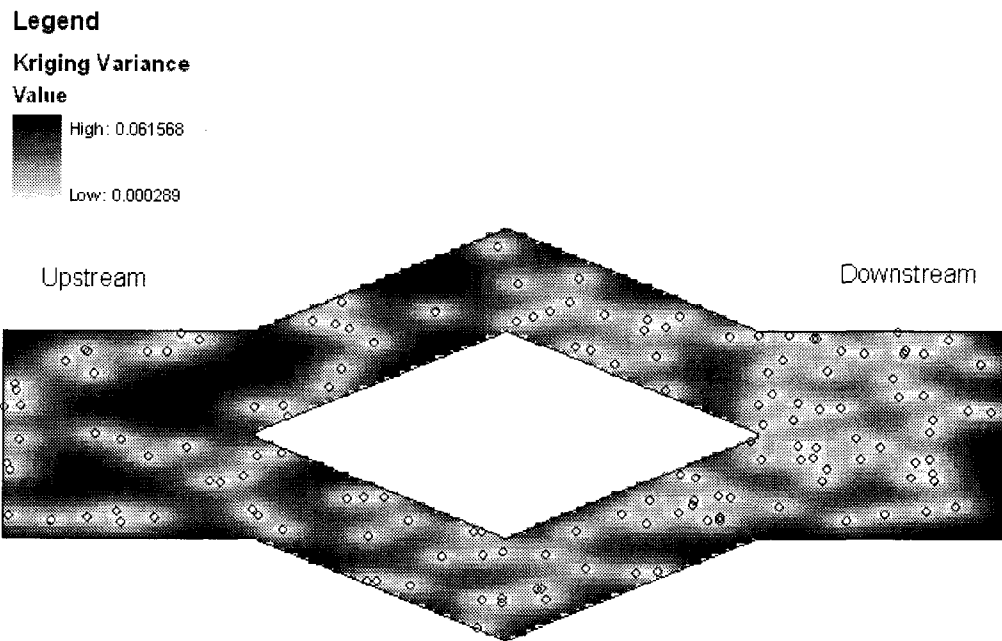
Figure 19: Kriging variances for sediment with grain size diameter of 0.05 mm using standard kriging on 150 samples in a channel with an island.

Legend

Kriging Variance
Value

High: 0.069883

Low: -0.083553

Upstream   Downstream
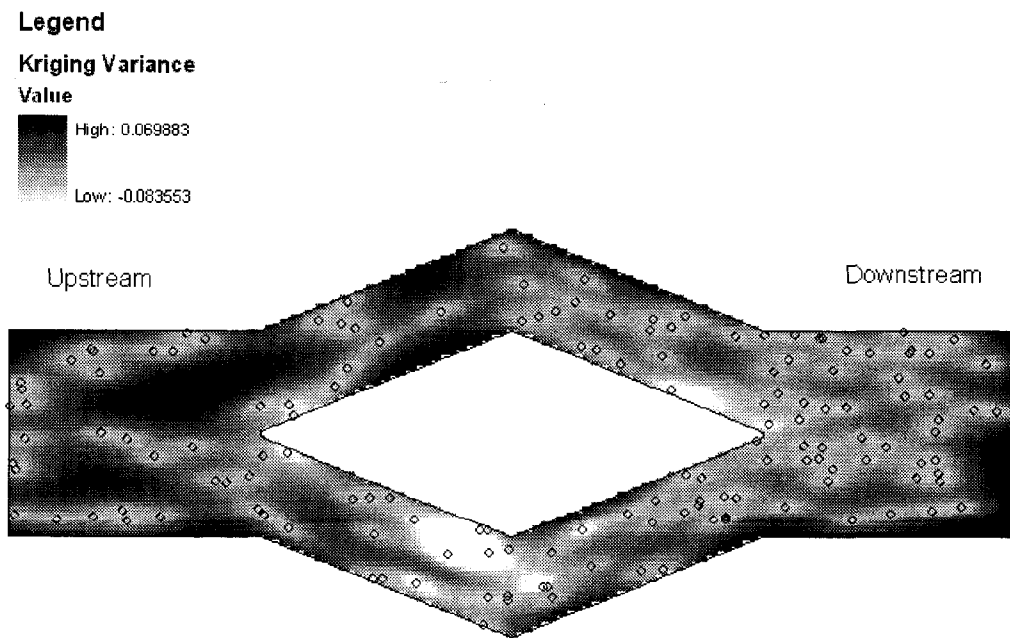
Figure 20: Kriging variances for sediment with grain size diameter of 0.05 mm using flowline kriging on 150 samples in a channel with an island.

47
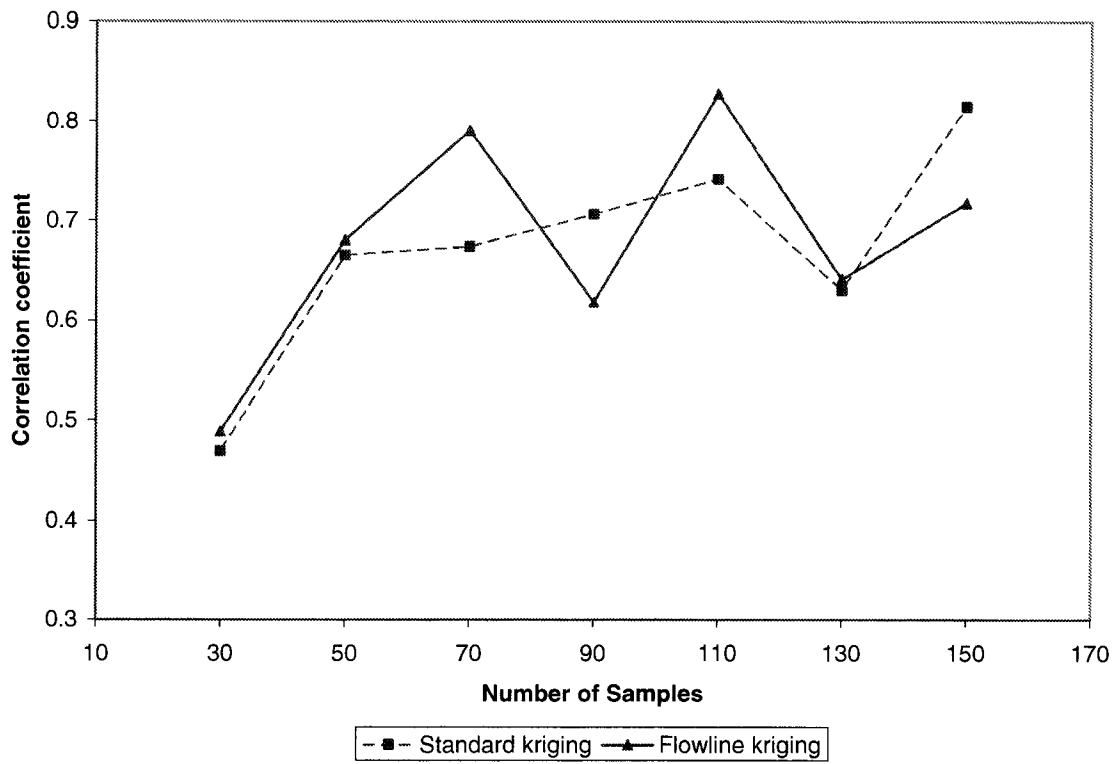
Figure 21: Graph of correlation vs. number of samples for a channel with an island.
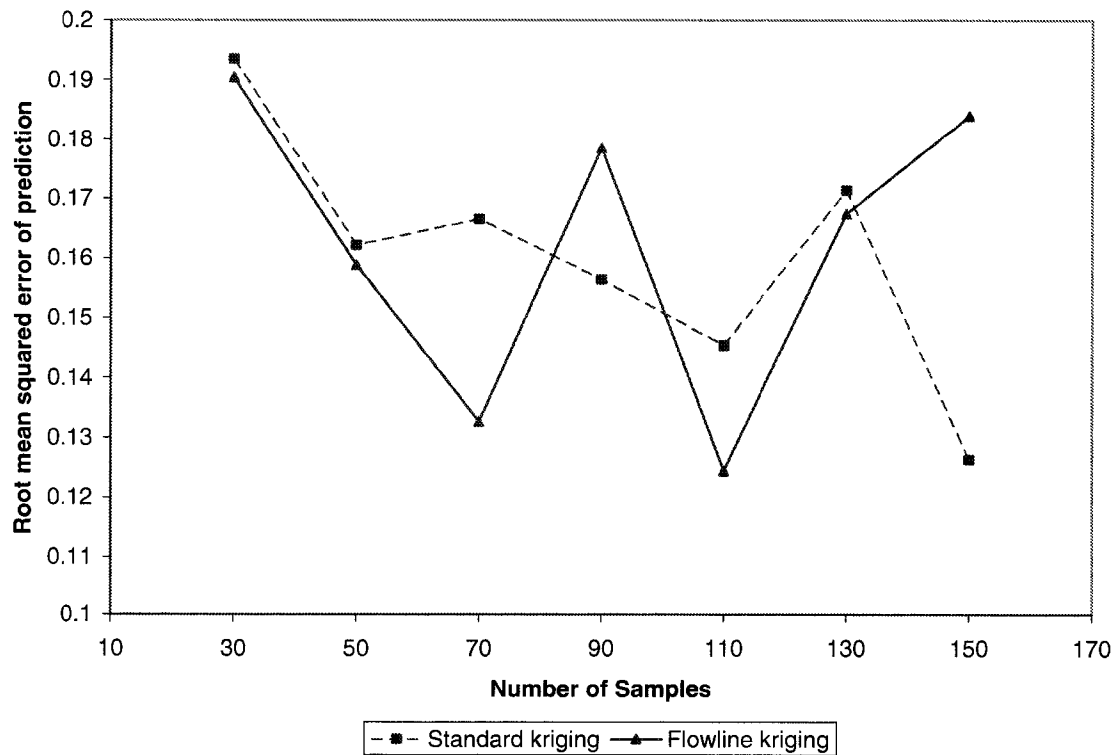
Figure 22: Graph of RMS vs. number of samples for a channel with an island.

48

3.2.4 Diverging Channel

As mentioned in Section 2.4, a domain transformation will likely distort the shape of the anisotropy ellipse under converging and diverging conditions. Although the results are not being compared to a domain transformation, sections of channel with diverging and converging widths are very common and an algorithm that behaves well under those flow conditions is desirable.

Figure 23 shows the actual sediment distributions as produced by the hydrodynamic model. The flow of water is from right to left so an average anisotropy direction of 90 degrees was used. For the CH3D simulation the six sediment sources were randomly placed in the channel, however two of the six sediment sources failed to generate plumes. The four plumes that were generated were deemed sufficient so no further attempt was made to generate additional plumes. The CH3D input files, random samples and kriging equations used in this test case can be found in Appendix E.

The graphs of correlation vs. number of samples (Figure 28) and RMS vs. number of samples (Figure 29) show that for test cases up to and including 70 samples, the results for standard kriging and flowline kriging produce results with roughly the same numerical accuracy. However, for larger sample sets, the standard kriging method continues to show small improvements in accuracy while the flowline method shows decreasing performance. The maps of kriging predictions for the simulations with 150 sample points (Figures 25 and 26) show some of the reasons why. It seems that in these simulations, like the island test case for 150 sample points, the flowline kriging method suffers from numerical sensitivity that causes prediction values less than 0% and greater than 100%. The effect is so pronounced that it actually causes the appearance of areas with large proportions of sediment where there actually is none, as seen in the bottom half of the channel in Figure 26. The plumes in the upper half of the channel cover roughly the same area for the standard and flowline kriging methods. However, the flowline method produces much larger values than actually exist.

49
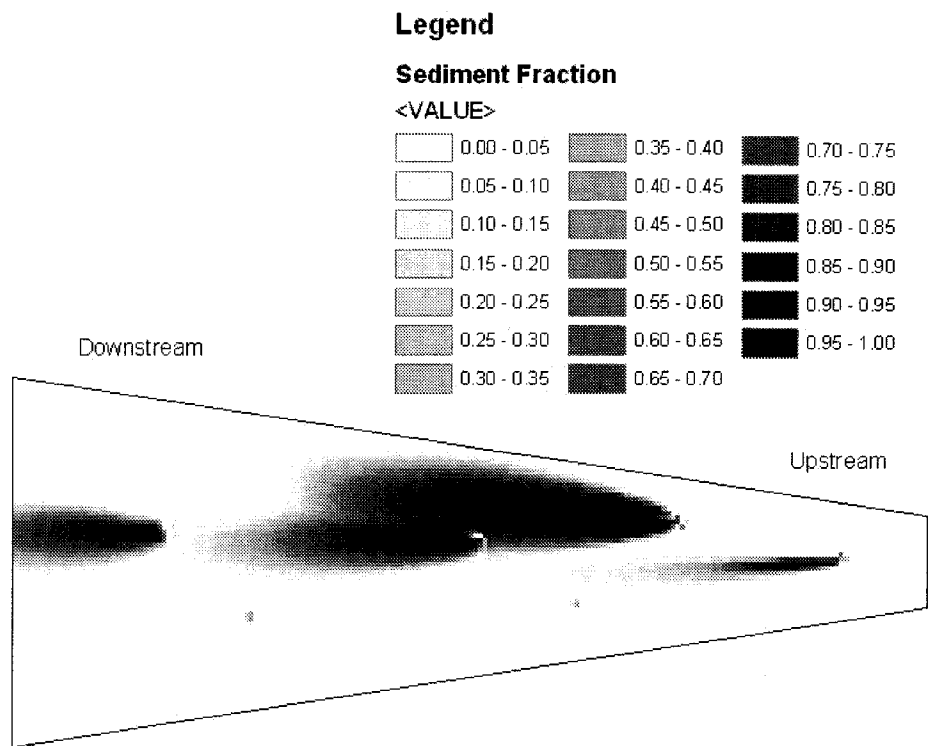
Figure 23: Mass fractions of sediment with grain size diameter of 0.01 mm for a diverging channel as output from the CH3D model.

50

Downstream

Upstream
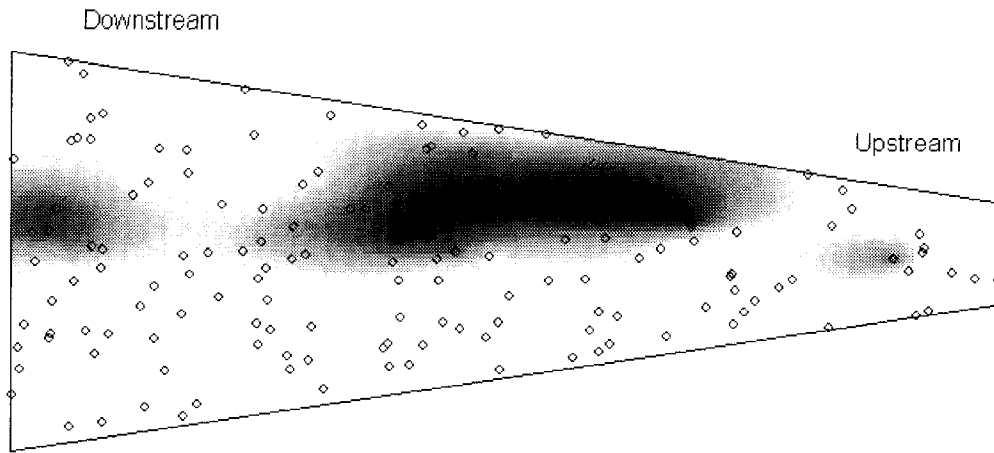
Figure 24: Predicted mass fractions of sediment with grain size diameter 0.01 mm using standard kriging on 150 samples in a diverging channel (Same legend as Figure 23).

Downstream

Upstream
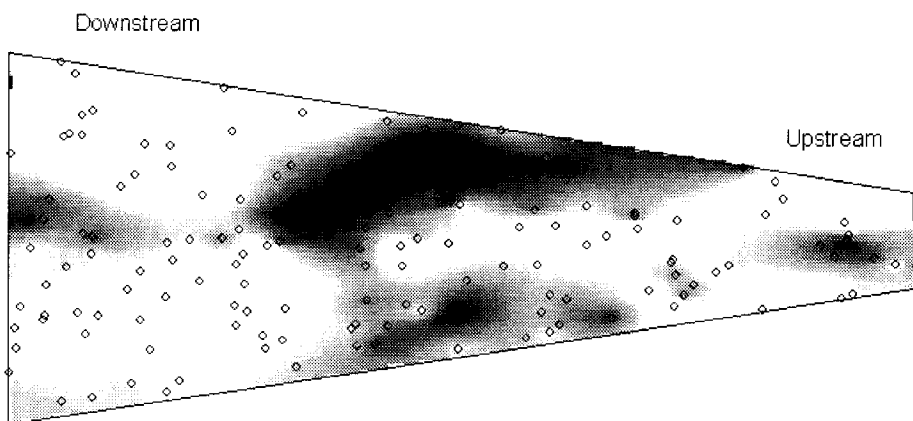
Figure 25: Predicted mass fractions of sediment with grain size diameter 0.01 mm using flowline kriging on 150 samples in a diverging channel (Same legend as Figure 23).

51

Downstream
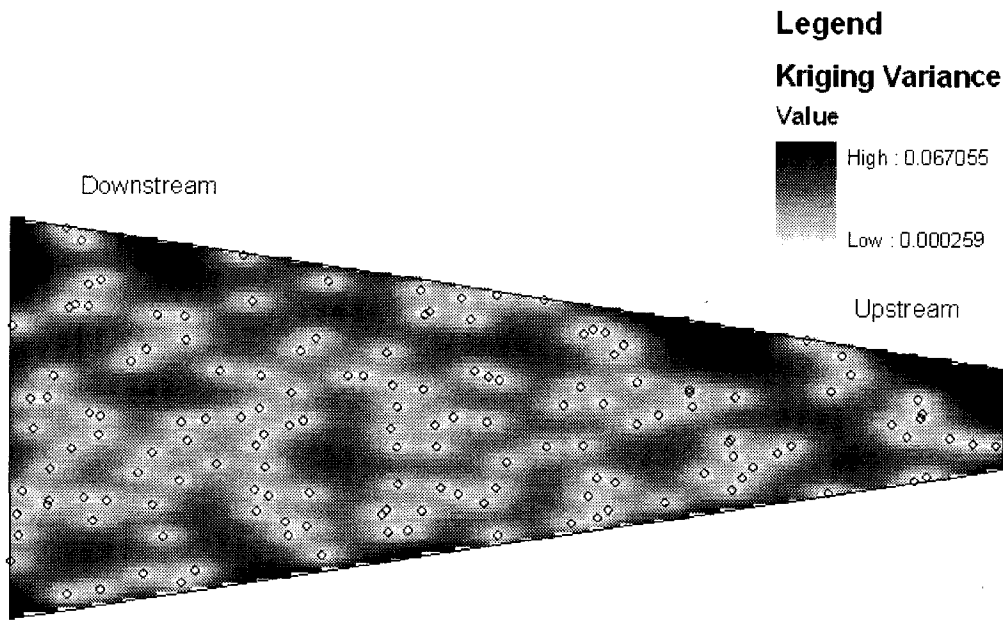
Figure 26: Kriging variances for sediment with grain size diameter of 0.01 mm using standard kriging on 150 samples in a diverging channel.

Downstream
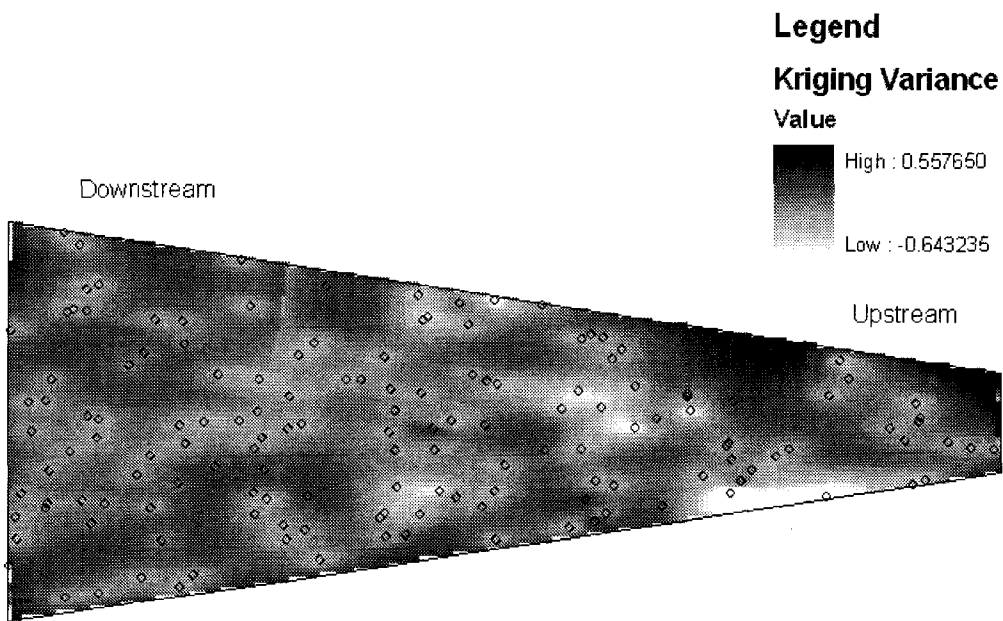
Figure 27: Kriging variances for sediment with grain size diameter of 0.01 mm using the flowline kriging method on 150 samples in a diverging channel.

52
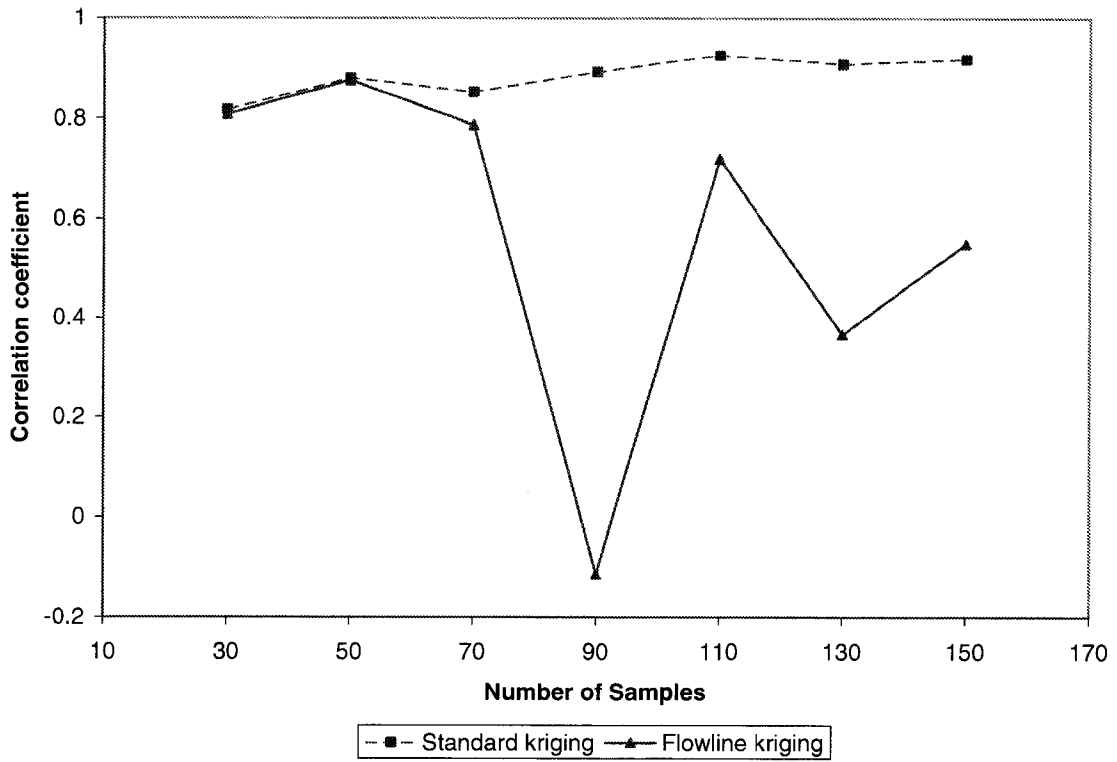
Figure 28: Graph of correlation vs. number of samples for a diverging channel.
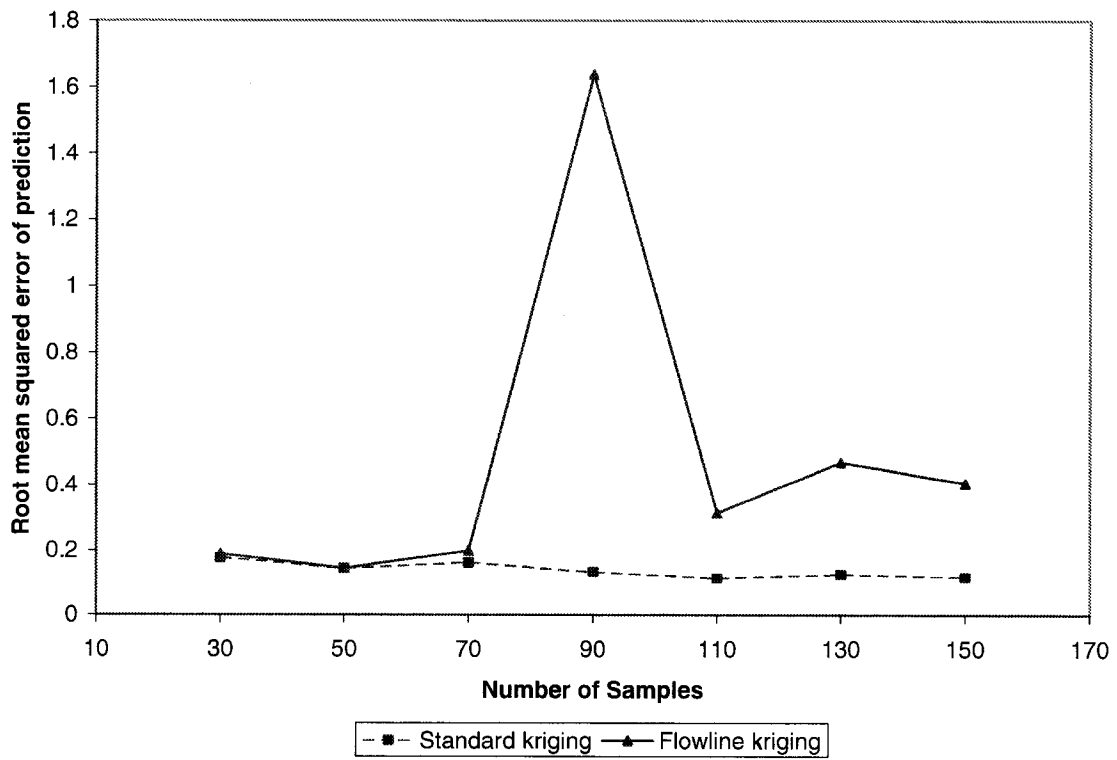
Figure 29: Graph of RMS vs. number of samples for a diverging channel.

53

The existence of prediction values greater than 100% and lower than 0% can occur with both the standard and flowline kriging methods. There is nothing in the kriging algorithm that specifies that percentages are being used and that therefore there are bounds on allowable values. This effect can be compensated for with better selection of a variogram model or by the application of various transformations on the data values. In order to objectively compare the standard and flowline kriging methods, only one attempt at fitting a variogram model was performed for each method so that 'selective tuning' would not bias the results. In practice, if these results were obtained, further attempts at variogram modelling and kriging would be conducted.

For the test cases with large numbers of samples, the flowline method also suffers from the existence of kriging artefacts. The existence of a large kriging artefact is part of the reason for the poor correlation and RMS observed in the flowline simulation with 90 sample points. A small kriging artefact can be seen in Figure 28 along the upper bank of the channel. Kriging artefacts are discussed in Section 5.1.

For the test cases with large numbers of samples, it appears that the flowline kriging method may also be suffering from poor specification of the variogram. It seems that the flowline method may be more sensitive to the underlying assumptions of kriging, the specification of the variogram model and/or the number of samples used in the calculation. If this is the case, it would explain why decreasing performance is observed with the increasing number of samples. Part of the problem for the flowline method in this test scenario may be the geometric arrangement of the sediment sources. Since the sources produce plumes that nearly all line-up and are clustered in the upper half of the channel, the variogram for the flowline method may be having difficulty describing the spatial structure. It is likely that, with a re-examination of the variogram model and some attempt to reduce kriging artefacts, results comparable to the standard kriging method could be obtained with the flowline method.

54

3.3   Assessment of the Results from Test Cases

The results of the above test cases suggest that the flowline kriging algorithm should perform well over a wide variety of channel geometries and sampling densities. Examining the spatial distributions from both a statistical and visual perspective seems to indicate that the flowline method should generally outperform standard kriging techniques in fluvial environments. Although the flowline kriging method seems to be more sensitive to the model inputs, especially for larger sample sets and certain geometries, it is likely that this can be dealt with by a closer examination of the data and the use of more advanced techniques for variogram model specification.

It should be noted that these test cases only examined sediment deposition from point sources. Non-point source deposition is likely to appear as a trend in the data. In most kriging applications, a trend would be removed prior to kriging the residuals and therefore there would be little point in examining the implications of the process on kriging. Another major process that affects sediment distributions in real rivers is erosion and the uncovering of historically deposited layers of sediment. In these situations, much of the spatial variability in the sediment distributions would be determined by that of the underlying layers. Test cases for erosion would be much more arbitrary than the cases tested in this study, since both a random bed surface and underlying historical sediment distributions would need to be generated. Rather than pursuing further simplified test cases through simulation, it was decided to test the method on a complex real-world test case.

4.0   Case Study: Sediment Distributions in the Detroit River

For large study areas, the amount of money required to adequately sample the area can be prohibitive. There may also be instances when the researchers have to work with data sets that were not collected with the intention of performing geostatistical analysis. As a result, researchers sometimes have to make do with data that is either too sparse or poorly

55

distributed in the problem domain to allow the proper use of standard geostatistical methods in producing spatial distributions.

A surficial sediment sampling survey conducted for the Detroit River Modelling and Management Framework will be examined as a real test case. The Detroit River study area was very large and consequently the data can be considered quite sparse, despite the large scope, budget and resources dedicated to the project. The new flowline transformation approach was attempted to evaluate whether it could improve upon the standard geostatistical methods and produce a better spatial distribution map for sediments in the river.

4.1   Background on the Detroit River Project

The Detroit River Modelling and Management Framework began in 1999 as an initiative of the Detroit River Canadian Cleanup Committee. This committee was formed in 1998 to manage Canadian obligations arising from Canada-US Great Lakes Water Quality Agreement for the Detroit River Area of Concern. The project was different than most other studies that had been previously conducted on the river. Its objective was to gain an overall indication of ecosystem health. Many studies had previously been conducted in the Detroit River, but they had always focused on a particular problem area. Since much of the data on the Detroit River was either out-of-date or focused on particular problem areas, the committee decided to conduct a completely new comprehensive study. The Great Lakes Institute for Environmental Research (GLIER) at the University of Windsor was given the responsibility of conducting and managing the new study. To get an overall picture of ecosystem health, the study was comprised of many components including environmental assessment studies, bioaccumulation modelling and hydraulic modelling of the river. In addition to the surficial sediment sampling survey data analyzed in this thesis, there were many other data sets collected for the project and analyzed by other researchers. These included: acoustically surveyed river bathymetry, sonar sediment classification, water surface elevation data, acoustic doppler current

56

profiler (ADCP) velocity data, sediment core data, and a wide variety of biological sampling data. Some of the findings from this related research can be found in *Detroit River Modelling and Management Framework: Modelling Report and Manual.* (GLIER, 2002)

4.2   The Detroit River

The Detroit River forms part of the international border between Wayne County, State of Michigan, USA and Essex County, Province of Ontario, Canada. The two largest communities on the river are Detroit, Michigan and Windsor, Ontario. The river is approximately 51 km long and varies in width from about 600 m to 3000 m. The depth of the river varies depending on location. In the deeper regions of the river, particularly in the navigation channels, depths can reach about 15 m. In other areas, such as the wetlands at the mouths of the various tributaries, depths may only be a few centimetres. There are a total of twelve major islands in the river of which some are natural islands and some are man-made. The Detroit River is often referred to as a connecting channel because flow through the river is not driven by topography but rather by the small difference in lake surface water elevations between Lake St. Clair and Lake Erie. The change in water surface elevation over the entire length of the river averages approximately 1 m.

57
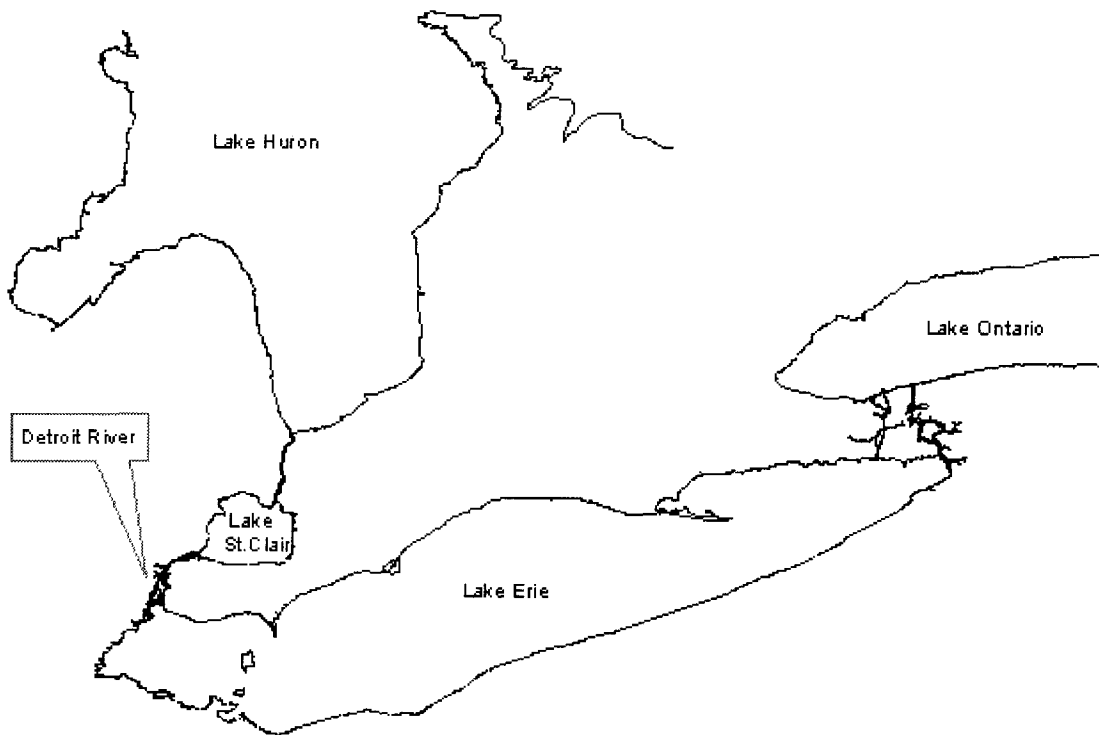
Figure 30: Location of the Detroit River.

Based on channel characteristics, the river can be considered to have 2 distinct reaches (OMOE, 1991). The upper reach runs from Lake St. Clair to the upstream tip of Fighting Island. This stretch is approximately 21 km long and varies in width from about 600 m to 1500 m and in centre line depth from about 9 m to 15 m. Over this length about 30% of the hydraulic head difference is dissipated. Peche Island and Belle Isle are the two islands in the upper reach and can be found a short distance downstream from Lake St. Clair. After the two islands, the river tends to form one well defined channel with a consistent cross section. Throughout much of this section, the river has an engineered shoreline since it flows through the downtown urban areas of Detroit and Windsor.

The lower reach runs from the upstream tip of Fighting Island to the mouth of the river at Lake Erie. This stretch covers the remaining 30 km and varies in width from about 1500 m to 3000 m and in centre line depth from about 0.6 m to 9 m. Over this length the remaining 70% of the hydraulic head difference is dissipated and 70% of those losses actually occur between Fighting Island and Bois Blanc Island. In the lower reach of the

58

river, the remaining 10 islands divide the river into many channels. In order to facilitate navigation in this area 5 navigational channels have been dredged (OMOE, 1991).

The long-term average flow rate of the river is approximately 5300 m^3/s which varies from a monthly winter low of about 4400 m^3/s to a monthly summer high of about 5700 m^3/s. (Holtschlag and Koschik, 2001) Seasonal variations in flow range from about 800 to 1300 m^3/s. The flow in the river is considered well-mixed vertically but lateral mixing of the river water occurs only gradually along the length of the river, leading to deposition of sediments and contaminant in an along-shore pattern. The average linear velocity of the water ranges from about 0.3 m/s to 0.6 m/s and gives an average retention time of about 21 hours for the river. Local channel properties and weather conditions can produce velocities significantly different than the average. In fact, water depth and flows in the river are highly dependent on current lake levels and wind conditions. Reversals in flow direction have even been known to occur with high winds and elevated lake levels in Lake Erie (Derecki, 1990).

The tributaries and sewers that discharge into the Detroit River drain approximately 2100 km^2 of land (OMOE, 1991). Approximately 1580 km^2 of this watershed is on the U.S. side while only 520 km^2 is on the Canadian side. The major tributaries of the Detroit River on the US side include: the Rouge River, Ecorse River, Huntington Creek, Frank and Poet Drain, and Brownstown Creek. The major tributaries on the Canadian side include: the Little River, Turkey Creek and Canard River. Despite this large watershed, the majority of flow in the Detroit River is drainage water from the Upper Great Lakes.

The total inflow from the tributaries is approximately 35 m^3/s, which represents less than 1% of the river's total flow (OMOE, 1991). Groundwater contributions to the river flow are considered negligible (OMOE, 1991). Groundwater discharges from the Michigan side of the river have been estimated at between 1.5 and 3 m^3/s. Given the relative contributing watershed areas on the US and Canadian sides, it is reasonable to assume

59

that groundwater discharges from the Canadian side are also negligible compared to the total flow in the river.

The mean annual river temperature is about 10 °C with monthly average temperatures ranging from about 0.6 °C to 22.2 °C (OMOE, 1991). Heated wastewater discharges and relatively swift currents in the river tend to prevent ice build-up in the river except in shallow areas surrounding the islands. Ice build-up around the lower islands can occasionally cause ice jams and, with incoming ice from Lake St. Clair, cause ice jams through the entire river.

Water from the Detroit River is used in a variety of ways depending on the need of the surrounding communities and the various land uses along the river's banks. Water uses which tend to have the largest impact on water quality are water supply and sewerage. Water from the Detroit River is taken for both domestic and industrial use by Detroit, Windsor and numerous other communities and industries along the river. The river acts as receiving water for municipal wastewater, industrial wastewater, storm sewer discharge, combined sewer overflow discharge, and agricultural runoff. Other important uses of the river include navigation and recreational activities such as fishing, hunting, swimming and boating. The Detroit River also provides important fish and wildlife habitat.

Surficial sediments in the Detroit River have been influenced by numerous factors. Agricultural and urban runoff has contributed sediments characteristic of the surrounding soils, while the dredging of navigational channels has exposed the bedrock in other areas. The soils around the Detroit River are dominantly clays and silts on the US side and clays on the Canadian side. Sandy soils exist around the Rouge River and the Ojibway area of Windsor. The depth to bedrock under the city of Detroit varies from 15 to 61 m (OMOE, 1991).

Sediments in the main channels tend to be coarse material due to the relatively high velocities. The upper reach of the river has mostly consolidated clays lining the bed. The

60

lower reach is much more varied. Dredging has exposed the bedrock in some areas and glacial boulders and other coarse sediments can be found in the main channels. Fine grained silts and clays can also be found near the shoreline and around the many islands in the lower reach.

Toxic concentrations of various chemicals, as defined in the *Stage I Remedial Action Plan for Detroit River Area of Concern* (OMOE, 1991), are known to exist in Detroit River sediments. In general, contaminant concentrations are higher on the Michigan side of the river than on the Ontario side or in the middle of the river. The area that appears to have the most contamination overall is the shoreline extending from the Rouge River, south through the Trenton Channel.

4.3   Surficial Sediments Data

A vast amount of data was collected and analyzed for the Detroit River Modelling and Management Framework project. Of primary interest to this thesis is the surficial sediment sampling survey conducted in 1999. In total, 150 locations were sampled over 21 days during May and June. The samples were analysed for: benthic community structure; grain size distribution, organic carbon, sulphur, nitrogen, 17 metals, 41 PCBs, 16 polycyclic aromatic hydrocarbons (PAHs) and at least 14 other organic compounds including some pesticides. The sampling was conducted with a Stainless Steel Ponar Dredge Sampler with a $0.05m^2$ horizontal cut. Field samples were taken in triplicate at 5 locations for quality control. All samples were analysed by GLIER staff at their laboratory which is accredited by the Canadian Association of Environmental Analytical Laboratories (CAEAL) and quality-assured by the Standards Council of Canada (SCC).

The sampling locations were stratified so that 30 stations were selected from each of the Upper and Middle Zones and 90 stations were chosen from the Lower Zone. Samples in each zone were equally divided between the American and Canadian sides. Then from within each zone and jurisdiction, sample locations were selected so that 2/3 of the

61

samples came from depths less than or equal to the median depth and the remaining 1/3 of the samples from depths greater than the median depth. When choosing sample locations from the stratified map of the river, locations were chosen at random, subject to the restriction that no two samples could be taken within 300 m. In an attempt to reduce spatial trending due to small scale temporal variability, sample locations were randomly assigned to sampling days.
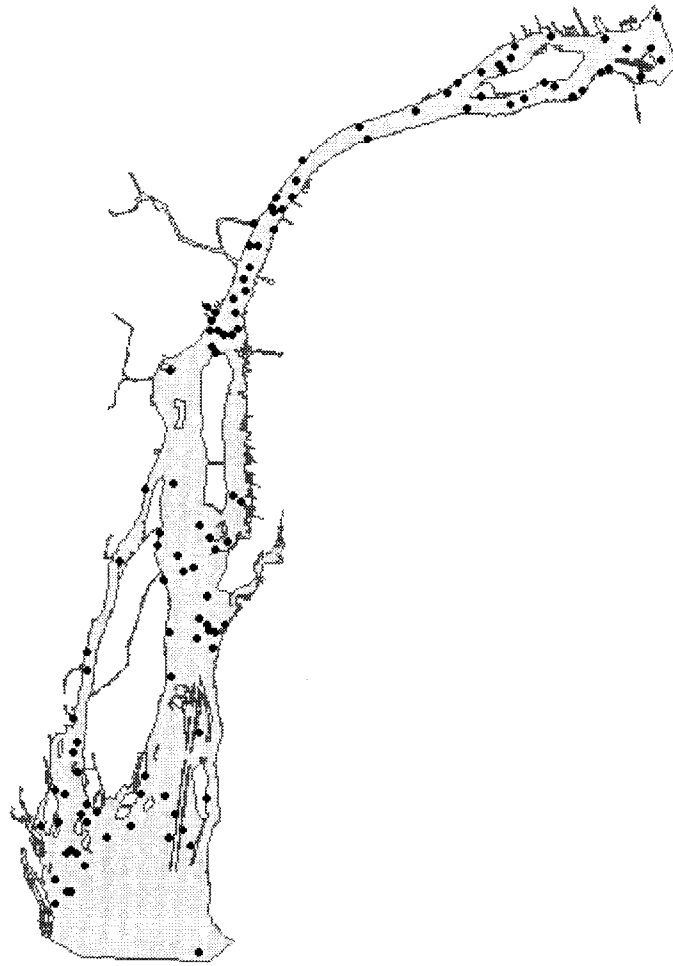
Figure 31: Point samples for the 1999 sampling survey.

62

4.4 Conventional Approaches on the Detroit River

In order to provide a point of comparison and to ensure that sample data from the Detroit River behaved as an anisotropic environment, a series of interpolations using standard techniques were performed. The property examined by the interpolation was the mass fraction of sediment with grain size diameter smaller than 0.075 mm. For the purposes of the Detroit River study, this was considered the fine-grained fraction. The interpolations were performed using ESRI's ArcGIS 8.1 software with the Geostatistical Analyst extension. Cross-validation results from ArcGIS are represented by the root mean squared error of prediction (RMS) and the average standard error of prediction (ASE).

When dealing with variograms, ArcGIS allows for the use of 11 different variogram models. Although all 11 models were examined for effectiveness, since the trends remained the same, only the results of two commonly used models, spherical and exponential are summarized below. The parameter optimization routines within Geostatistical Analyst were used to determine the best sets of the model parameters.

4.4.1 Statistical Results

If the Detroit River does behave as an anisotropic environment, there should be an improvement seen in the RMS and ASE as new techniques are applied that deal with the anisotropy. To start, Inverse Distance Weighting was attempted. Ordinary kriging was attempted, with and without anisotropy. In case a trend existed in the data, methods were applied to remove a first-order trend, a second-order trend and a third-order trend. Universal kriging was also attempted with a first-order trend, a second-order trend and a third-order trend. Finally, the river was broken up into three roughly straight sections of river. Refer to Figures 32-46 for the extents of the three areas. Universal kriging was applied to each section individually using a first-order trend and a second-order trend.

63

Table 1 summarizes the cross-validation results of interpolating the mass fraction of the fine-grained sediments (i.e. grain size diameter smaller than 0.075 mm) in the Detroit River using standard kriging techniques.

Table 1: Cross-validation Results of Standard Interpolations on the Detroit River

Section	Method	Trend	Model	Isotropy		Anisotropy	
				RMS	ASE	RMS	ASE
All	IDW	None	P=1.1255	16.85	NA	NC	NA
All	Ordinary	None	Spherical	14.06	15.77	14.52	15.86
			Exponential	13.69	15.54	14.06	15.95
		First	Spherical	14.03	15.72	14.26	15.58
			Exponential	13.64	15.43	13.83	15.57
		Second	Spherical	13.49	15.05	13.41	14.99
			Exponential	13.64	15.35	13.65	15.31
		Third	Spherical	15.57	14.79	15.57	14.71
			Exponential	15.49	15.00	15.55	14.93
All	Universal	None	Spherical	14.06	15.77	14.52	15.86
			Exponential	14.10	15.79	14.64	15.92
		First	Spherical	13.47	14.91	13.48	14.86
			Exponential	13.42	15.14	13.51	15.08
		Second	Spherical	13.56	15.06	13.54	15.00
			Exponential	13.59	15.31	13.63	15.24
		Third	Spherical	15.34	11.89	15.36	11.82
			Exponential	15.38	11.84	15.28	11.93
Upper	Universal	None	Spherical	13.13	8.35	13.76	8.09
			Exponential	NC	NC	NC	NC
		First	Spherical	14.68	9.32	14.11	9.23
			Exponential	14.20	9.48	13.47	9.53
		Second	Spherical	12.97	8.73	12.60	8.46
			Exponential	13.07	9.03	12.65	8.56
Lower	Universal	None	Spherical	15.64	16.48	15.99	16.40
			Exponential	14.86	15.92	15.15	16.21
		First	Spherical	15.65	12.30	15.74	11.83
			Exponential	15.51	12.14	15.51	12.14
		Second	Spherical	17.98	14.80	18.53	14.67
			Exponential	17.94	15.25	18.27	15.13
Middle	Universal	None	Spherical	10.66	17.61	10.87	15.56
			Exponential	10.59	17.64	10.75	15.04
		First	Spherical	11.41	16.77	11.68	15.43
			Exponential	11.41	16.77	11.54	15.52
		Second	Spherical	18.12	16.28	20.13	14.91
			Exponential	18.11	16.38	19.84	14.71

4.4.2 Assessment of the Statistical Results

When looking at the cross-validation results for the entire river using ordinary kriging and the spherical model on the fine-grained fraction, the RMS improved from 14.06 to 13.49 by incorporating a second order trend in the data. This could be explained by the shape of the river. There is likely a linear trend in the sediment mass fraction in the downstream direction. However, since the river is curved, the linear trend appears as a second-order trend. When universal kriging is applied, modelling a first-order trend (RMS = 13.47) appears to produce a very slight improvement over a second-order trend (RMS = 13.56). There appears to be no substantial improvement in using universal kriging over ordinary kriging when considering the entire river. Modelling anisotropy using ordinary kriging produces a RMS value of 13.41, only 0.08 better than no anisotropy. Modelling anisotropy using universal kriging produces a RMS value of 13.48, only 0.01 worse than no anisotropy. There appears to be no substantial improvement when modelling anisotropy over the entire river.

Breaking the river up into three relatively straight sections and applying universal kriging with a spherical model reveals that each section of the river has its own unique characteristics. The Upper reach produces a RMS of 13.13 and an ASE of 8.35 with no trend, a RMS of 12.97 and an ASE of 8.73 with a second-order trend and a RMS of 14.68 and an ASE of 9.32 with a first-order trend. Given the results of the cross-validation, it is likely safe to model the Upper reach of the river without any trend. When modelling anisotropy, a slight improvement is seen in modelling anisotropy with a second order trend (RMS = 12.60).

The Middle reach produces a RMS of 10.66 with no trend and increasing RMS values of 11.41 and 18.12 with first-order and second-order trends, respectively. Modelling anisotropy produces best results with no trend (RMS = 10.87), although this is still not a better RMS than observed for isotropic modelling. Given the results of the cross-validation, it is likely safe to model the Middle reach of the river as isotropic with no trend.

66

The Lower reach produces a RMS of 15.64 with no trend, 15.65 with a first-order trend and 17.98 with a second-order trend. When examining the ASE, modelling a first-order trend produces a value of 12.30 while modelling no trend produces a value of 16.48. Modelling anisotropy produces best results with a first-order trend (RMS = 15.74), although this is still not a better RMS than observed for isotropic modelling. It is likely best to model the Lower reach of the river as isotropic with a first-order trend.

In terms of prediction errors, it is obvious that different sections of the river are contributing different proportions of the overall error. The Upper reach has roughly the same RMS as the overall average, but substantially lower ASE. The Middle reach has lower RMS values than the overall analysis, but substantially larger ASE. The Lower reach also has higher RMS values to the overall analysis.

The results of these preliminary analyses provide some insight into what could be expected when applying the flowline kriging algorithm and how the problem should be approached. The different characteristics of the three sections indicate non-stationarity in the river data. Although modelling the entire river together appears to be a serious violation of the stationarity assumption, modelling each piece individually may be a less serious violation. Since there exist only slight trends in the data, it would be appropriate to use universal kriging or ordinary kriging with a neighbourhood. It would also appear that modelling anisotropy will provide little benefit for most of the river. However, it may be that the river is too complex to be properly modelled by the sparse sample data. The flowline method may be able to help in such situations by accounting for some of the flow complexities.

4.5   Flowline Transformation Approach on the Detroit River

In order to test the applicability and effectiveness of the flowline kriging method for real-world applications, kriging analysis was performed on the Detroit River using both

67

standard ordinary kriging and ordinary kriging using flowlines. The sediment samples used for the interpolations were collected as part of a 1999 sampling program and are described in Section 4.3. As with the simplified test cases described in Section 3.2, a velocity vector field was required to construct the flowline for each sample location. A velocity vector field for the Detroit River, obtained from Dr. Stan Reitsma, was created as part of the research for the *Detroit River Modelling and Management Framework: Modelling Report and Manual.* (GLIER, 2002) Otherwise, the algorithm and methods used were the same as those described for the simplified test cases and are described in Section 3.2 and Appendix A. The particular sediment property examined in this case study was also the bed sediment mass fraction of grain size diameter less than 0.075 mm.

As mentioned in Section 4.4.2, any attempt to model the entire river as a whole would be a serious violation of the assumption of stationarity. Instead, the three sections of the river were examined individually. Although the use of universal kriging would be a more appropriate method to use in the river because of the slight trend in the data, variogram modelling of data with a trend requires the use of more sophisticated techniques that have not yet been developed for the flowline method. As a result ordinary kriging was used in the analysis despite the lack of confidence in the assumption of stationarity. Since the assumption of stationarity is often violated in fluvial environments, this may help to reveal the overall effectiveness of the method in fluvial environments.

In the simple test cases, an average angle of anisotropy was assumed based on the known flow directions of the water. Since the Detroit River is a real test case and processes other than just the flow of water may be involved, the selection of an average anisotropy angle was determined using only the distribution of sample data (i.e. no subjective user input) and ArcGIS. Similarly, the lag distances used for variogram modelling were also chosen by ArcGIS for the standard kriging method and the same lags were used for the flowline method. Although to some extent this may bias the results towards the standard kriging method, it ensures that variability is being modelled over the same spatial scale. For these test cases, the problem domains were gridded into cells 20 m^2 upon which

68

predictions were made. The sample points and variogram equations used in the interpolations can be found in Appendix F.

4.5.1 Spatial Distribution

The Upper reach of the river (Figures 32-36) provides an excellent example of how the use of flowlines can improve the interpolation. It is clear to see from the figures how flowlines track sediment plumes through the river. Examining the south side of Belle Isle is quite revealing. On the south side of the island, at Site 25, a sample was collected with a very high proportion of fine grain sediments. Two other samples, at Sites 22 and 26, were collected further out from shore, upstream and downstream, each with significantly lower proportions of fine grain sediments. The standard method (Figure 33) created a plume of high concentrations between Sites 22 and 26. The plume was so large that it stretched all the way across the island and influenced points on the far side. The flowline method (Figure 34) predicts a much more plausible distribution. Since the anisotropy follows a flowline and flowlines do not cut across islands, Site 25 has very little effect on the far side of the island. The method also strings together Sites 22 and 26 into one plume and shows a patch with a high proportion of fine grained sediment hugging the shore of the island with a patch composed of a lower proportion of fine grained sediments bounding it offshore. Figures 35 and 36, which show the kriging variances, also show a more realistic pattern for the flowline method. Examining the southern end of the reach, two samples were taken near opposite shores. The deeper centre of the river runs between the two. The map of kriging variances using standard techniques (Figure 35) shows that the areas of good predictability stretch into the centre of the channel, while the flowline technique (Figure 36) shows the areas of good predictability hugging the shore and leaves the deeper centre of the river poorly predicted, which is much more likely.

In the Middle reach (Figures 37-41), there are less obvious deviations between the results. This stretch of channel has no islands and is very straight which means that an average anisotropy angle and the standard kriging techniques should produce very similar

69

results to the flowline method. Although the results are quite similar, there are some distinguishing characteristics. In the northern section of the channel, where the channel turns from the average anisotropy angle, the flowline method (Figure 39) shows an along-shore pattern of sediments that stretches all the way out of the reach while the standard method (Figure 38) does not. Also, the standard method shows a small sediment plume stretching out into the middle of the channel from Site 34 while the flowline method keeps the plume along the shoreline. With the high flow conditions that exist in the Middle reach, the along-shore pattern shown with the flowline method is a more likely scenario. Comparing the maps of kriging variances (Figures 40 and 41) shows similar behaviour. In addition, the flowline method (Figure 41) shows a more distinct pattern of variability that is more like the known behaviour of the river, especially near the southern end of the channel where the flowlines prepare to flow around Fighting Island just off the edge of the map.

The Lower reach (Figures 42-46) is an extremely complex region of the river. To aid in interpreting the resulting prediction maps (Figures 43 and 44), the mass fractions were reclassified into ranges of 5% for display, rather than using a continuous spectrum as seen in the previous figures. The prediction maps for the Lower reach provide a different picture than observed in the other test scenarios. In the previous studies the flowline method seemed to generate elongated plumes that followed the direction of flow while the standard method created much wider ones that did not follow the flow. In the Lower reach it is the Standard method (Figure 43) that creates elongated plumes in the direction of flow. The flowline method (Figure 44) produces wide, stunted plumes that appear more like bands across the channel or blobs rather than plumes. The boundary between display ranges is also much smoother for the standard method, while the flowline method produces patches with very rough edges. Other than the shape of the prediction regions, the flowline method also produces some regions of high and low fine grained fractions that do not appear in the standard method. These regions can be seen off the southwest corner of Fighting Island, the southwest corner of Grosse Ile and south of Crystal Bay. The maps of kriging variance (Figures 45 and 46) do not show any noticeable differences in pattern. However, the map of standard kriging variances (Figure 45) shows a much

70

wider range of values than the flowline variances (Figure 46). This is likely due to the larger proportion of nugget obtained in the flowline variogram equation. One notable difference is that the flowline method shows that the area off the northeast corner of Fighting Island has high variability, while the standard method shows that predictions in the area are not as variable relative to the rest of the values in the river. Given that there are no sample points in that area and that the area is sheltered by the islands, it is likely that the area is poorly predicted. The standard method shows a much larger area of low predictability in the southern end of the river than the flowline method does. Since there is a gap of nearly 5.5 km between sample points in that area, it is likely that the larger area of poor predictability shown by the standard method is more representative.

For the Lower reach of the river, the flowline method suffers from the existence of kriging artefacts. The reclassification applied to the prediction values has masked most of the effect. However, some of the kriging artefacts can still be observed in maps. The cause of kriging artefacts and the characteristics of flowlines needed to prevent them are discussed in Section 5.1. From visual inspection, there does not appear to be a good reason to recommend either kriging method over the other for the Lower reach. The following section, Section 4.5.2, will examine the results from a statistical viewpoint in an attempt to determine which method is more effective.

71
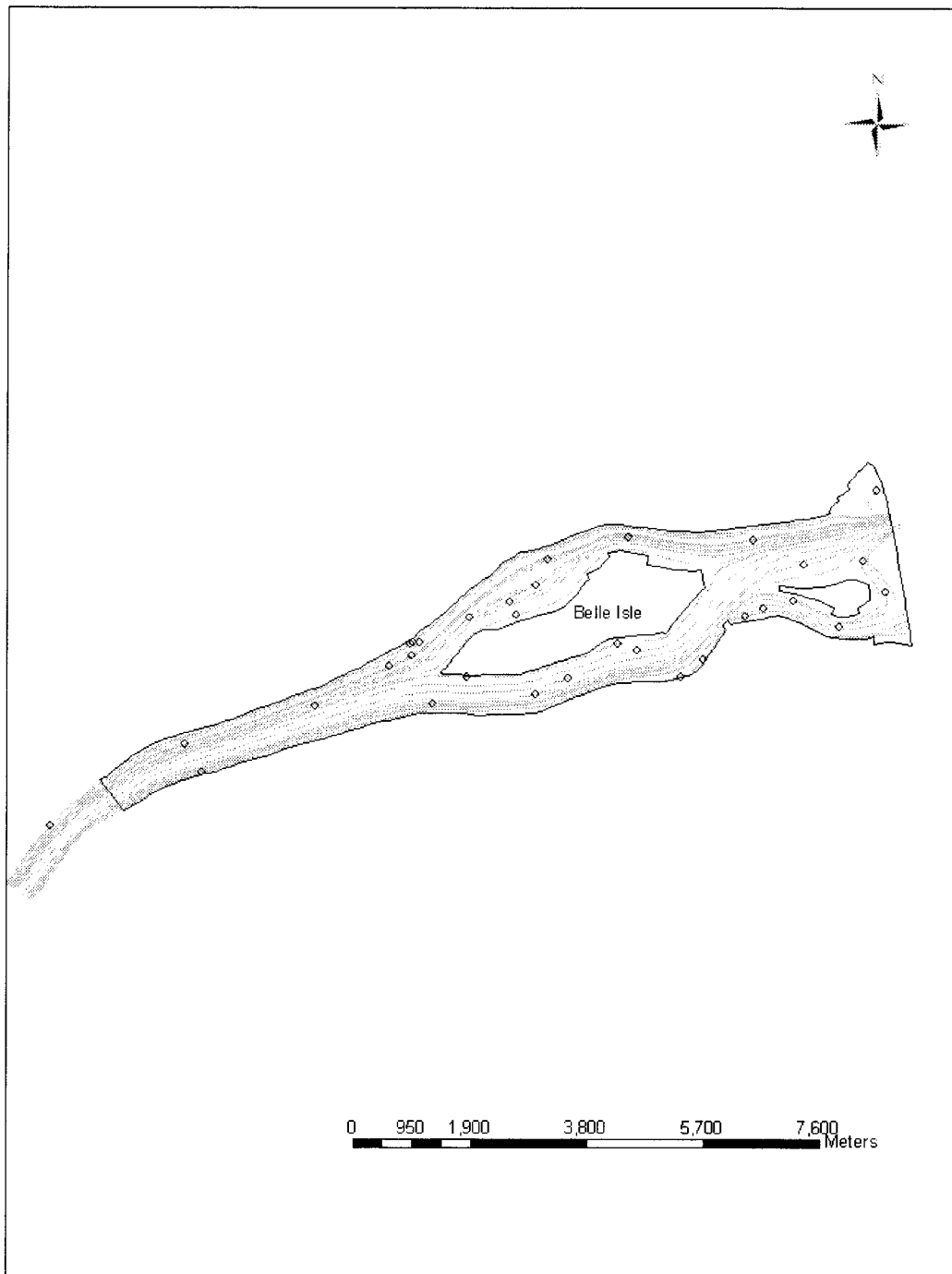
Figure 32: Flowlines used for interpolation of the Upper reach of the Detroit River.

72
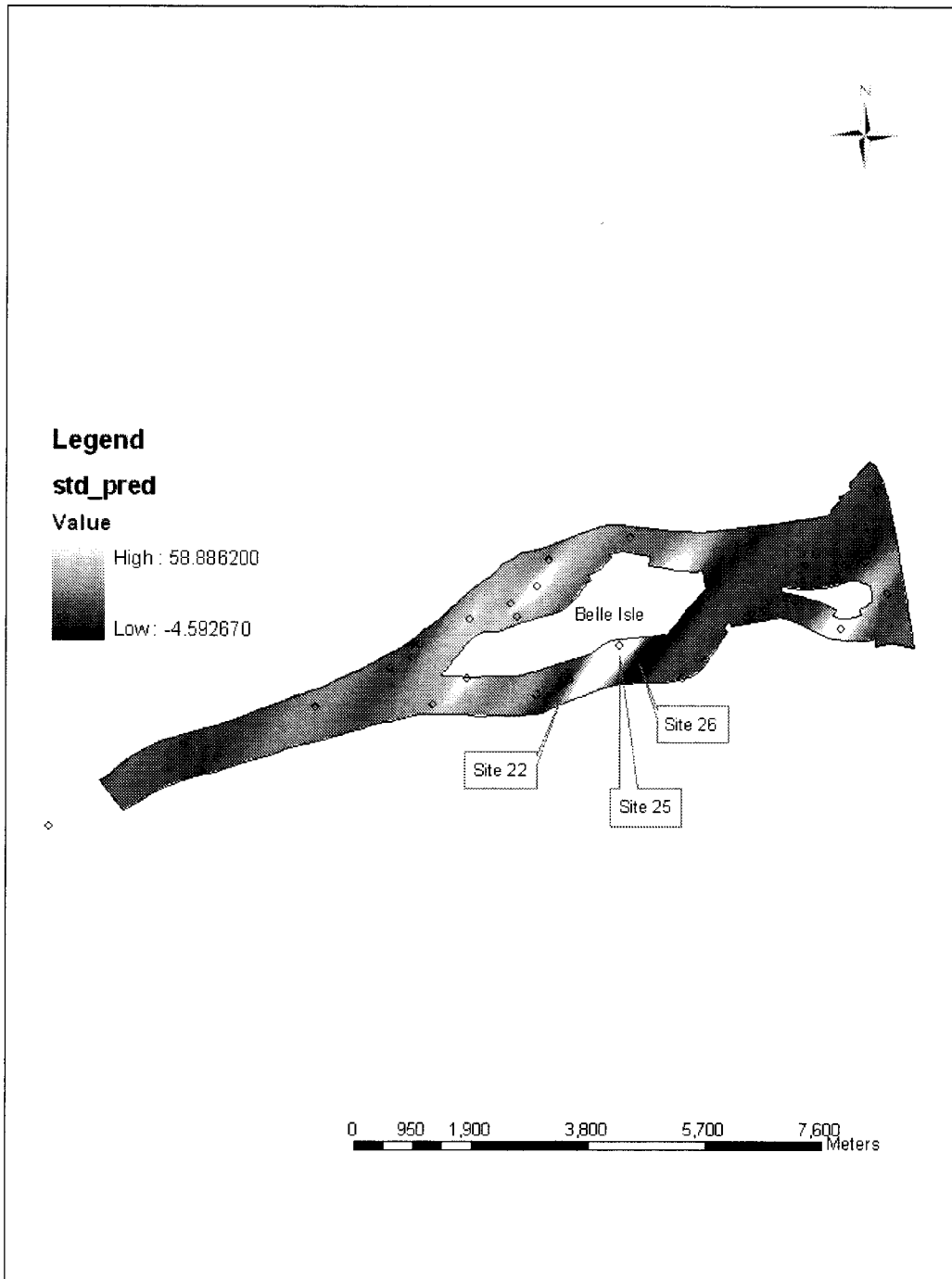
Figure 33: Predicted mass fraction of sediment with grain size diameter less than 0.075 mm for the Upper reach of the Detroit River using standard kriging.

73
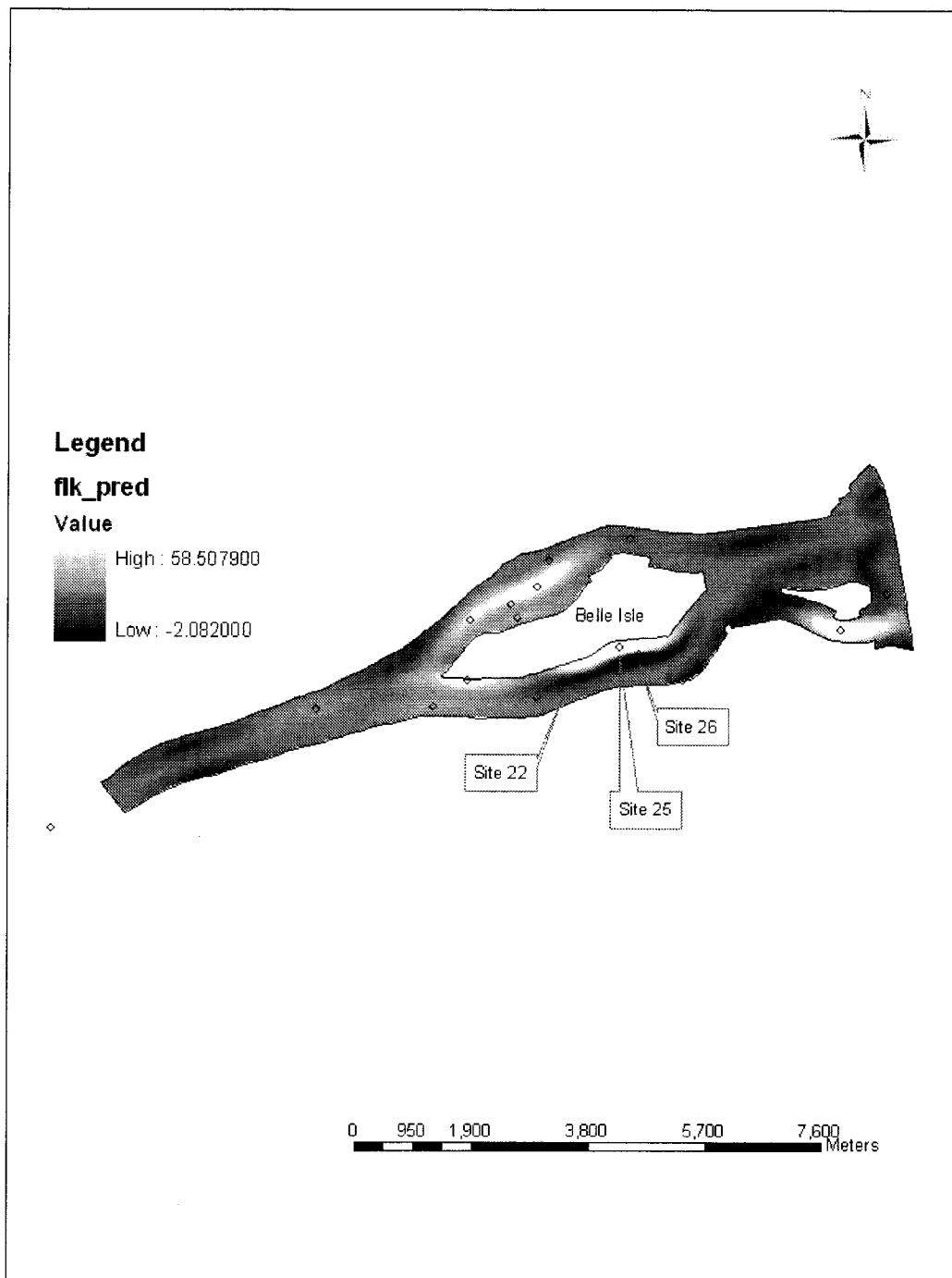
Figure 34: Predicted mass fraction of sediment with grain size diameter less than 0.075 mm for the Upper reach of the Detroit River using flowline kriging.

74
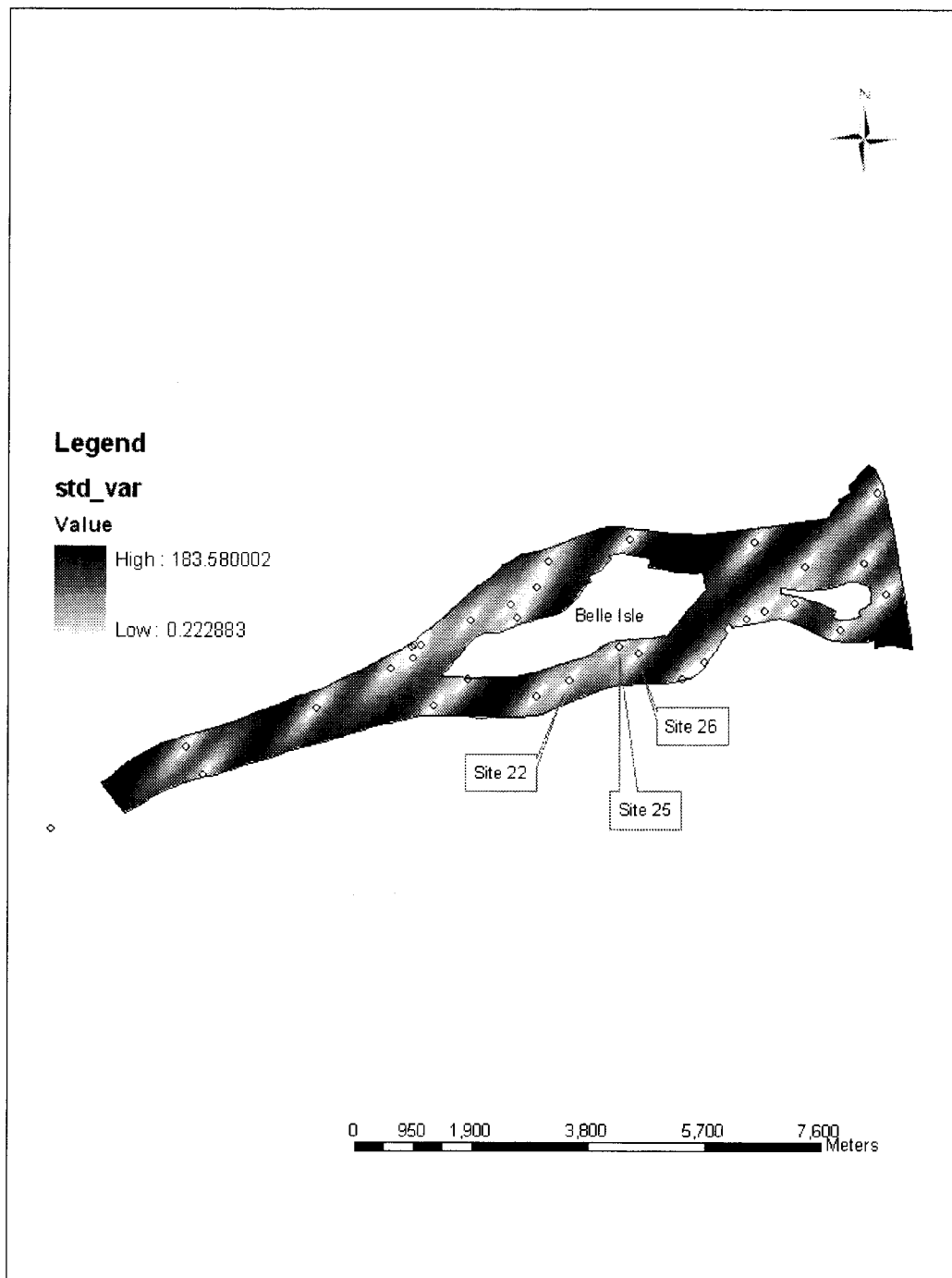
Figure 35: Kriging variances for sediment with grain size diameter less than 0.075 mm for the Upper reach of the Detroit River using standard kriging.

75
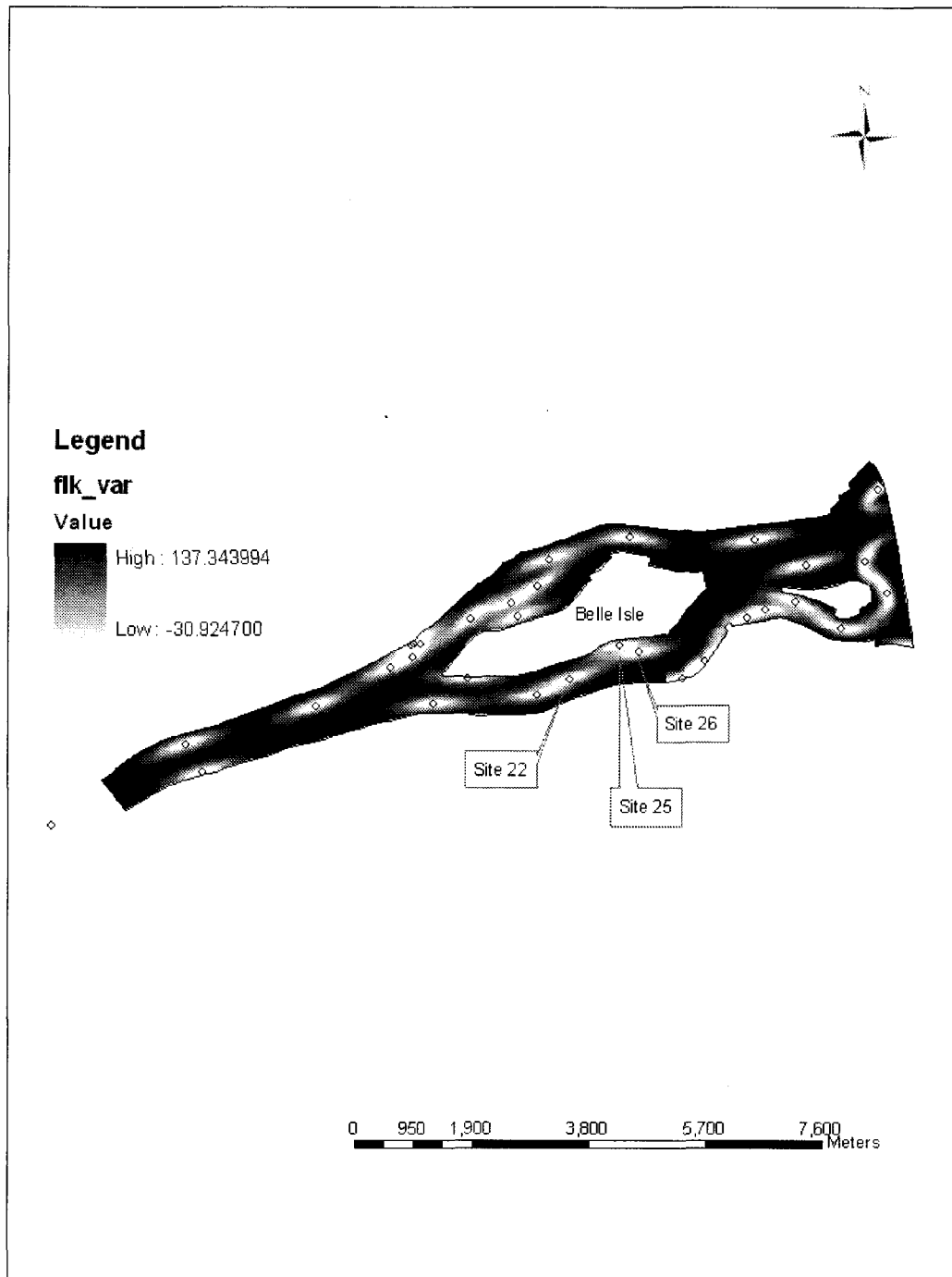
Figure 36: Kriging variances for sediment with grain size diameter less than 0.075 mm for the Upper reach of the Detroit River using flowline kriging.
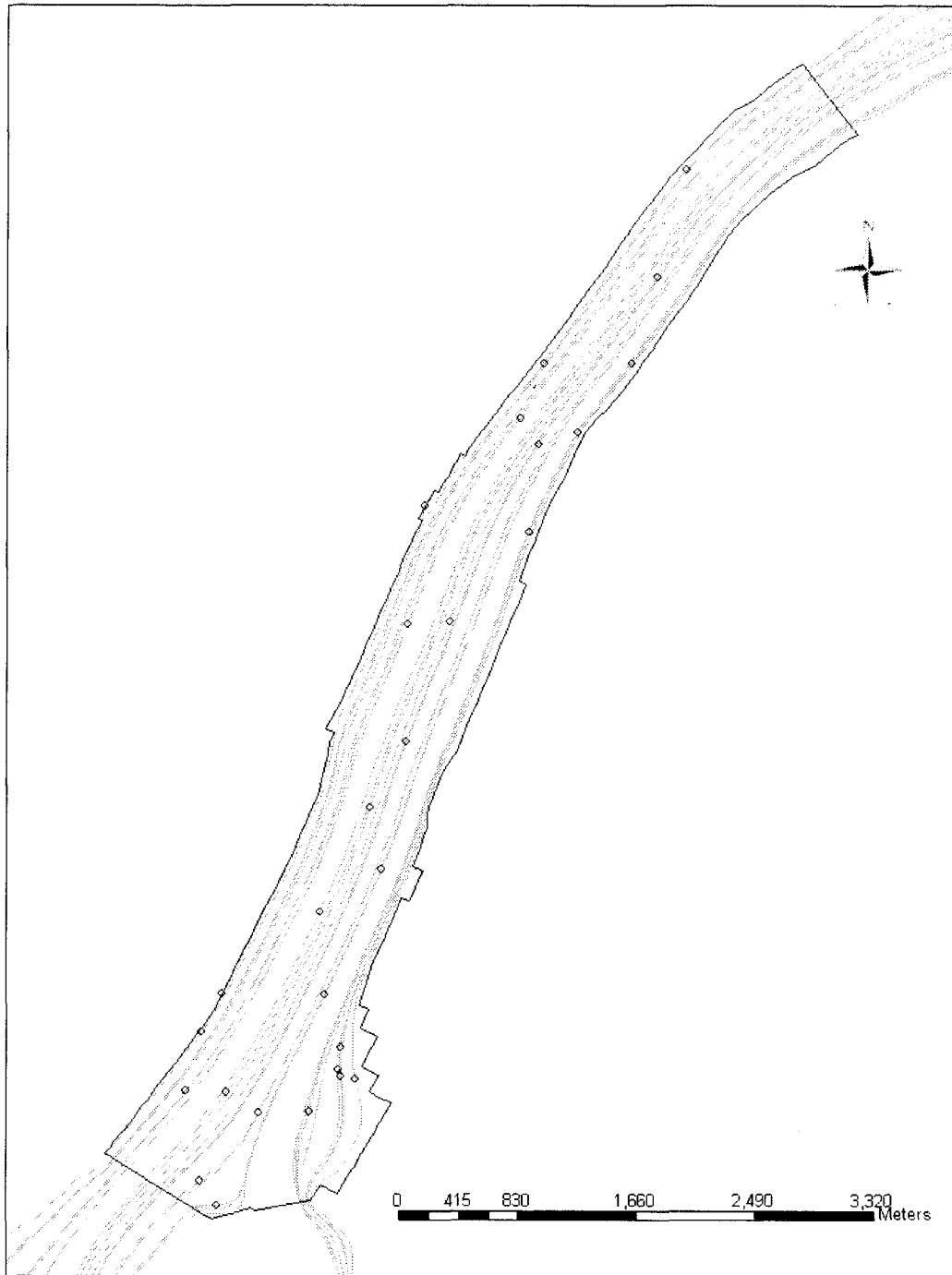
Figure 37: Flowlines used for interpolation of the Middle reach of the Detroit River.

77
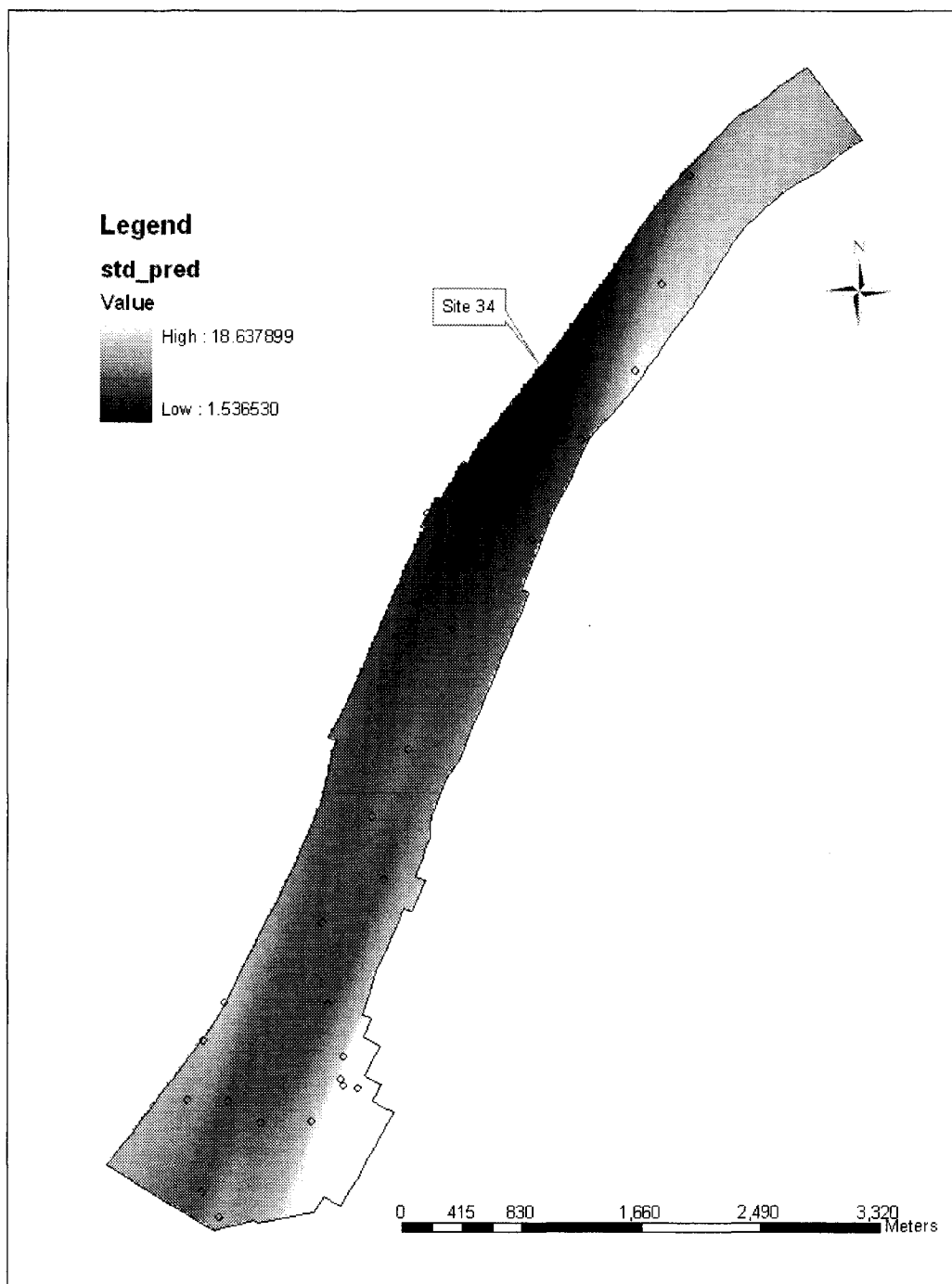
Figure 38: Predicted mass fraction of sediment with grain size diameter less than 0.075 mm for the Middle reach of the Detroit River using standard kriging.

78
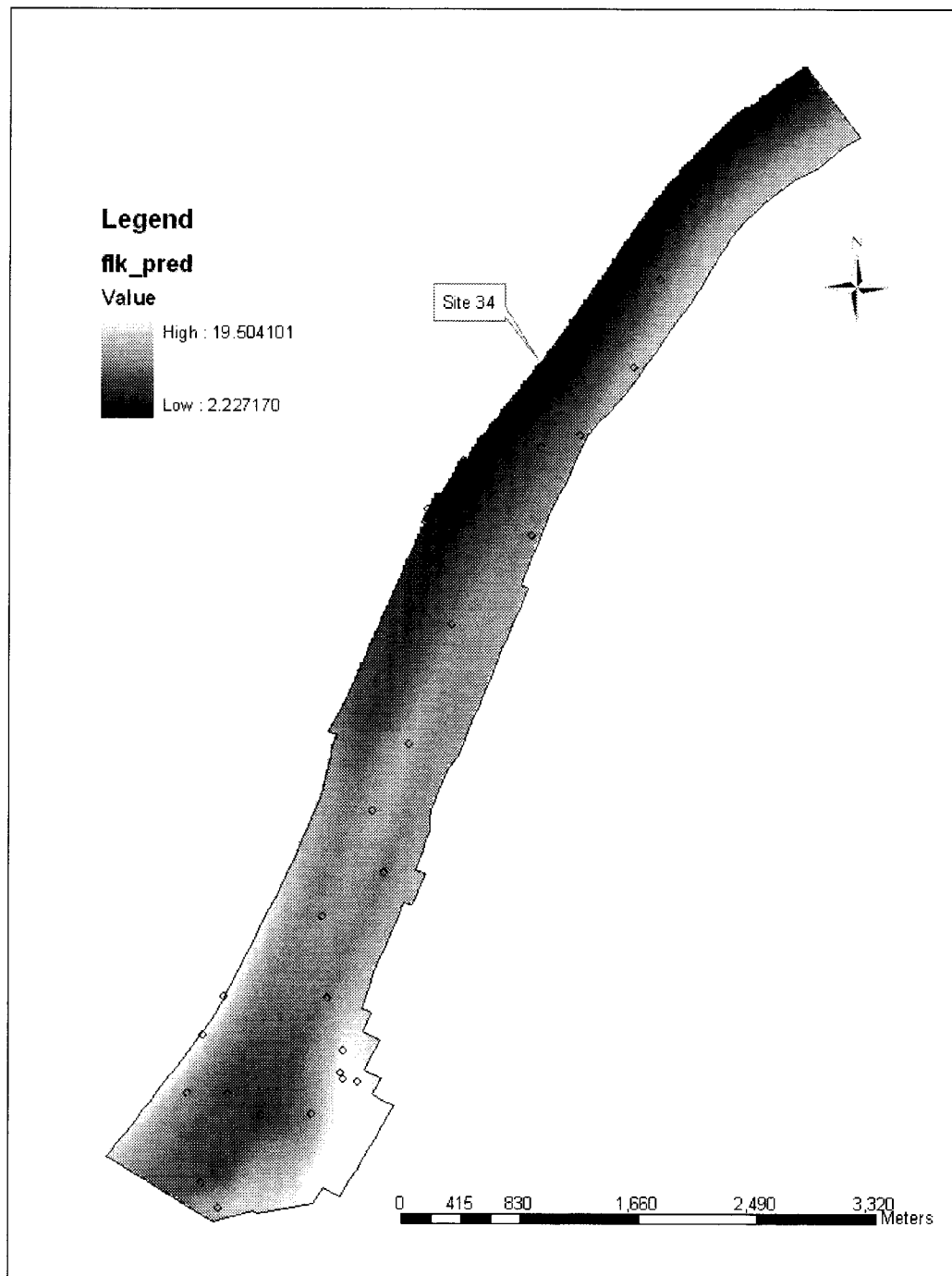
Figure 39: Predicted mass fraction of sediment with grain size diameter less than 0.075 mm for the Middle reach of the Detroit River using flowline kriging.

79
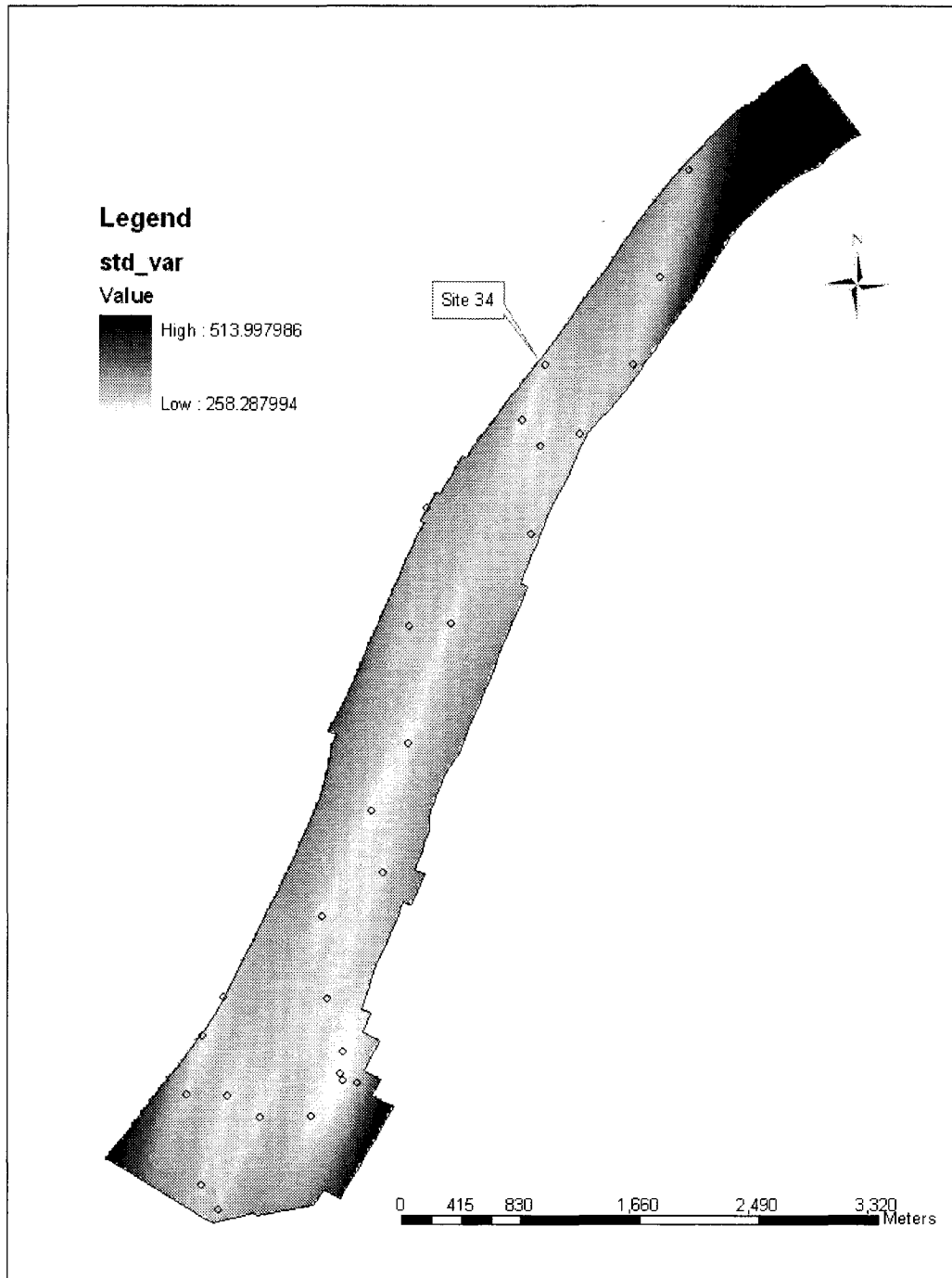
Figure 40: Kriging variances for sediment with grain size diameter less than 0.075 mm for the Middle reach of the Detroit River using standard kriging.

80
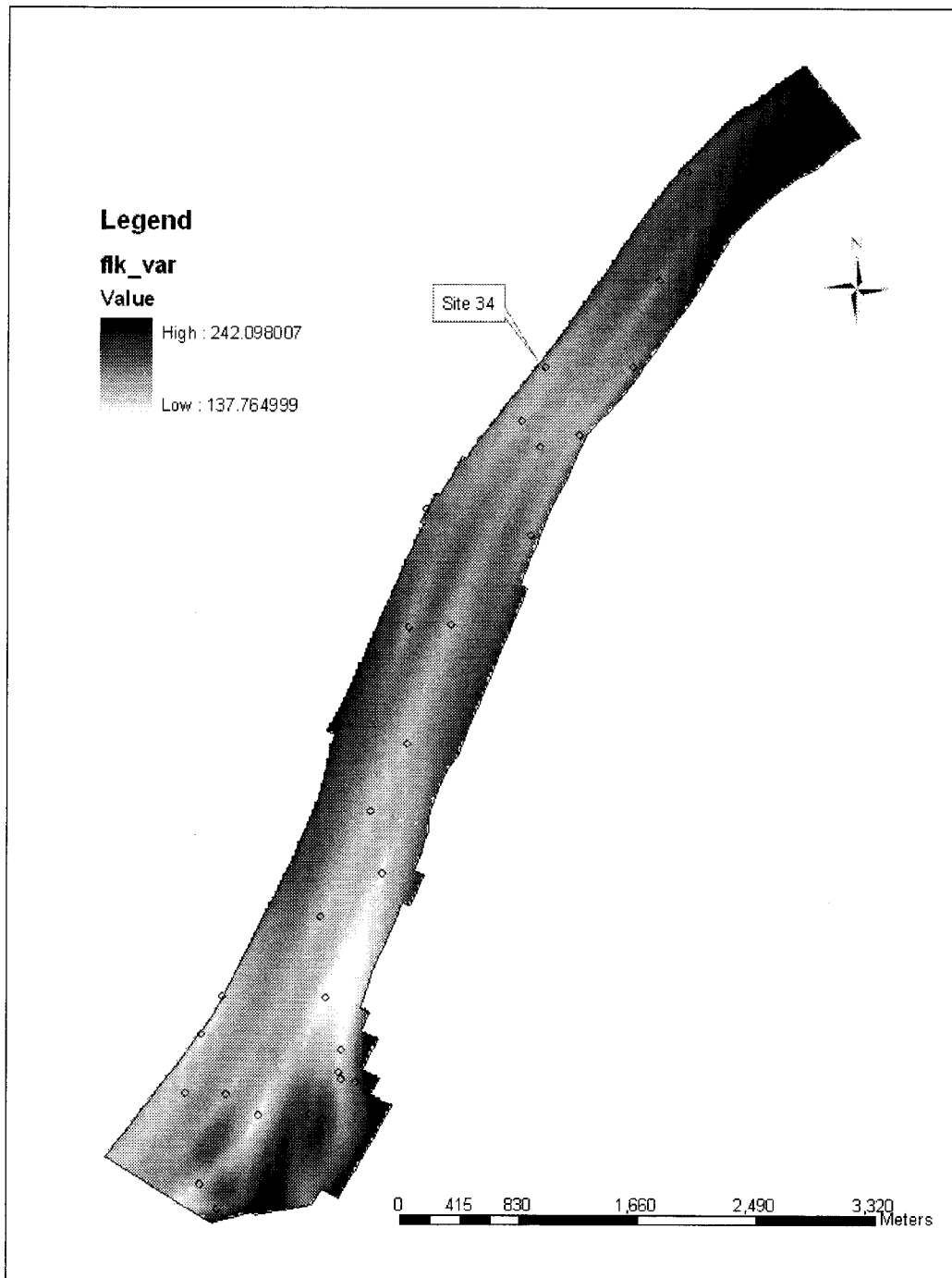
Figure 41: Kriging variances sediment with grain size diameter less than 0.075 mm for the Middle reach of the Detroit River using flowline kriging.

81
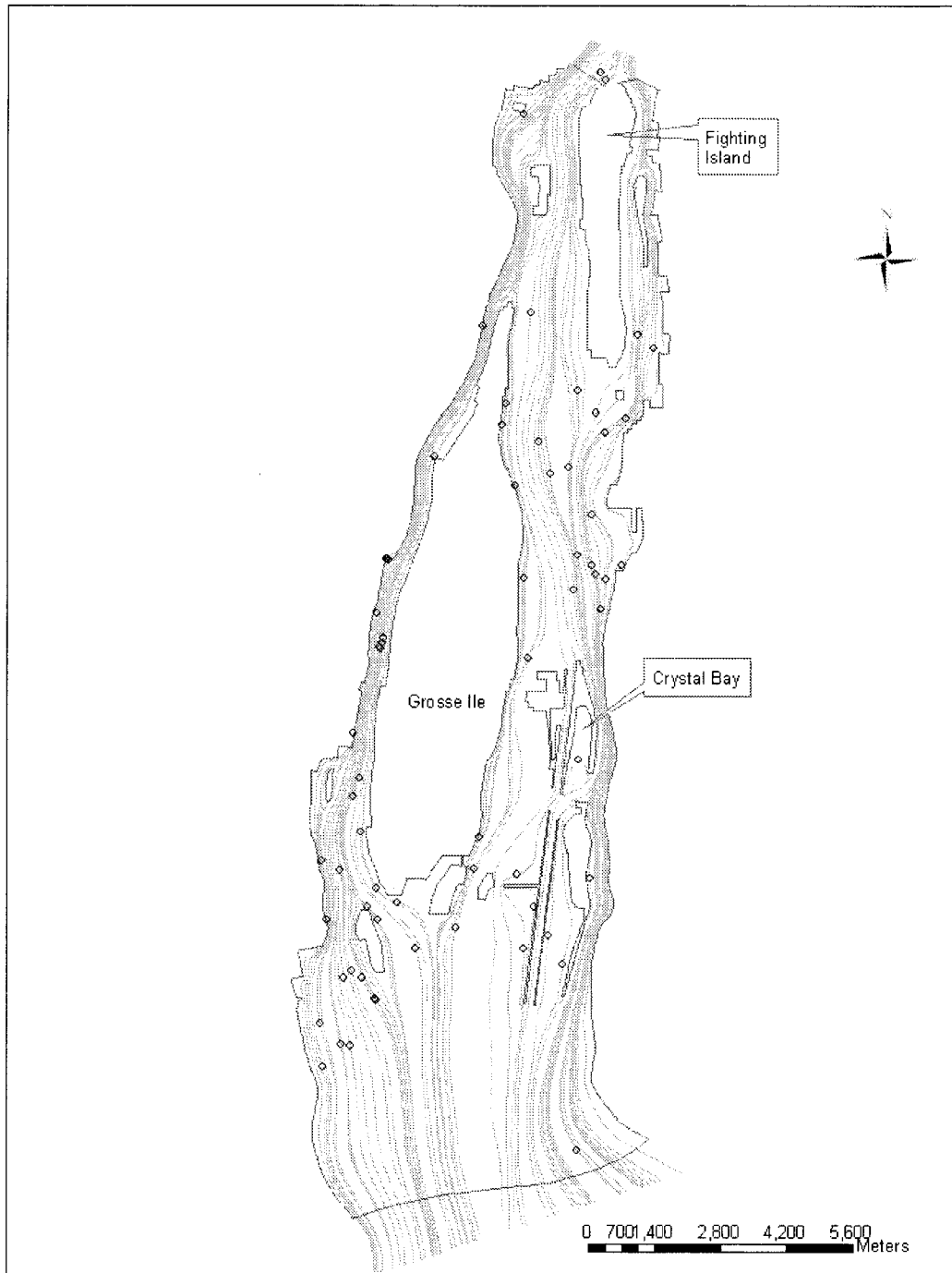
Figure 42: Flowlines used for interpolation of the Lower reach of the Detroit River.

82
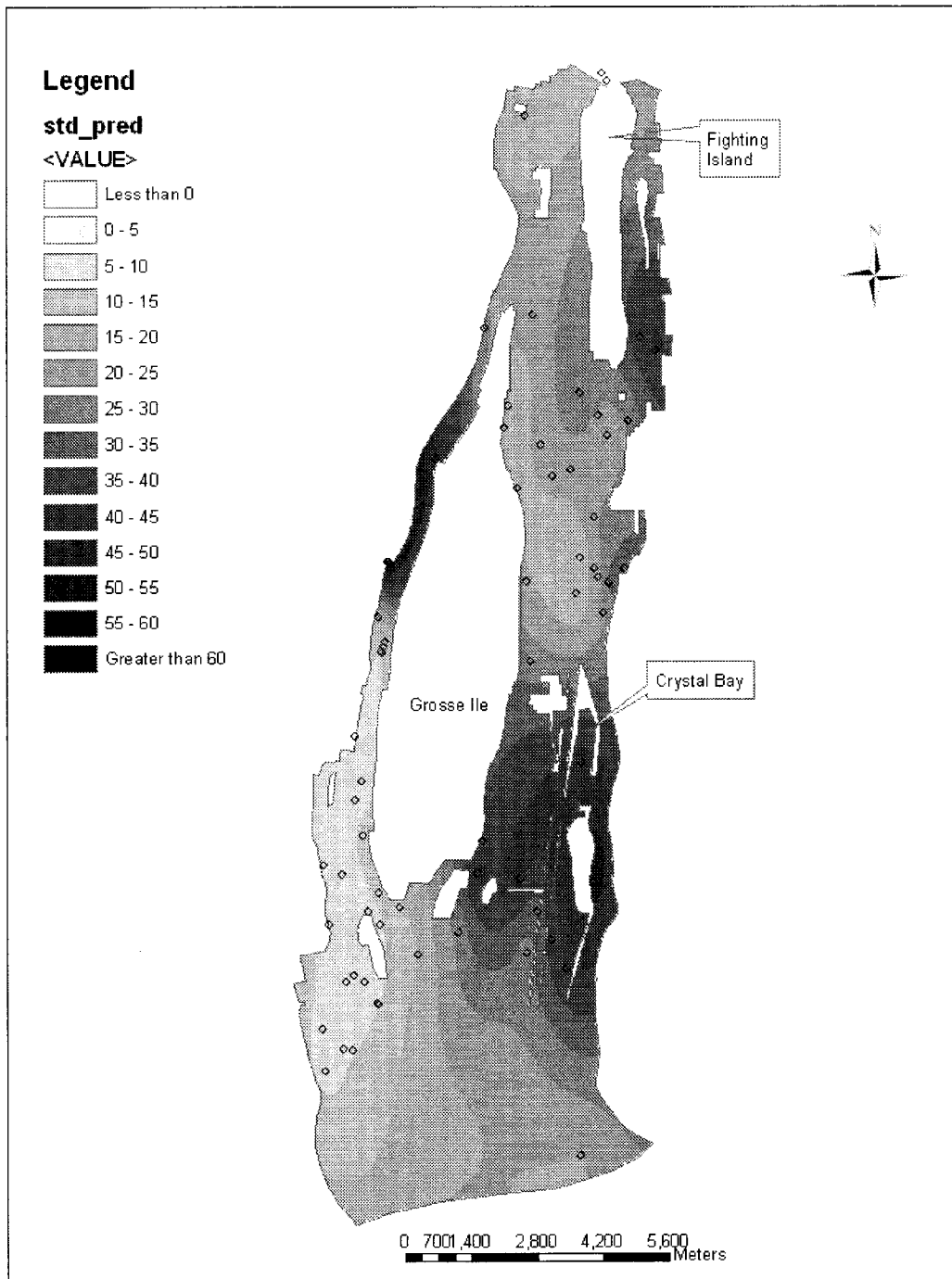
Figure 43: Predicted mass fraction of sediment with grain size diameter less than 0.075 mm for the Lower reach of the Detroit River using standard kriging.

83
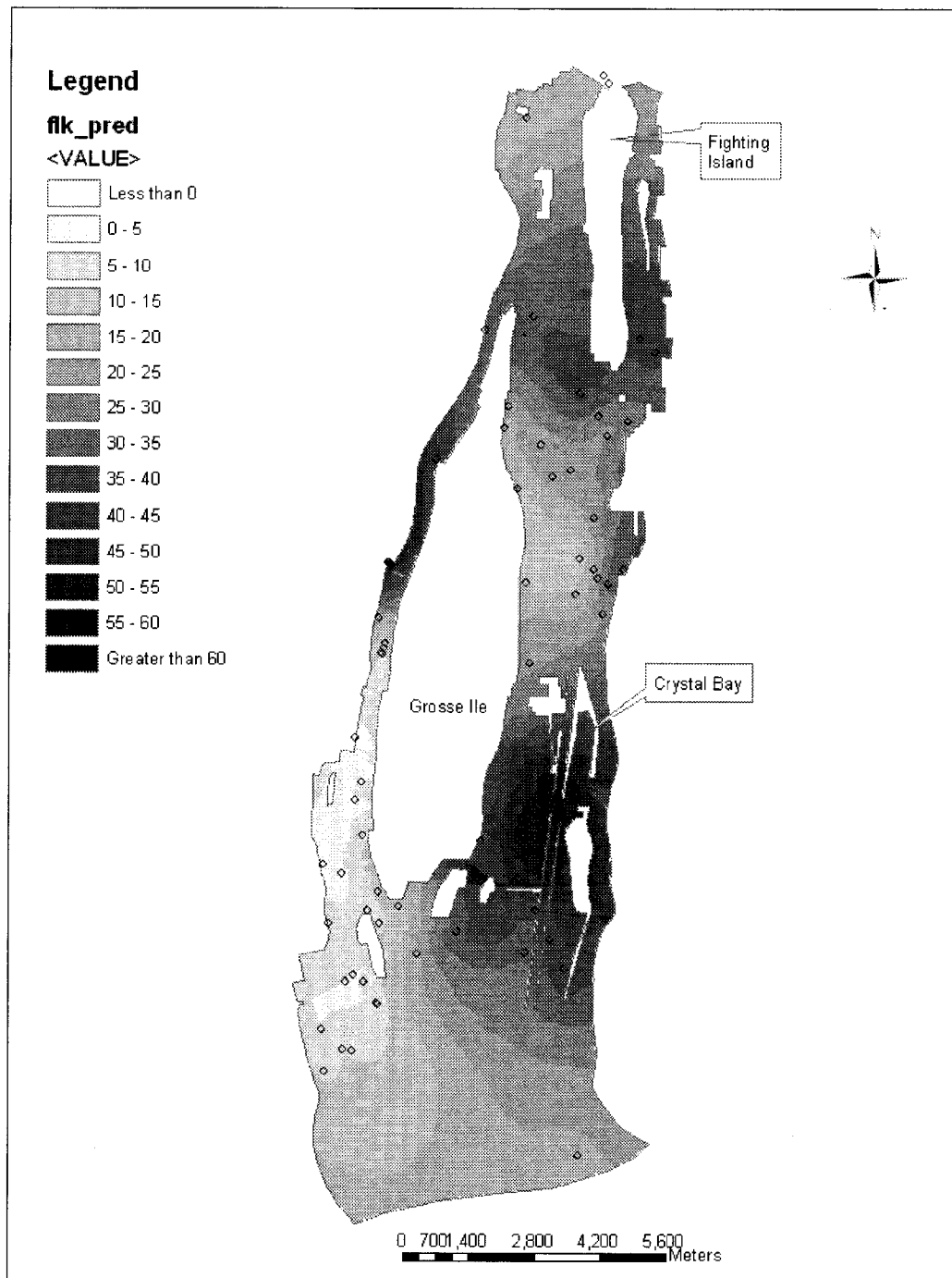
Figure 44: Predicted mass fraction of sediment with grain size diameter less than 0.075 mm for the Lower reach of the Detroit River using flowline kriging.

84
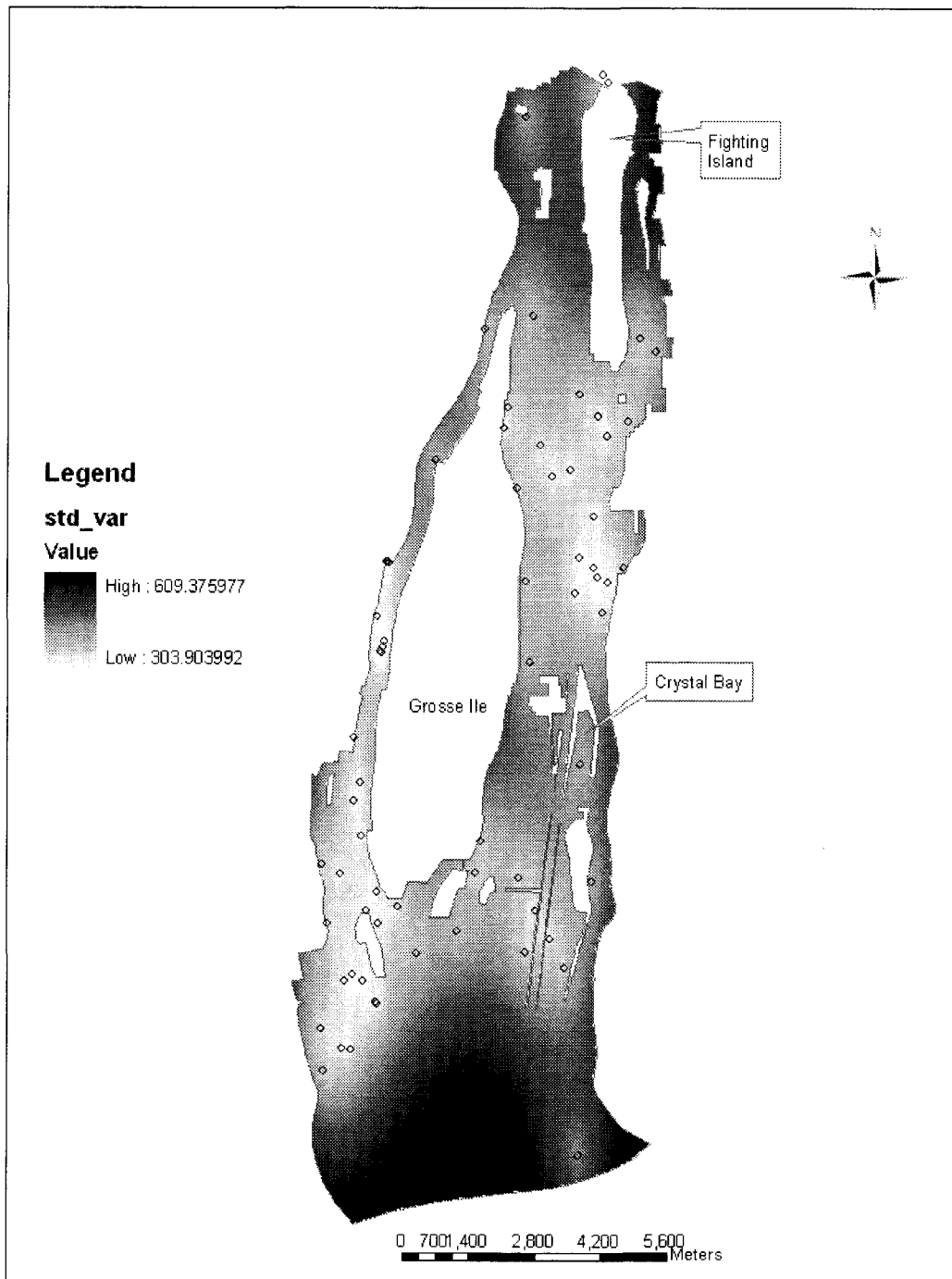
Figure 45: Kriging variances for sediment with grain size diameter less than 0.075 mm for the Lower reach of the Detroit River using standard kriging.

85
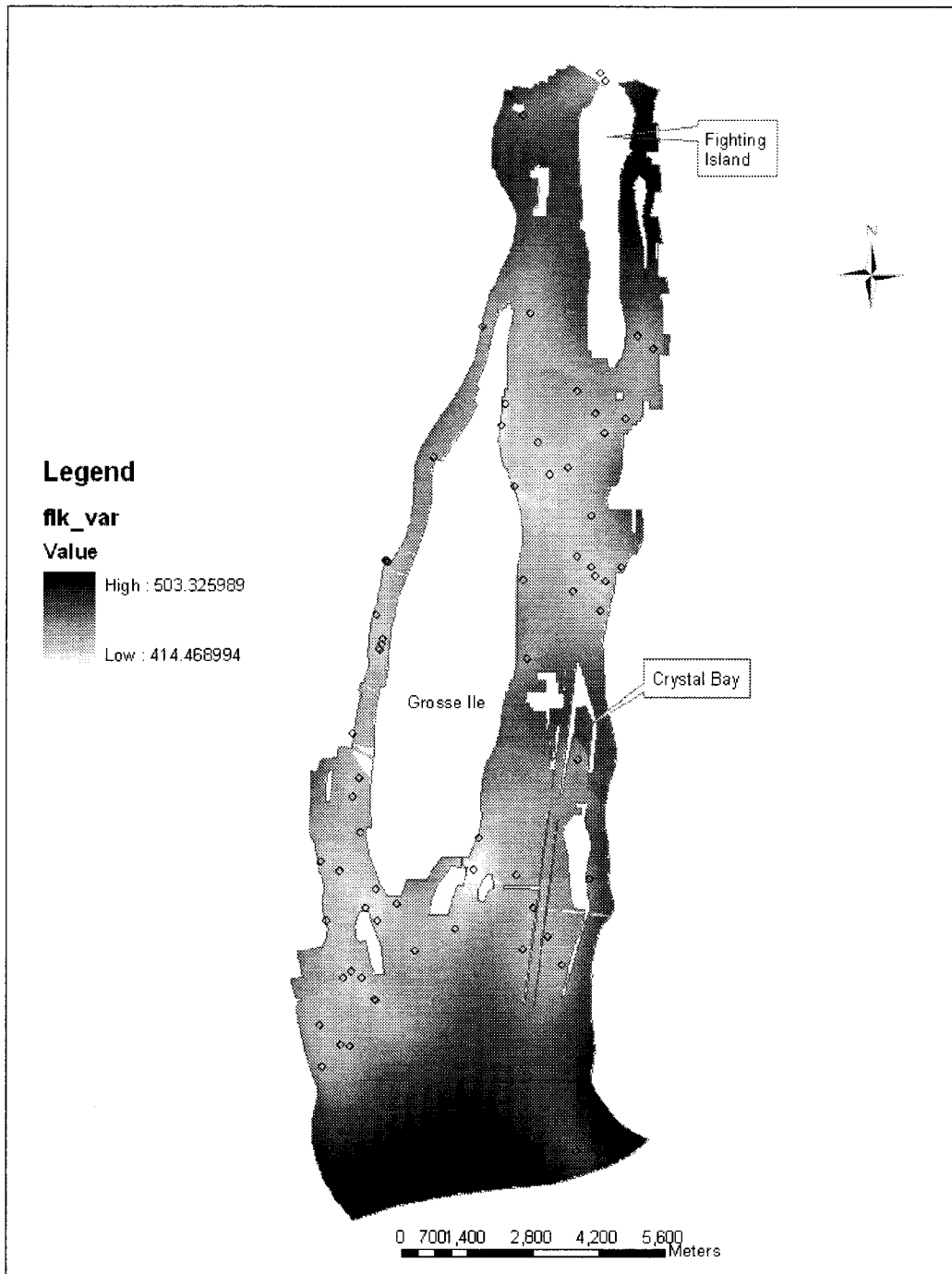
Figure 46: Kriging variances for sediment with grain size diameter less than 0.075 mm for the Lower reach of the Detroit River using flowline kriging.

86

4.5.2 Assessment of the Statistical Results

Other than the appearance of some interpolation artefacts, from the appearance of the resulting spatial distributions the flowline method appears to produce more reasonable spatial distributions for the fine grained fraction of sediments than the standard methods do when looking at the Detroit River data. The results were also examined statistically to see which method performed better numerically. GSTAT reports the results of cross-validation using different statistics than ArcGIS and therefore the results are not directly comparable to those from Section 4.4. Instead GSTAT uses the correlation coefficient as a statistical measure of how well the kriging method is predicting sample values.

Table 2: Correlation results from Cross-Validation on the Detroit River

	Standard	Flowline
Upper	-0.07229	-0.07993
Middle	0.02377	-0.06752
Lower	0.5892	0.6536

The cross-validation results from the Upper and Middle reaches, using both kriging techniques, show essentially no correlation between the predicted and sampled data. The implication is that the sampling program was insufficient to model the spatial variability in the data for either method. This does not mean that all areas of the river are necessarily predicted poorly. An individual point may be predicting well for its immediate neighbourhood. It simply means that the sample points are spread so far apart that they can not be used to infer sample values at other locations. Given the limitations of the data, unless additional sampling is conducted, it becomes simply a matter of professional judgement as to which method performs better. In that case, since the flowline method produces a much more realistic pattern of sediment distribution, the flowline method would be recommended for the Upper and Middle reaches.

While there was little in the visual representations of the spatial distributions for the Lower reach to recommend one method over the other, examination of cross-validation

87

results reveals that the flowline method performs somewhat better than the standard method. Although the elongated plumes of the standard method would seem to make more sense for a fluvial environment, they are in fact causing poor predictability at the sample locations. Based on the results of the cross-validation, the flowline method would also be recommended for the Lower reach.

5.0 Discussion

5.1 Flowlines and the Causes of Interpolation Artefacts

The results obtained from the flowline kriging method are highly dependent upon the shape and areal coverage of the flowlines. If accurate results are expected from the flowline kriging method, special care must be taken to ensure that the flowlines used in the method behave well.

The most important property of a flowline is that the line must be traced completely through the problem domain. Flowlines that terminate prematurely in the middle of the problem domain can cause kriging artefacts that affect both the visual and numerical results. The use of prematurely terminating flowlines was partly to blame for the poor correlation and RMS seen in the 90 sample point test cases for the island and diverging channel simulations. Figure 47 shows an example from an initial attempt on the Lower reach of the Detroit River. It can be seen that flowlines terminating in the middle of the river cause very noticeable kriging artefacts. The premature termination of a flowline causes a sudden jump in prediction values across a line that stretches perpendicular from the termination point of the flowline all the way across the channel. The existence of multiple terminating lines compounds the problem. The artefact is caused by the flowline Δx (i.e. length along the flowline) and Δy (i.e. length of the cross-line) values that are returned from the flowline method. If the flowline terminates, then any cells beyond the endpoints of the flowline will always return the same flowline Δx value. The modelling

88

of anisotropy compounds the problem since the x-direction provides a greater contribution to the variance.

The solution to the problem is to ensure that the flowlines are traced completely through the problem domain. In practice, flowlines will not always flow out of the problem domain. Sources, sinks, circulation zones and areas of very low velocity may all cause the effective termination of a flowline before it exits the problem domain. Realistically, some termination criteria must be chosen for the construction of a flowline. In this study, most of the prematurely terminated flowlines were caused by either low velocities in the shallow areas near the banks of the river, or by flowlines that, due to numerical limitations of the hydraulic model, intersected the banks of the channel. One possible solution, and the one used in this study, is to complete the flowline by forcing it to follow the shoreline all the way out of the problem domain. The results described in Section 4.5 were generated after the manual correction of the terminated flowlines, so they were not affected by artefacts similar to the one shown in Figure 47.

Figure 48 shows a kriging artefact caused by the existence of a small circulation zone. The circulation zone also produces discontinuities in the returned values of flowline Δx and Δy. Inside the interior of the circulation zone, the flowline Δx distance may be extremely long even though the Euclidean distance is very short. On the outside of the circulation zone, an odd pattern of flowline Δx and Δy values are returned as the cross-lines keep being measured to different locations on the exterior of the circulation zone. In reality the circulation zones are generally not temporally stable. Some flow disturbance eventually comes along and alters the flow regime causing the flow to temporarily break out of the circulation pattern. The results described in Section 4.5 attempted to reduce the kriging artefact by forcing the flowline out of the circulation pattern. After one loop, the flowline was made to cross over itself and was extended out into the main channel where the flowline then continued downstream and out of the problem domain.

89

The flowline method shows two other types of kriging artefacts (Figures 49 and 50). They are caused by sharp curves in the flowlines. Figure 49 shows a kriging artefact caused by a concave bend in a flowline. The white lines represent the cross-lines that would be constructed. One prediction cell measures its cross-line north of the flowline's curve. The adjacent prediction cell measures its cross-line south of the flowline's curve. This results in very different flowline Δx distances being returned even though the prediction cells are adjacent. As mentioned earlier, with anisotropy the flowline Δx distances have a greater effect on the prediction results. The effect is to cause a sudden jump in values between prediction cells. In the particular example shown in Figure 49, several flowlines are compounding the problem and increasing the effect. It should be pointed out that under most circumstances this type of kriging artefact should have very little effect on the overall results. In Figure 49, the gray-scale has been adjusted to aid in the display of the artefact. There is only about a 1% difference in the predicted values observed on either side of the artefact.

Figure 50 shows the complementary situation to Figure 49. Figure 50 shows a kriging artefact caused by a convex bend in a flowline. In this example, a triangular pattern is exhibited where all the cross-lines are drawn to the exact same point on the flowline. Therefore, they will all have the same flowline Δx distance. Eventually, an adjacent prediction cell will break from the pattern and begin drawing cross-lines further down the flowline. This causes a discontinuity just as discussed above. In Figure 48, there is somewhere between a 5% and 10% difference in predicted values between the interior of the artefact and the outside of the artefact. The effect of the artefact is to cover up a gradient of 5% to 10% that is occurring over the over that area.

In essence, the flowline method relies on the fact that the flowlines curve and follow the true direction of flow. The recommendation is not to make any attempt at reducing the existence of artefacts caused by concave and convex bends in the flowlines. These artefacts are pointed out here so that their appearance will be recognized, understood and properly interpreted and accommodated.

90
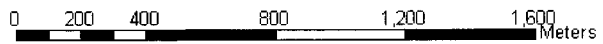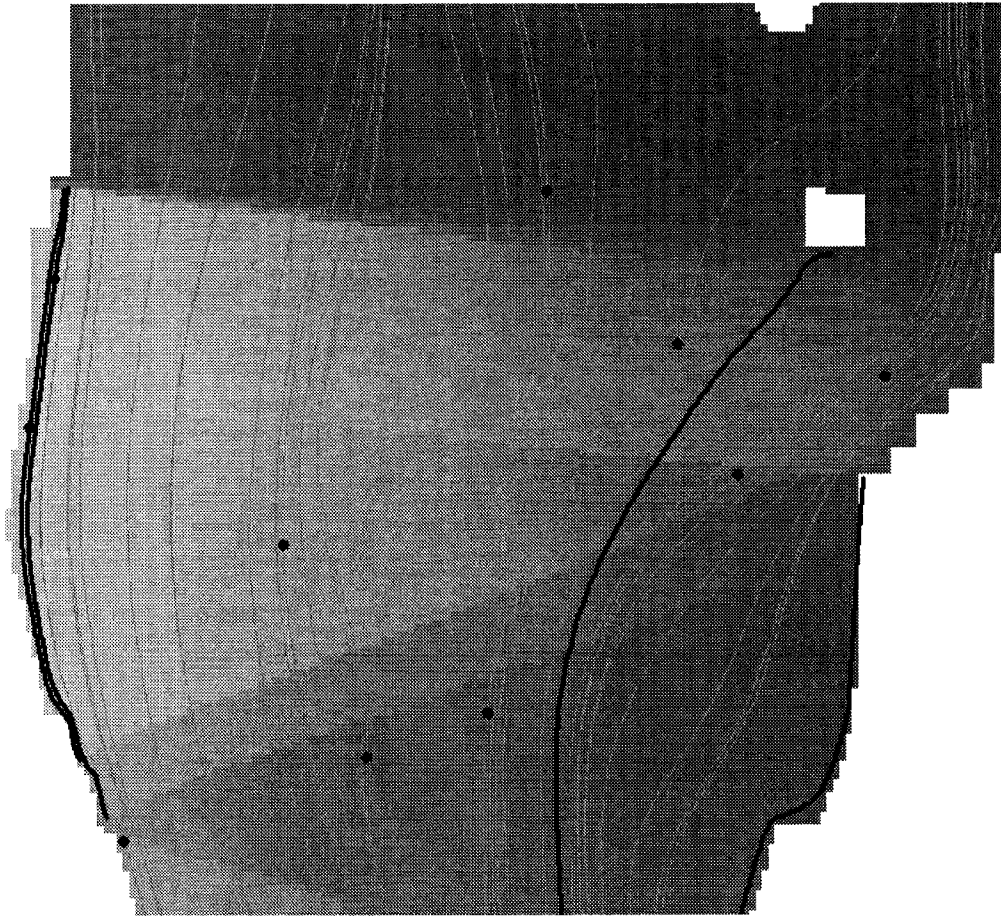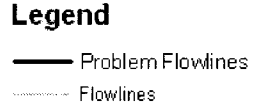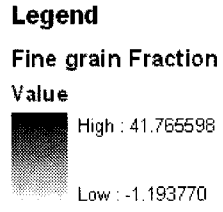
Figure 47: Kriging artefacts caused by the termination of flowlines within the problem domain.

91
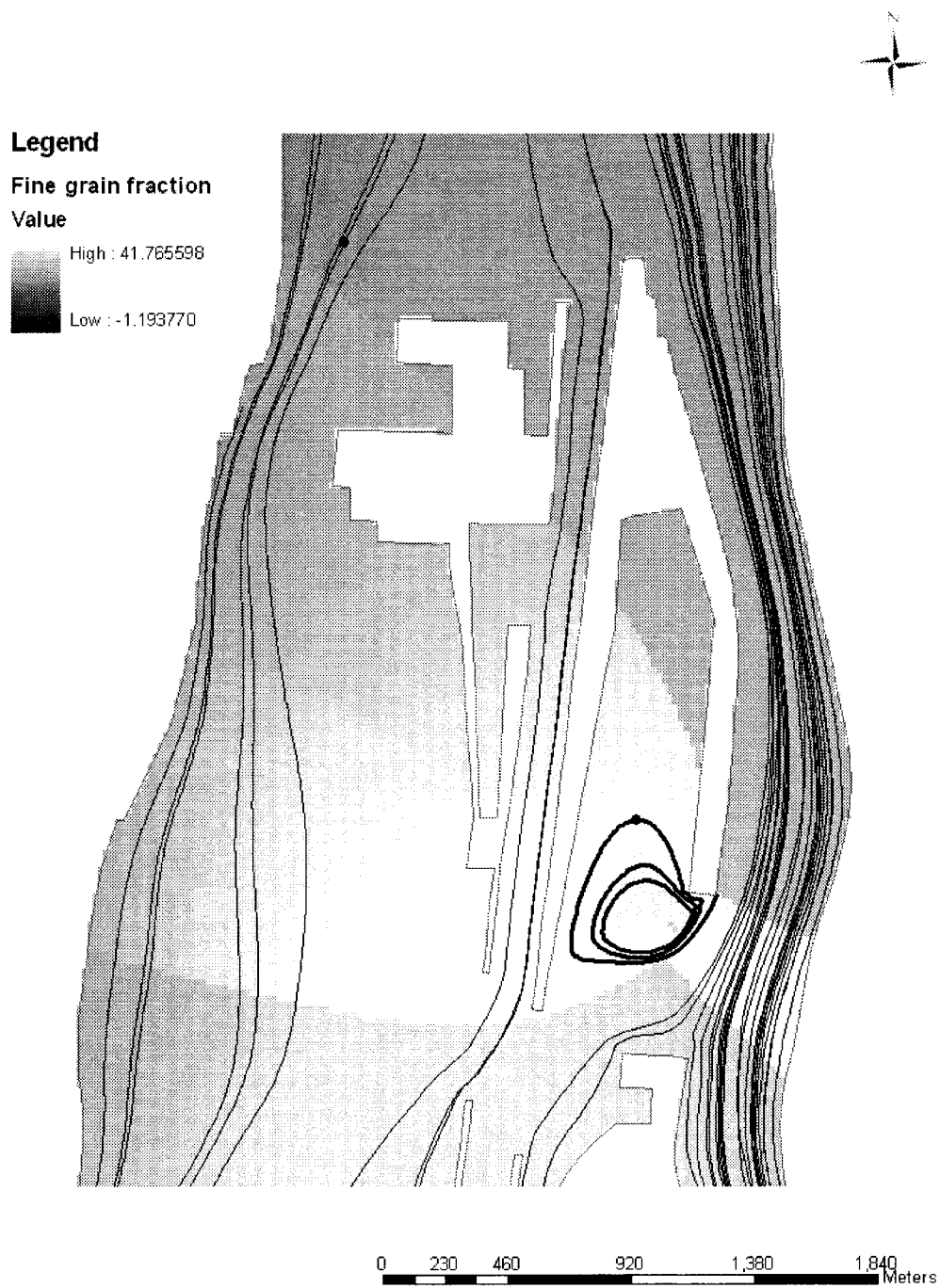
Figure 48: Kriging artefact cause by a circulation zone.

92
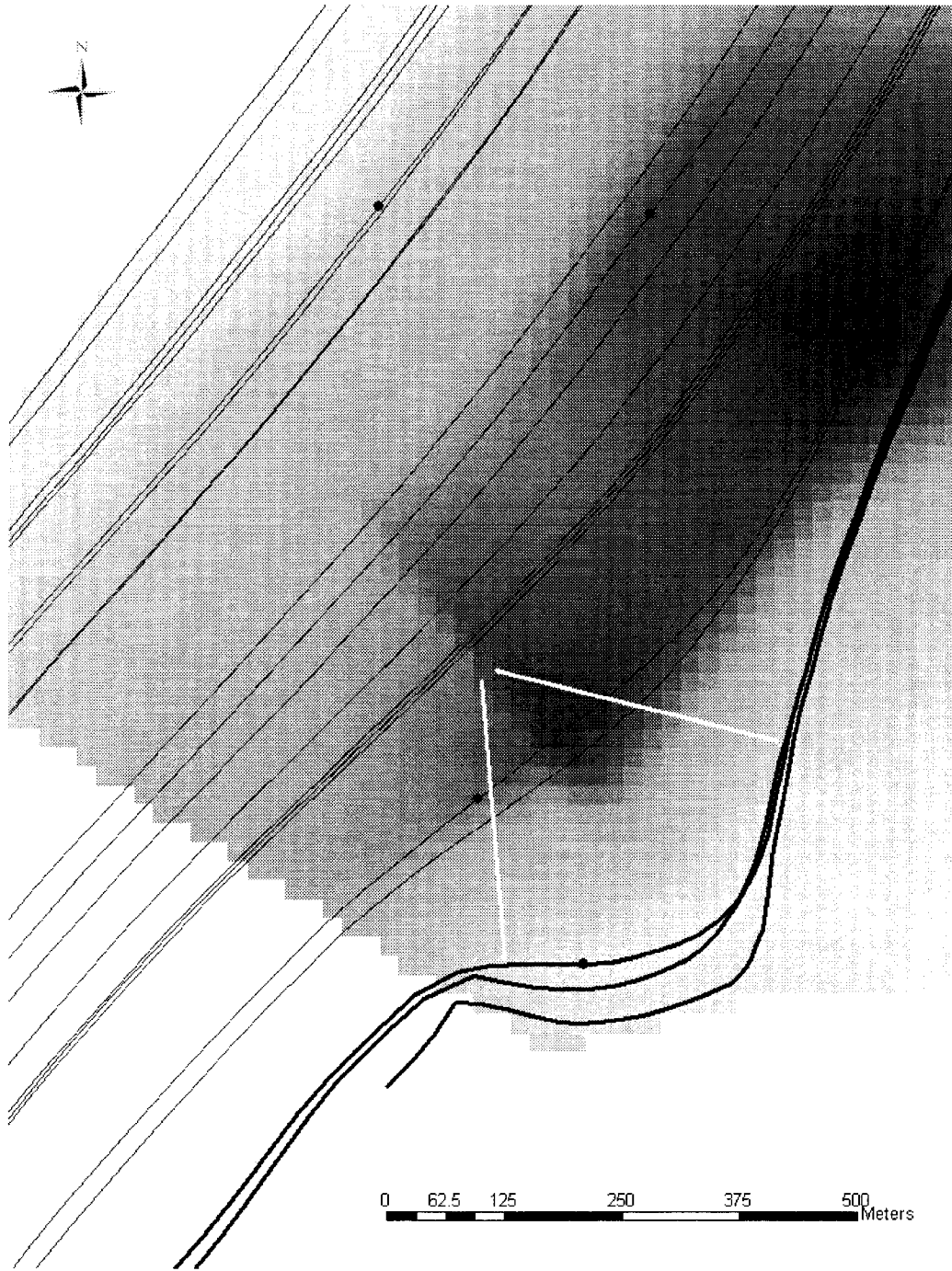
Figure 49: Kriging artefact cause by a concave turn in the flowlines.

93
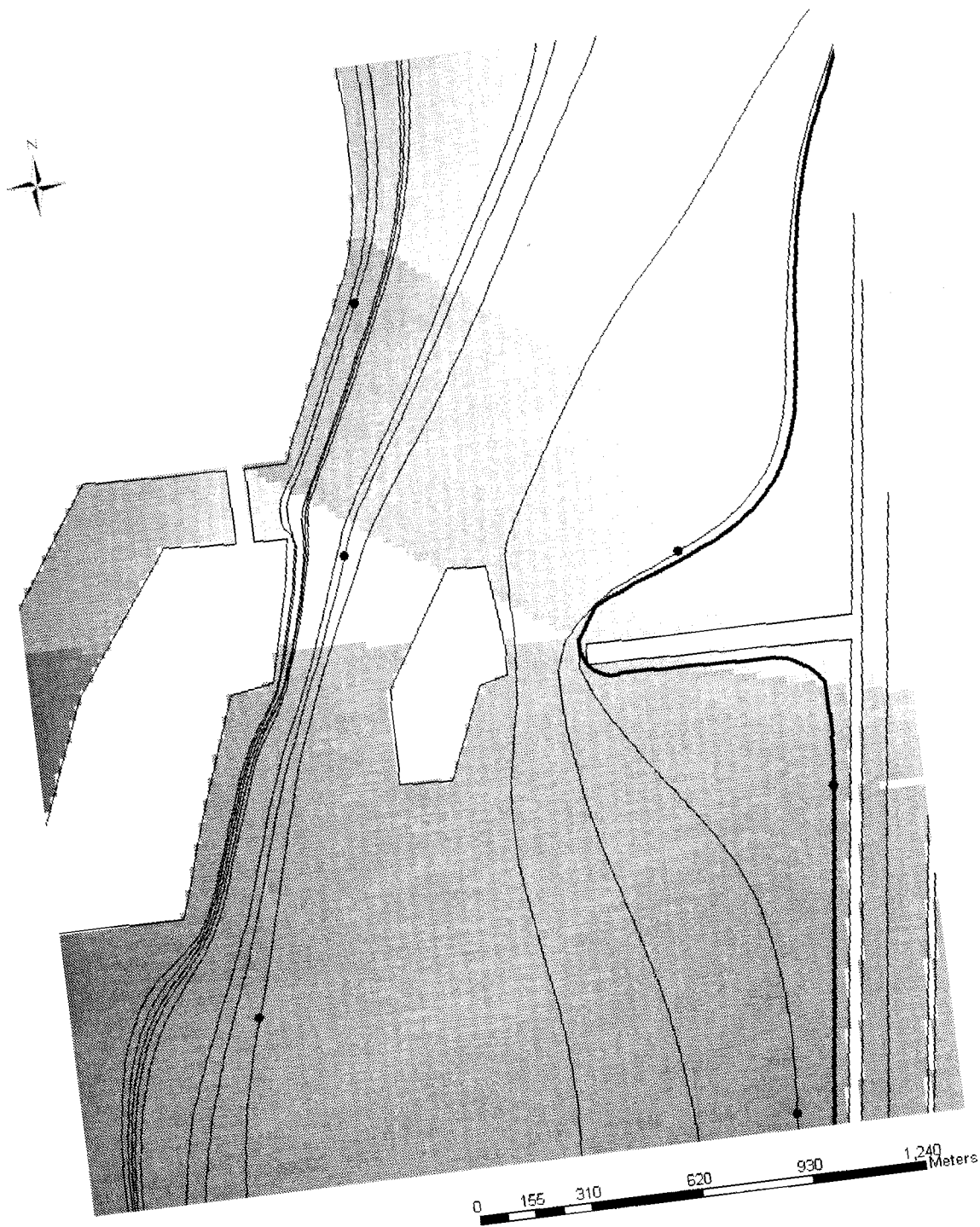
Figure 50: Kriging Artefact caused by a convex curve in a flowline.

94

5.2　Method Applicability and Limitations

Like the other forms of kriging, methods of kriging that use flowlines are based on the same assumptions of Gaussian distribution and stationarity in the data. Although the assumptions were not strictly adhered to in this proof of concept study, in other studies where sampling has been adequately performed and the predicted values are critical, the importance of the underlying assumptions should not be ignored. Although normalization techniques can be applied to the data to make it Gaussian, the assumption of stationarity is often, perhaps nearly always, violated in fluvial environments and needs to be addressed.

Any investigation using flowline kriging should begin with an examination of the processes involved in generating the spatial distributions. In the method, flowlines are generated by fluid flow and the attributes being examined are assumed to be transported by the fluid. If the environment being modelled is not dominated by these processes then it is unlikely that kriging with flowlines will provide an improvement over standard techniques. Special care will need to be taken when dealing with highly erosive environments. Although erosion on the bed is certainly a process dominated by fluid flow, the end result is the uncovering of historically deposited layers. The uncovering of substantial areas of the underlying layers will reveal the influences of historical processes and can create additional complexity in the spatial distributions.

Using kriging with flowlines, situations still arise where distance measurements between two points can cross over land. Since the flowline paths are traced through the water, a flowline will not cross over land. However, a cross-line could still cross over land. These situations certainly occur with islands, but they can also occur around sheltered inlets along a shoreline. Special care must be taken in these environments to ensure that an appropriate method of accounting for the decay of spatial autocorrelation across the land is being used. Also, the existence of prematurely terminating flowlines and circulation zones must also be examined and perhaps dealt with manually to ensure that they are not creating kriging artefacts that adversely affect the final results.

95

5.3   Applicability to Other Studies

Based on the above test cases it would seem that kriging with flowlines is a method that could be applied to a wide range of fluvial environments. In trying to extend the applicability of the method to situations other than fluvial environments, special attention must be paid to the processes generating the spatial distributions and anisotropy. Any environment where the distribution of sampled parameters is dominated by transport processes could be expected to see improvements through the use of the flowline method.

While the test parameter used in this thesis was fine grain surficial sediments, there are many other possible attributes that would be suitable for examination using the flowline method. The most obvious of these would be chemical contaminants in the bed sediments. In many cases, the purpose of looking for fine grain sediments on the bottom of a river is that chemical contaminants are often associated them. In addition to the parameters from the bed of the river, suspended sediments and chemical contaminants are also likely candidate parameters to benefit from the flowline method. It is also possible that the spatial distribution of some biological species could be examined with the method. Spatial distributions of species that are passively carried along by the flow of water and those that rely on the flow of water to transport their offspring to other areas are most likely to benefit from the use of the method.

Some non-fluvial aquatic environments may also benefit from the use of flowline kriging. Although the flow of water in lakes and oceans is not channelized, some parameters may still be controlled by the flow of water. For example, it may be possible to use flowline kriging on large circulation zones in lakes and oceans. For the current flowline implementation, small circulation zones can create conceptual problems in the method. However, the problems may eventually be overcome. It may be that large circulation zones will not even suffer from the same problems. In large circulation zones, a flowline may not converge in on itself as tightly. If the variogram range is sufficiently short that it does not overlap a flowline in multiple places and if the sample spacing is small relative to the circulation size, the fact that the flow is circular may not matter.

96

Hydrogeology may benefit from the use of these techniques as well. Although the issues involving groundwater plumes are mentioned in Section 1.1, the field may also benefit from the use of more simplified techniques. The use of flownets for obtaining initial estimates of groundwater flow is a good example. There is an obvious analogy between the creation of flownets and the generation of flowlines for this kriging method. If the creation of a flownet is to be performed, it may be that a substantial portion of the work for flowline kriging has already been performed.

Hydrologic studies may also be able to make use of the method. A common technique in simple GIS hydrologic models is the tracing of the path of water as it flows across the landscape using a digital elevation model. By treating this path as a flowline, this may improve the modelling of spatial distributions tied to the flow of water across a landscape.

Finally, it may be that air quality studies could use this method under certain circumstances. The applicability is likely limited since for most air quality studies, the flow of air is dominated by regional wind patterns that are not changing direction as they move across the landscape. Exceptional circumstances where the method could apply would be modelling with jet streams or wind patterns in a downtown core dominated by tall buildings.

5.4   Recommendations for Future Research

The use of kriging with flowlines for more quantitatively based studies requires more research into the underlying theory. The violation of the assumptions of stationarity and Gaussian distributions is common in many kriging applications. However, the implications for the flowline method in particular should be further examined as they may be different than the implications for standard kriging techniques. Based on some

97

ancillary work not included in this thesis, there is some indication that the flowline method may be more sensitive to the assumption that the data has a Gaussian distribution.

A related issue that could be examined is the non-symmetric nature of flow-dominated environments. Since the flow of water only goes downstream, it could be expected that a point in the middle of a river would have less influence on points upstream than it would on points downstream. The degree of the correlation upstream and downstream is likely different. However, a means of quantifying the correlation in opposite directions and conducting computations with it would need to be devised.

The current implementation of the flowline distance metric has its own theoretical problem that needs to be addressed. Strictly speaking, the flowline distance metric is not a metric at all. Rathbun (1998) and Løland et al. (2003) point out that a metric space is required to be symmetric; that is, the distance between two points is the same regardless of the direction it is measured. This is not true for the current implementation of the flowline method since measuring the distances in opposite directions uses different flowlines. The consequence of not using a true metric space is that the resulting spatial covariance model may not be valid. It is likely that some modification of the current flowline implementation could overcome this issue. One possible modification would be that measurements are only made from upstream to downstream. However, from a practical standpoint the issue may not be that serious. As long as the distances from both directions are used in the variogram plot, as was done in this study, the results will, to some extent, average out. This doubles the number of points in the variogram plot and introduces more noise into the model fitting. However, once a variogram model is fit to the plot, the model is used from that point on and the issue never arises again.

To aid in future studies, a more sophisticated algorithm should be implemented. The current implementation is highly inefficient since it carries considerable overhead embedded in the GIS application programming interface. The current implementation also lacks a good, integrated piece of variogram modelling software. Integrated variogram modelling software would allow for much easier construction of variogram

98

models, help to avoid model specification problems and allow the examination of kriging methods other than just ordinary kriging.

In order for the method to gain more widespread applicability, alternate methods for the construction of flowlines should also be examined. For any particular study area, the researchers involved may not have the inclination or the ability to generate the fine resolution flow fields that existed for this study. An investigation regarding the accuracy of the flowlines versus the improvements seen in the kriging results could be quite helpful. If it turns out that, as with the construction of groundwater flownets, hand drawn estimates for flowlines still produce the desired results, this could greatly improve the accessibility of the method.

6.0   Summary and Conclusions

The process of predicting reasonable spatial distribution of surficial sediments in fluvial environments using interpolation techniques can be quite challenging. The process of sediment transport dominates these environments and influences the distributions of many attributes to a large degree. The process of sediment transport also creates anisotropy along the direction of flow in the resulting distributions. The geographic bearing of the flow direction can change throughout the channel due to influences such as: changes in the shape of the channel bed, dredging for navigational purposes, flow diversions due to hydraulic structures and islands, meanders along the channel length and a variety of other local influences.

Most standard geostatistical software packages allow for the incorporation of only one geographic bearing of anisotropy for the entire problem domain. This is problematic for fluvial environments because an average bearing will often misrepresent the local changes in anisotropy throughout the river.

99

A distance transformation technique based on the use of flowlines was applied in an attempt to improve the way geostatistical algorithms deal with anisotropy. The standard geostatistical method of ordinary kriging was modified so that distances measured along flowlines and perpendicular to the flowlines were substituted for the Cartesian coordinate system distances typically used.

Five geometrically and hydrodynamically simple test cases were generated using the CH3D hydrodynamic model with sediment transport to test how the method performs in idealized environments. The first two test cases were straight horizontal and vertical channels that were used to determine whether the modified flowline kriging algorithm was performing as expected. The results showed that the current implementation of the flowline algorithm reproduced the expected interpolation values to an accuracy of 5 decimal places for these two test cases.

The other three test cases were: a channel in the shape of a 90-degree bend, a symmetrical channel with an island in the centre, and a channel with diverging width. Seven datasets with 30, 50, 70, 90, 110, 130 and 150 random samples were extracted from the CH3D model for each of these three test cases. These 21 scenarios were used to examine the effectiveness of the flowline kriging method in comparison to the standard kriging method. For the curved channel test case, the flowline method outperformed the standard method over the entire range of sampling densities examined, both in terms of visual and numerical representation. The channel with an island test case also showed that, in general, the flowline method outperforms the standard method. Two particular situations appeared in the island test cases where kriging artefacts, poor specification of the spatial structure and numerical sensitivity to the problem size lead to decreased performance of the flowline method relative to the standard method. The diverging channel test case showed similar performance between the standard and flowline methods with sample sets of 30 to 70 sample points. With larger data sets the diverging channel test case also suffered decreased performance due to kriging artefacts, poor specification of the spatial structure and numerical sensitivity to the problem size.

100

Sediment sampling conducted on the Detroit River was also examined as a test case to evaluate how the flowline method performs in real environments. The river was divided into three relatively straight sections with internally similar flow conditions. Each section was examined individually. The use of flowline kriging on the Upper and Middle sections of the river generated more realistic looking sediment distributions than the standard kriging method. Unfortunately the sampling conducted in these two areas was insufficient to determine which method performed better numerically. When applied to the Lower section of the river, the two kriging methods produced different but equally plausible looking sediment distributions. Statistical examination of the results using cross-validation indicted that the flowline kriging method was performing better numerically.

The test case results indicate that the flowline-based kriging method should perform well in a variety of flow-dominated environments. The ability of the flowline method to properly track sediment patterns and plumes around curves, corners and islands in the channels allows for predictions of spatial distributions that appear much more reasonable upon visual inspection. This ability alone can greatly improve upon predictions of sediment distributions in fluvial environments, especially for studies where delineation is the objective or the sampling is insufficient to statistically analyze the resulting distributions. Statistical examination of the test cases revealed that, under most circumstances, the flowline based kriging method performs equally well or better than the standard kriging methods. It appears that with some particular spatial distribution and sampling patterns, the flowline method has more difficulty determining the spatial structure of sediments. However, this study is a first attempt at dealing with these issues. It is likely that with refinement of the method and the application of more advanced kriging techniques, the flowline kriging method can overcome these particular shortcomings.

References

ASCE Task Committee on Geostatistical Techniques in Geohydrology. *Review of Geostatistics in Geohydrology, Parts I and II.* Journal of Hydraulic Engineering 116(5): 612-658, 1990.

Barabás, Noémi, Pierre Goovaerts and Peter Adriaens. *Geostatistical Assessment and Validation of Uncertainty for Three-Dimension Dioxin Data from Sediments in an Estuarine River.* Environmental Science and Technology, 35: 3294-3301, 2001.

Baudo, Renato, John P. Giesy and Herbert Muntau. *Sediments: Chemistry and Toxicity of In-Place Pollutants.* Lewis Publishers. Ann Arbor, Michigan, 1990.

Ben-Jemaa, Fethi, Miguel A. Mariño and Hugo A. Loaiciga. *Sampling Design for Contaminant Distribution in Lake Sediments.* Journal of Water Resources Planning and Management 121(1): 71-79,1995

Butcher, Jonathan B. *Co-Kriging to Incorporate Screening Data: Hudson River Sediment PCBs.* Water Resources Bulletin 32(2): 349-356, April 1996.

Büttner, O., A. Becker, S. Kellner, B. Kuehn, K. Wendt-Potthoff, D.W. Zachmann and K. Friese. *Geostatistical Analysis of Surface Sediments in an Acidic Mining Lake.* Water, Air and Soil Pollution 108: 297-316, 1998.

Chapman, R. S., B. H. Johnson and S. R. Vemulakonda. *User's Guide for the Sigma Stretched Version of CH3D-WES; A Three-Dimensional Numerical Hydrodynamic, Salinity, and Temperature Model,* Technical Report HL-96-21. U. S. Army Engineer Waterways Experiment Station, Vicksburg, MS, 1996.

Clark, I. *Practical Geostatistics.* Applied Science Publishers, London, 1979.

Cressie, Noel A.C. *Statistics for Spatial Data*, Revised Edition. John Wiley & Sons. New York, 1993.

Cressie, Noel and Dale. L. Zimmerman. *On the Stability of the Geostatistical Method.* Mathematical Geology 24(1): 45-59, 1992.

Critto, Andrea, Claudio Carlon and Antonio Marcomini. *Characterization of Contaminated Soil and Groundwater Surrounding an Illegal Landfill (S. Giuliano, Venice, Italy) by Principal Component Analysis and Kriging.* Environmental Pollution 122: 235-244, 2003.

D'Agostino, V., E. A. Greene, G. Passarella, and M. Vurro. *Spatial and Temporal Study of Nitrate Concentration in Groundwater by means of Coregionalization.* Environmental Geology 36(3-4): 285-295, 1998.

Danielsson, Å., R. Carman, L. Rahm, and J. Aigars. *Spatial Estimation of Nutrient Distributions in the Gulf of Riga Sediments using Cokriging.* Estuarine, Coastal and Shelf Science 46: 713-722, 1998.

Delhomme, J. P. *Kriging in the Hydrosciences.* Advances in Water Resources 1(5): 251-266, 1978.

Derecki, J. A. and F. H. Quinn. *Comparison of Measure and Simulated Flows During the 15 December 1987 Detroit River Flow Reversal.* Journal of Great Lakes Research 16(3): 426-435, 1990.

Duetsch, Clayton V. *Geostistical Reservoir Modeling.* Oxford University Press, New York, 2002.

Deutsch, Clayton V. and André G. Journel. *GSLIB: Geostatistical Software and User's Guide,* Second Edition. Oxford University Press, New York, 1998.

103

Gaus, I., D. G. Kinniburgh, J. C. Talbot and R. Webster. *Geostatistical Analysis of Arsenic Concentration in Groundwater in Bangladesh using Disjunctive Kriging.* Environmental Geology 44: 939-948, 2003.

Great Lakes Institute for Environmental Research, University of Windsor (GLIER). *Detroit River Modelling and Management Framework: Modelling Report and Manual.* Prepared for the Detroit River Canadian Cleanup Committee, 2002.

Haan, Charles T. Statistical Methods in Hydrology, Second Edition. Blackwell Publishing, 2002.

Holtschlag, David J. and John A. Koschik. *Steady-State Flow Distribution and Monthly Flow Duration in Selected Branches of St. Clair and Detroit Rivers within the Great Lakes Waterway.* U.S. Geological Survey. Lansing, Michigan, August 2001.

Journel, A. G. and C. J. Huijbregts. *Mining Geostatistics.* Academic Press, New York, 1978.

Jounel, A. G. and M. E. Rossi. *When Do We Need a Trend Model in Kriging?* Mathematical Geology 21(7): 715-739, 1989.

Kitanidis, P. K. *Introduction to Geostatistics: Applications in Hydrogeology.* Cambridge University Press, New York. 1997.

Kitanidis, P. K. *Geostatistics,* Chapter 20 in Handbook of Hydrology, edited by David R. Maidment, McGraw-Hill, New York, 1993.

Little, Laurie S., Don Edwards and Dwayne E. Porter. *Kriging in estuaries: as the crow flies, or as the fish swims?* Journal of Experimental Marine Biology and Ecology 213: 1-11, 1997.

104

Lo, C. P. and Albert K. W. Yeung. *Concepts and Techniques of Geographic Information Systems.* Prentice Hall. Upper Saddle River, New Jersey, 2002.

Lo, S. L., J. T. Kuo and S. M. Wang. *Water Quality Monitoring Network Design of Keelung River, Northern Taiwan.* Water Science and Technology 34(12): 49-57, 1996.

Løland, Anders and Gudmund Høst. *Spatial covariance modelling in a complex coastal domain by multidimensional scaling.* Environmetrics 14:307-321, 2003.

Lu, X. X., P. Ashmore, and J. Wang. *Sediment yield mapping in a large river basin: the Upper Yangtze, China.* Environmental Modelling & Software 18: 339-353, 2003.

Marvin, C. H., M. N. Charlton, G.A. Stern, E. Braekevelt, E. J. Reiner and S. Painter. *Spatial and Temporal Trends in Sediment Contamination in Lake Ontario.* Journal of Great Lakes Research 29(2): 317-331, 2003.

Matherson, G. *Principles of Geostatistics.* Economic Geology 58:1246-1266, 1963.

Merwade, V. M., D. R. Maidment and B. R. Hodges. *Geospatial Representation of River Channels.* submitted, ASCE Journal of Hydrologic Engineering., July 2003.

Metcalfe, Tracey L., Chris D. Metcalfe, Erin R. Bennett and G. Douglas Haffner. *Distribution of Toxic Organic Contaminants in Water and Sediments in the Detroit River.* Journal of Great Lakes Research 26(1): 55-64, 2000.

Ontario Ministry of the Environment (OMOE). *Stage I Remedial Action Plan For Detroit River Area of Concern.* Sarnia, Ontario, June 1991.

Ouyang, Ying, John Higman, Jeanne Thompson, Tim O'Toole and Dean Campbell. *Characterization and spatial distribution of heavy metals in sediment from Cedar and Ortega rivers subbasin.* Journal of Contaminant Hydrology 54: 19-35, 2002.

Ouyang, Ying, Peter Nkedi-Kizza, Robert S. Mansell and Jim Y. Ren. *Spatial Distribution of DDT in Sediments from Estuarine Rivers of Central Florida.* Journal of Environmental Quality 32: 1710-1716, 2003.

Pebesma, Edzer J. *GSTAT User's Manual.* Utrecht University, Utrecht, The Netherlands.

Poon, Ka-Fai, Raymond Wai-Hang Wong, Michael Hon-Wah Lam, Hung-Yui Yeung and Tony King-Tung Chiu. *Geostatistical Modelling of the Spatial Distribution of Sewage Pollution in Coastal Sediments.* Water Research 34(1): 99-108, 2000.

Rathbun, Stephen L. *Spatial Modelling in Irregular Shaped Regions: Kriging Estuaries.* Environmetrics 9: 109-129, 1998.

Roth, D. A., H. E. Taylor, J. Domagalski, P. Dileanis, D. B. Peart, R. C. Antweiler and C. N. Alpers. *Distribution of Inorganic Mercury in Sacramento River Water and Suspended Colloidal Sediment Material.* Archives of Environmental Contamination and Toxicology 40: 161-172, 2001.

Rubin, Yoram. *The Spatial and Temporal Moments of Tracer Concentration in Disordered Porous Media.* Water Resources Research: 27(11): 2845-2854, 1991.

Wackernagel, Hans. *Multivariate Geostatistics: An Introduction with Applications.* Second, completely revised edition. Springer-Verlag, Berlin, Heidelberg, 1998.

Zhang, Chaosheng and Olle Selinus. *Spatial Analyses for copper, lead, and zinc contents in the sediments of the Yangtze River basin.* The Science of the Total Environment 204: 251-262, 1997.

Appendix A – Flowline Generation Algorithm

The output of the CH3D hydrodynamic model is a series of text files that contains an ordered list of attribute values predicted for the center of each modelling mesh element. However, the geometry of the modelling mesh is described by an ordered list of nodes that represent the corners of the mesh elements.

The first step in generating flowlines is to import the geometry and produce coordinates for the centroid of each mesh element. The corresponding attribute values, in this case both the flow velocities and sediment mass fractions, are then matched up to each centroid. Then a grid is constructed using these centroids as the corners of the grid cells. When an attribute value is required for a particular point, the cells in the grid are searched to determine which cell contains the point. Then linear interpolation is then applied to the cell's four corners (i.e. the mesh centroids) to produce the desired value for the point. If the point happens to lie outside the grid but still within the problem domain, the attribute value from the nearest centroid is used.

A flowline is represented as an ordered list of vertices. Functionally the creation of a flowline is based on predicting the locations of a series of sequential vertices. The flowline construction begins at the sample point and proceeds downstream. A velocity is determined at the sample point using the attribute grid as previously discussed. Using the velocity and one time step, the location of the next vertex is created. The velocity at that vertex is then determined and the process repeats itself until a predicted vertex leaves the problem domain. Then the flowline is traced upstream. The process is the same as tracing the flowlines downstream except that the x and y components of the velocities are multiplied by -1 to reverse their direction. As these vertices are created they are added to the beginning of the vertex list rather than the end.

In order to prevent circulation zones, every 1000 time steps a check is performed to ensure that the flowline has not crossed over itself. If a flowline does cross over itself, vertices are removed until this no longer occurs and the flowline is terminated. In some

107

circumstances the flow velocities may become so small that the flowline essentially stops. Therefore, a tolerance distance was used. If the line segment for one time step is drawn shorter than the tolerance distance, the flowline is terminated. These terminated flowlines can then be dealt with manually on a case by case basis.

Several algorithms exist that can help create smooth lines with fewer vertices. With fewer vertices, the computational effort is also decreased. However, the effect of these methods is to trim the corners of lines, which consequently decreases the length of the lines. Since the lengths of the lines are so important to the kriging algorithm, it was decided not to use any of these smoothing techniques. Sufficiently small time steps must be used to make the flowlines smooth and the increased computational requirements simply have to be dealt with.

When determining flowline and cross-line distances there are two particular sections of the algorithm that may affect the results. To calculate the distances, the ArcObjects method QueryPointandDistance was used. When a perpendicular cannot be drawn to a flowline, because of a terminated flowline for example, a tangent is extended off the end of the flowline and the cross-line is drawn to the tangent. The cross-line distance is returned as expected, but the flowline distance is only measured to the end of the flowline. The distance along the tangent is not added into the returned flowline distance. This is part of the reason why it is so critical that flowlines do not terminate in the middle of the problem domain. The other section of algorithm also involves calculation of cross-line distances. In order to prevent unrealistic cross-line measurements from being returned when a flowline begins to run cross-channel, a cut-off value is implemented. The cut-off value implemented is the width of the channel (including islands) at that location. Any cross-line distances returned that exceed this cut-off are reduced back to the cut-off value.

108

Appendix B – Straight Channel Simulation Inputs

CH3D Channel Geometry (grid.inp)

Although the CH3D grid file describing the channel geometry is too large to include in an appendix, a brief description of the channel follows.

The channel is rectangular, 200 m wide by 1000 m long and divided into a 20 m^2 square mesh for computations.

CH3D Main Input File (main.inp)

```
TITLE(A80)
Jason Wintermute, Test run.
      IT1       IT2        DT  ISTART     ITEST   ITSALT     ISCOM   NTSED0NDTINDTS
        1     53600         1       0         0        0         1     28600         1
  WPRCRD
        0
  WXCEL1    WXCEL2    WYCEL1    WYCEL2    WZCEL1    WZCEL2    WPRINT    WPRSTR    WPREND    WPRVAR
  SNPCRD
        1
  SXCEL1    SXCEL2    SYCEL1    SYCEL2    SZCEL1    SZCEL2    SNPINT    SNPSTR    SNPEND    SNPVAR
        1        10         1        50         1         2         1     53600     53600UVECDB
   NRANG
        0
  RANGDR     RPOS1     RPOS2     RPOS3    RRNAME
      IGI       IGH       IGT       IGS       IGU       IGW       IGC       IGQ       IGP
        0         1         0         0         0         0         0         0         0
     XREF      ZREF      UREF       COR        GR       RO0       ROR        T0        TR
     2000       200        45       1.0     981.0      1.00     1.021        20        20
    THETA
      0.6
    ITEMP     ISALT       ICC       IFI    ifitim       IFA       IFB       IFC       IFD
        0         0         0         0         0         0         0         0         1
      TWE       TWH       FKB
        0         0         0
     IEXP       IAV       AVR       AV1       AV2       AVM      AVM1       AHR
        1         0         1        0.        0.     0.002     0.002     10000
     IVIS       IQW       IPT
        0         0         0
    GAMAX     GBMAX
    60000     60000
    IWIND      TAUX      TAUY
        0      0.00      0.00
    ISPAC(I),I=1,10
        0         0         0         1         0         0         0         0         0         0
    JSPAC(I),I=1,10
        1         1        -1         0         0         0         0         0         0         0
    RSPAC(I),I=1,10
 0.035000         0   0.00000   0.00000         0         0         0     0.000      0.00         0
     IBTM      HADD      HMIN        H1        H2      SSS0      HMAX
        4       0.0       0.0       0.0       0.0       1.0   999999.
   ISMALL       ISF       ITB    ZREFBN       CTB       BZ1    ZREFTN       TZ1
        1         0         5         5     0.003     0.200         5       2.0
     XMAP    ALXREF    ALYREF
    100.0         0         0
    ITRAN     IBD(1)    IBD(2)    IBD(3)    IBD(4)
```

109

```
         2         4         4         4         4
ITBRK(1)     (2)       (3)       (4)       (5)       (6)       (7)       (8)       (9)      (10)
         0         0         0         0         0         0         0         0         0         0
     NSTA  NFREQ  NSTART    (CURRENT STATIONS)
        0      0      0
IST JST  STATID(K)     (2I4,A48)      ( ONE CARD FOR EACH STATION )
     NSTAS  NFREQS  NSTRTS    (TIDE STATIONS)
        0       0       0
IST JST  STATID(K)     (2I4,A48)      ( ONE CARD FOR EACH STATION )
     MSTA   MFREQ  MSTART    (SALINITY STATIONS)
        0       0      0
IST JST  STATID(K)     (2I4,A48)      ( ONE CARD FOR EACH STATION )here
   NRIVER
        0
  IJRDIR  IJRROW  IJRSTR  IJREND     ( ONE CARD FOR EACH RIVER )
       I        J  QRIVER            ( ONE CARD FOR EACH CELL )
     NBAR
        0
  IJBDIR  IJBROW  IJBSTR  IJBEND     ( ONE CARD FOR EACH BAR )
  TIDFNO  TIDBND
       5       5
  TIDSTR       2       3       4       5       6       7       8       9      10
       1       1       1       1       1
  IJTDIR  IJTROW  IJTSTR  IJTEND  TIDTYP  TIDFN1  TIDFN2
       4      50       1      10CONSTANT      1       0
       2       1       1      10CONSTANT      2       0
       4      40       8       8CONSTANT      3       0
       4      10       5       5CONSTANT      4       0
       4      25       2       2CONSTANT      5       0
RESET HS(I,J)  TO ZERO AT THE FOLLOWING CELLS
RESET HU(I,J)  TO ZERO AT THE FOLLOWING CELLS
RESET HV(I,J)  TO ZERO AT THE FOLLOWING CELLS
RESET HS(I,J)  TO THE FOLLOWING DEPTHS
    END OF DATA
    END OF FILE
```

CH3D Sediment Input File (sed.inp)

```
    99999   99999   99999   99999   99999   99999   99999   99999   99990   99999
    99999   99999   99999   99999   99999   99999   99999   99999   99999   99999
    99999   99999   99999   99999   99999   99999   99999   99999   99999   99999
    99999   99999   99999   99999   99999   99999   99999   99999   99999   99999
    99999   99999   99999   99999   99999   99999   99999   99999   99999   99999
    99999   99999   99999   99999   99999   99999   99999   99999   99999   99999
    99999   99999   99999   99999   99999   99999   99999   99999   99999   99999
    99999   99999   99999   99999   99999   99999   99999   99999   99999   99999
    99999   99999   99999   99999   99999   99999   99999   99999   99999   99999
    99999   99999   99999   99999   99999   99999   99999   99999   99999   99999
    99999   99999   99999   99999   99999   99999   99999   99999   99999   99999
    99999   99999   99999   99999   99999   99999   99999   99999   99999   99999
    99999   99999   99999   99999   99999   99999   99999   99999   99999   99999
    99999   99999   99999   99999   99999   99999   99999   99999   99999   99999
    99999   99999   99999   99999   99999   99999   99999   99999   99999   99999
    99999   99999   99999   99999   99999   99999   99999   99999   99999   99999
    99999   99999   99999   99999   99999   99999   99999   99999   99999   99999
    99999   99999   99999   99999   99999   99999   99999   99999   99999   99999
    99999   99999   99999   99999   99999   99999   99999   99999   99999   99999
    99999   99999   99999   99999   99999   99999   99999   99999   99999   99999
        1       1       1       0       0
0 0 0 0 0 0 0 0 0 1 0 0 1 0 0 0 0 0 0 0 0 0 0
1 1 1 1 1 1 1
        0       0
          1.00e-6         3.17e-6         1.00e-5         3.17e-5         1.00e-4
        0.00000114
     2.65     0.4
     0.60     0.10    0.100    0.030    0.010
        0.0000001        0.00000001
```

110

```
   100
   0.01
      0
1.4e-5  1.3e-5  5.4e-6  1.3e-7        0
9.3e-6  8.0e-6  3.0e-6  4.5e-8        0
1000.
      0
      1       1       2
0.100         100
      1   0.20    0.20    0.20    0.20    0.20
     -2   0.20    0.20    0.20    0.20    0.20
      1     50       1       1       1
      2     50       1       1       1
      3     50       1       1       1
      4     50       1       1       1
      5     50       1       1       1
      6     50       1       1       1
      7     50       1       1       1
      8     50       1       1       1
      9     50       1       1       1
     10     50       1       1       1
      8     40       1       1       2
      2     25       1       1       2
      5     10       1       1       2
      1      1      -1
      2      1      -1
      3      1      -1
      4      1      -1
      5      1      -1
      6      1      -1
      7      1      -1
      8      1      -1
      9      1      -1
    -10      1      -1
      0      0
             -1   0.20    0.20    0.20    0.20    0.20
              1  1.4e-5  1.3e-5  5.4e-6  1.3e-7        0
                 9.3e-6  8.0e-6  3.0e-6  4.5e-8        0
              2  1.4e-4  1.3e-4  5.4e-5  1.3e-6        0
                 9.3e-5  8.0e-5  3.0e-5  4.5e-7        0
      2       3
             -1   0.20    0.20    0.20    0.20    0.20
              1  1.4e-5  1.3e-5  5.4e-6  1.3e-7        0
                 9.3e-6  8.0e-6  3.0e-6  4.5e-8        0
              2  1.4e-4  1.3e-4  5.4e-5  1.3e-6        0
                 9.3e-5  8.0e-5  3.0e-5  4.5e-7        0
```

CH3D Boundary Conditions (tide.inp)

```
FORTRAN 16 FILE: TIDE TABLE DATA
1  1  98  0 0      1.00    1.00    1.00    1.00    1.00
1  1  98  1 0      1.00    0.90   0.981    0.92   0.952
8  2  98  3 0      1.00    0.90   0.981    0.92   0.952
```

Sample Points

X	Y	Attr.
613.7534	37.31479	0.26725
310.3279	126.4922	0.27
609.7043	17.05808	0.268517
477.3509	101.1303	0.27981
224.7918	129.0449	0.263817
485.4493	141.6437	0.26515

111

156.5906	60.45262	0.270034
75.10363	83.26195	0.273197
139.2557	131.5975	0.276049
716.6244	164.6173	0.2734
438.6321	22.16332	0.27559
673.8563	65.39361	0.267532
53.7196	134.1501	0.275306
947.7995	187.5909	0.21401
986.5184	65.55786	0.207606
271.609	47.52527	0.273006
30.56271	61.43814	0.273
240.3538	135.2999	0.27081
329.9391	153.004	0.269877
197.5857	36.07619	0.280184
946.0266	63.99076	0.219571
205.6841	76.58961	0.276734
611.9806	114.7147	0.271
796.3384	18.20785	0.270264
860.4905	66.54338	0.254926
436.8592	99.56319	0.27387
158.8669	158.1092	0.276923
394.0911	0.339504	0.277
338.2999	193.9481	0.27
231.3798	46.38889	0.277421

Variogram Equation

Variogram Equation is specified in the format required by GSTAT. (Pebesma, 1999)

A Nug(0) + B Sph(C)

where A is the nugget, B is the partial sill (sill − nugget), C is the range. Sph denotes a spherical variogram model.

<u>Both Standard and Flowline</u>
2.1973e-006 Nug(0) + 7.9262e-005 Sph(237.07)

112

Appendix C – Curved Channel Simulation Inputs

CH3D Channel Geometry (grid.inp)

Although the CH3D grid file describing the channel geometry is too large to include in an appendix, a brief description of the channel follows.

The curved channel is a regular 90-degree bend, 200 m wide throughout and 1000 m long through its centre. The computational mesh was created with cells approximately 5m^2. Mesh nodes were evenly spaced across the channel's width perpendicular to the channel banks and evenly spaced along the channel's length.

CH3D Main Input File (main.inp)

```
TITLE(A80)
Jason Wintermute, Test run.
      IT1       IT2        DT  ISTART     ITEST   ITSALT     ISCOM  NTSED0NDTINDTS
        1      2000         1       0         0        0         1       300        1
    WPRCRD
        0
   WXCEL1    WXCEL2    WYCEL1   WYCEL2    WZCEL1   WZCEL2    WPRINT    WPRSTR    WPREND    WPRVAR
    SNPCRD
        1
   SXCEL1    SXCEL2    SYCEL1   SYCEL2    SZCEL1   SZCEL2    SNPINT    SNPSTR    SNPEND   SNPVAR
        1       200         1      40         1        2        10       300     2000CB
    NRANG
        0
    RANGDR    RPOS1     RPOS2    RPOS3    RRNAME
      IGI       IGH       IGT      IGS       IGU      IGW       IGC       IGQ       IGP
        0         1         0        0         0        0         0         0         0
     XREF      ZREF      UREF      COR        GR      RO0       ROR        T0        TR
      500       200        20      1.0     981.0     1.00     1.021        20        20
    THETA
      0.6
    ITEMP     ISALT       ICC      IFI    ifitim      IFA       IFB       IFC       IFD
        0         0         0        0         0        0         0         0         1
      TWE       TWH       FKB
        0         0         0
     IEXP       IAV       AVR      AV1       AV2      AVM      AVM1       AHR
        1         0         1       0.        0.    0.002     0.002     10000
     IVIS       IQW       IPT
        0         0         0
    GAMAX     GBMAX
    60000     60000
    IWIND      TAUX      TAUY
        0      0.00      0.00
    ISPAC(I),I=1,10
        0         0         0        1         0        0         0         0         0         0
    JSPAC(I),I=1,10
        1         1        -1        0         0        0         0         0         0         0
    RSPAC(I),I=1,10
 0.035000         0   0.00000  0.00000         0        0         0     0.000      0.00         0
     IBTM      HADD      HMIN       H1        H2     SSS0      HMAX
        4       0.0       0.0      0.0       0.0      1.0   999999.
   ISMALL       ISF       ITB   ZREFBN       CTB      BZ1    ZREFTN       TZ1
```

113

```
    1        0        5        5   0.003   0.200        5      2.0
  XMAP   ALXREF  ALYREF
  100.0        0        0
  ITRAN   IBD(1)   IBD(2)   IBD(3)   IBD(4)
     2        4        4        4        4
ITBRK(1)    (2)      (3)      (4)      (5)      (6)      (7)      (8)      (9)     (10)
     0        0        0        0        0        0        0        0        0        0
  NSTA    NFREQ   NSTART    (CURRENT STATIONS)
     0        0        0
IST JST  STATID(K)    (2I4,A48)      ( ONE CARD FOR EACH STATION )
  NSTAS   NFREQS   NSTRTS    (TIDE STATIONS)
     0        0        0
IST JST  STATID(K)    (2I4,A48)      ( ONE CARD FOR EACH STATION )
  MSTA    MFREQ   MSTART    (SALINITY STATIONS)
     0        0        0
IST JST  STATID(K)    (2I4,A48)       ( ONE CARD FOR EACH STATION )here
  NRIVER
    -6
IJRDIR  IJRROW   IJRSTR   IJREND      ( ONE CARD FOR EACH RIVER )
     2       12       65       65
     2        7       20       20
     2       17       98       98
     2       17      167      167
     2       33       77       77
     2       39       57       57
     I        J   QRIVER                  ( ONE CARD FOR EACH CELL )
    65       12        0
    20        7        0
    98       17        0
   167       17        0
    77       33        0
    57       39        0
  NBAR
     0
IJBDIR  IJBROW   IJBSTR   IJBEND      ( ONE CARD FOR EACH BAR )
TIDFNO  TIDBND
     2        2
TIDSTR        2        3        4        5        6        7        8        9       10
     1        1        1        1        1        1
IJTDIR  IJTROW   IJTSTR   IJTEND   TIDTYP   TIDFN1   TIDFN2
     1        1        1       40CONSTANT        1        0
     3      200        1       40CONSTANT        2        0
RESET HS(I,J) TO ZERO AT THE FOLLOWING CELLS
RESET HU(I,J) TO ZERO AT THE FOLLOWING CELLS
RESET HV(I,J) TO ZERO AT THE FOLLOWING CELLS
RESET HS(I,J) TO THE FOLLOWING DEPTHS
  END OF DATA
  END OF FILE
```

CH3D Sediment Input File (sed.inp)

```
  99999   99999   99999   99999   99999   99999   99999   99999   99990   99999
  99999   99999   99999   99999   99999   99999   99999   99999   99999   99999
  99999   99999   99999   99999   99999   99999   99999   99999   99999   99999
  99999   99999   99999   99999   99999   99999   99999   99999   99999   99999
  99999   99999   99999   99999   99999   99999   99999   99999   99999   99999
  99999   99999   99999   99999   99999   99999   99999   99999   99999   99999
  99999   99999   99999   99999   99999   99999   99999   99999   99999   99999
  99999   99999   99999   99999   99999   99999   99999   99999   99999   99999
  99999   99999   99999   99999   99999   99999   99999   99999   99999   99999
  99999   99999   99999   99999   99999   99999   99999   99999   99999   99999
  99999   99999   99999   99999   99999   99999   99999   99999   99999   99999
  99999   99999   99999   99999   99999   99999   99999   99999   99999   99999
  99999   99999   99999   99999   99999   99999   99999   99999   99999   99999
  99999   99999   99999   99999   99999   99999   99999   99999   99999   99999
  99999   99999   99999   99999   99999   99999   99999   99999   99999   99999
  99999   99999   99999   99999   99999   99999   99999   99999   99999   99999
```

114

```
99999    99999    99999    99999    99999    99999    99999    99999    99999    99999
99999    99999    99999    99999    99999    99999    99999    99999    99999    99999
99999    99999    99999    99999    99999    99999    99999    99999    99999    99999
99999    99999    99999    99999    99999    99999    99999    99999    99999    99999
      1        1        1        0        0
0 0 0 0 0 0 0 0 0 1 0 0 1 0 0 0 0 0 0 0 0 0
1 1 1 1 1 1 1
         0             0
             1.00e-6              1.00e-5
         0.00000114
  2.65      0.4
  0.60      0.10      0.100    0.030    0.010
         0.0000001       0.00000001
   100
   0.01
      0
      0             0
      0             0
1000.
      1
      1        1        1
0.100              100
      2        1        2
0.100              100
     -1       12       65        65
      2        1        2
0.100              100
     -1        7       20        20
      2        1        2
0.100              100
     -1       17       98        98
      2        1        2
0.100              100
     -1       17      167       167
      2        1        2
0.100              100
     -1       33       77        77
      2        1        2
0.100              100
     -1      -39       57        57
      1    1.000    0.000
     -2    0.000    1.000
      1        1        1        1        1
      1        2        1        1        1
      1        3        1        1        1
      1        4        1        1        1
      1        5        1        1        1
      1        6        1        1        1
      1        7        1        1        1
      1        8        1        1        1
      1        9        1        1        1
      1       10        1        1        1
      1       11        1        1        1
      1       12        1        1        1
      1       13        1        1        1
      1       14        1        1        1
      1       15        1        1        1
      1       16        1        1        1
      1       17        1        1        1
      1       18        1        1        1
      1       19        1        1        1
      1       20        1        1        1
      1       21        1        1        1
      1       22        1        1        1
      1       23        1        1        1
      1       24        1        1        1
      1       25        1        1        1
      1       26        1        1        1
      1       27        1        1        1
      1       28        1        1        1
      1       29        1        1        1
```

115

```
    1       30       1          1          1
    1       31       1          1          1
    1       32       1          1          1
    1       33       1          1          1
    1       34       1          1          1
    1       35       1          1          1
    1       36       1          1          1
    1       37       1          1          1
    1       38       1          1          1
    1       39       1          1          1
    1       40       1          1          1
  200        1      -1
  200        2      -1
  200        3      -1
  200        4      -1
  200        5      -1
  200        6      -1
  200        7      -1
  200        8      -1
  200        9      -1
  200       10      -1
  200       11      -1
  200       12      -1
  200       13      -1
  200       14      -1
  200       15      -1
  200       16      -1
  200       17      -1
  200       18      -1
  200       19      -1
  200       20      -1
  200       21      -1
  200       22      -1
  200       23      -1
  200       24      -1
  200       25      -1
  200       26      -1
  200       27      -1
  200       28      -1
  200       29      -1
  200       30      -1
  200       31      -1
  200       32      -1
  200       33      -1
  200       34      -1
  200       35      -1
  200       36      -1
  200       37      -1
  200       38      -1
  200       39      -1
 -200       40      -1
   65       12       1          2          2
   20        7       1          2          2
   98       17       1          2          2
  167       17       1          2          2
   77       33       1          2          2
  -57       39       1          2          2
    0        0
             1   1.000      0.000
            -2   1.000      0.000
             1   0.000      0.000
                 0.000      0.000
             2   0.000      1.000
                 0.000      1.000
    2        3
             1   1.000      0.000
            -2   1.000      0.000
             1   0.000      0.000
                 0.000      0.000
             2   0.000      1.000
                 0.000      1.000
```

116

CH3D Boundary Conditions (tide.inp)

```
FORTRAN 16 FILE: TIDE TABLE DATA
1   1   98   0 0      1.00      1.00
1   1   98   0 1      1.20      0.80
8   2   98   3 0      1.20      0.80
```

Sample Points

30

X	Y	Attr	X	Y	Attr	X	Y	Attr
-1438.23	-651.646	0.000927	-1783.54	-440.855	0.598889	-1830.07	-71.0274	0
-1770.07	-229.229	0.476849	-1698.78	-488.295	0.903707	-1537.58	-628.58	0.000487
-1316.09	-555.886	0.018592	-1777.57	-292.181	6.03E-06	-1471.56	-563.61	0.001589
-1497.9	-663.147	0.001544	-1623.91	-569.915	0.004137	-1851.42	-128.161	0
-1598.42	-428.96	0.434	-1732.91	-284.345	0.925357	-1911.47	-44.4565	0
-1545.87	-575.617	0.308901	-1344.94	-675.971	3.99E-05	-1300.84	-574.509	0.002972
-1750.72	-360.767	7.87E-07	-1645.27	-627.048	0.000718	-1839.58	-200.413	0
-1922.74	-65.8301	0	-1705.31	-543.344	0.004731	-1775.25	-493.819	0.000425
-1706.06	-352.931	0.026401	-1805.83	-309.157	3E-11	-1273.99	-643.096	0.665
-1910.9	-138.082	3E-11	-1817.29	-332.111	3.08E-06	-1745.57	-292.913	0.001517

50

X	Y	Attr	X	Y	Attr	X	Y	Attr
-1347.13	-601.329	0.000414	-1941.5	-7.49919	0	-1884.69	-119.381	0
-1424.61	-689.253	0.000906	-1817.11	-384.609	0.671238	-1489.45	-646.371	0.000635
-1960.37	-240.82	1.3E-06	-1851.61	-85.4529	0	-1754.34	-347.817	1.46E-06
-1790.02	-156.512	0	-1530.09	-619.707	0.003443	-1821.29	-223.955	0
-1683.63	-611.625	0.000519	-1832.47	-96.3337	0	-1367.31	-550.611	0.033791
-1539.77	-553.938	0.004847	-1560.3	-530.252	0.000455	-1463.53	-526.125	0.109934
-1842.14	-30.5648	0	-1437.22	-623.324	0.262963	-1921.43	-84.9742	0
-1803.11	-463.344	0.000355	-1485.43	-611.871	0.128686	-1855.42	-20.0047	0
-1658.31	-594.489	0.000706	-1835.08	-265.877	0	-1992.95	-24.224	4.54E-09
-1960.69	-71.1158	7.64E-05	-1581.65	-587.385	0.00678	-1854.11	-304.043	0.000471
-1565.44	-598.106	0.005971	-1641.7	-503.681	0.005003	-1421.01	-634.044	0.95699
-1864.84	-0.39532	0	-1973.54	-81.2645	0.019795	-1787.16	-427.905	0.773523

117

X	Y	Attr	X	Y	Attr	X	Y	Attr
-1836.5	-449.807	6.12E-05	-1569.82	-659.637	0.00026	-1486.58	-522.987	0.109378
-1826.71	-47.6078	0	-1645.62	-389.186	0.855	-1345.69	-539.637	0.027523
-1680.6	-462.791	2.06E-07	-1857.37	-134.179	0	-1357.98	-643.412	0.939801
-1838.18	-70.5622	0	-1618.02	-648.185	0.000507	-1359.58	-730.554	5.88E-06
-1794.82	-516.308	1.19E-05	-1592.67	-434.313	0.336443			

70

X	Y	Attr	X	Y	Attr	X	Y	Attr
-1429.99	-618.547	0.094247	-1385.99	-666.081	3.92E-05	-1945.88	-249.17	0.003293
-1363.98	-553.578	0.032262	-1572.1	-563.641	0.401029	-1744.01	-538.356	0.000132
-1693.58	-604.032	0.000519	-1783.85	-308.634	2.41E-06	-1801.08	-380.314	0.004891
-1917.36	-278.353	0.30548	-1497.23	-645.261	0.000468	-1849.28	-368.862	0.043543
-1337.32	-623.745	0.020166	-1840.91	-150.593	0	-1912.31	-359.494	1.1E-06
-1340.3	-698.082	0.000811	-1656.48	-611.407	0.000426	-1290.97	-676.18	0.000806
-1679.69	-413.115	0.006674	-1732.29	-340.956	0.950743	-1362.48	-615.43	0.010282
-1477.83	-702.301	7.62E-06	-1944.04	-85.9489	4.32E-07	-1961.26	-157.629	0.523378
-1780.2	-178.928	0	-1657.42	-422.575	0.539937	-1621.5	-537.802	0.733362
-1710.37	-377.448	0.345767	-1482.78	-547.969	0.003302	-1476.7	-668.947	0.001523
-1787.85	-465.372	0.005673	-1674.45	-492.675	0.266146	-1306.35	-584.64	0.0013
-1349.62	-605.281	0.00057	-1463.64	-558.85	0.00287	-1383.83	-672.564	1.32E-05
-1505.15	-687.503	3.95E-05	-1604.15	-637.406	0.00013	-1569.94	-570.124	0.525314
-1605.66	-453.317	0.609855	-1846.48	-197.738	0	-1781.69	-315.117	3.12E-06
-1948.04	-242.687	0.003336	-1906.52	-114.033	0	-1495.07	-651.744	0.000495
-1746.18	-531.873	0.00011	-1295.9	-644.086	0.789774	-1853.2	-254.367	1.07E-09
-1803.24	-373.831	0.000241	-1834.64	-269.99	0	-1654.32	-617.89	0.000723
-1851.45	-362.379	0.382507	-1764.34	-414.721	0.001436	-1730.13	-347.439	0.952636
-1914.48	-353.011	1.27E-06	-1329.09	-628.968	0.071652	-1941.88	-92.4319	1.36E-07
-1293.13	-669.697	0.003035	-1311.29	-552.546	0.016785	-1655.26	-429.058	0.04608
-1290.14	-595.36	0.001328	-1388.77	-640.469	0.947084	-1603.5	-459.8	0.578943
-1963.43	-151.146	0.459175	-1924.52	-192.036	0.025646	-1308.51	-578.157	0.000685
-1761.56	-440.332	0.214296	-1647.79	-562.842	0.00077	-1502.99	-693.986	4.82E-05
-1478.86	-662.464	0.001232						

118

X	Y	Attr	X	Y	Attr	X	Y	Attr
-1520.95	-505.418	0.204332	-1854.34	-95.6469	0	-1291.15	-607.925	0.00038
-1376.14	-636.563	0.935545	-1296.66	-580.572	0.00082	-1829.89	-233.828	0
-1430.69	-678.578	0.001225	-1921	-338.223	1.28E-06	-1573.1	-576.206	0.270606
-1695.58	-380.024	0.914757	-1776.19	-469.368	0.007904	-1796.69	-248.947	4.9E-09
-1276.74	-585.131	0.001151	-1720.44	-343.372	0.631246	-1887.05	-224.781	5.57E-06
-1831.24	-24.2874	0	-1966.59	-157.228	0.00381	-1433.06	-551.438	0.000503
-1826.58	-329.195	1.67E-05	-1879.32	-404.725	7.82E-06	-1932.64	-43.7856	0
-1998.24	-129.464	0	-1936.38	-246.683	0.09099	-1793.81	-323.604	5.7E-10
-1796.29	-147.418	0	-1734.52	-535.869	0.000505	-1517.45	-599.204	0.205378
-1605.52	-554.765	0.753559	-1564.17	-451.562	0.261	-1306.63	-665.379	0.005288
-1907.9	-31.3913	0	-1904.75	-152.209	0	-1484.25	-614.322	0.065241
-1911.53	-283.335	0.54928	-1281.07	-572.165	0.008831	-1361.18	-707.394	0.000412
-1788.45	-376.407	3.68E-06	-1835.56	-11.3215	0	-1869.05	-146.779	0
-1978.85	-64.2667	0.000154	-1830.9	-316.229	6.75E-06	-1377.58	-698.254	0.000775
-1301.28	-718.182	0.000201	-1310.9	-577.916	0.000657	-1932.08	-137.411	3.5E-10
-1771.02	-204.779	0	-1614.59	-508.124	2.28E-05	-1492.17	-656.565	0.001104
-1511.67	-672.716	0.000349	-1395.29	-625.682	0.133752	-1883.13	-339.276	0.190729
-1842.58	-439.131	7.77E-05	-1726.2	-392.097	2.29E-05	-1447.88	-553.523	0.001192
-1937.12	-56.2704	2E-11	-1845.27	-142.288	0	-1354.65	-652.346	0.392098
-1948.22	-174.431	0.836723	-1905.32	-58.5831	0	-1666.81	-531.171	0.007014
-1746.36	-463.617	7E-05	-1812.08	-157.406	0	-1652.36	-433.88	0.009857
-1311.11	-677.864	0.000395	-1591.47	-559.002	0.667089	-1695.63	-454.521	7.02E-07
-1929.29	-285.26	3.89E-05	-1829.14	-424.241	0.000281	-1774.42	-258.407	1.62E-06
-1727.42	-574.446	0.000426	-1907.93	-228.126	0.03111	-1785.52	-376.568	2.83E-06
-1784.48	-416.405	0.409055	-1959.49	-195.805	0.003963	-1583.65	-665.754	0.000439
-1508.12	-692.004	6.5E-05	-1546.82	-551.166	0.004308	-1551.2	-490.46	0.305988
-1397.82	-523.992	0.0547	-1751.66	-336.317	3.24E-06	-1710.08	-551.813	0.001453
-1787.02	-314.716	1.26E-07	-1669.7	-456.513	2.15E-05	-1993.72	-140.849	7.2E-10
-1393.08	-557.667	0.014908	-1636.51	-471.632	0.001429	-1822.6	-50.2194	0
-1882.87	-385.436	2.02E-05	-1513.43	-564.704	0.001546	-1863.9	-78.9246	0

X	Y	Attr	X	Y	Attr	X	Y	Attr
-1335.79	-662.194	0.004729	-1780.8	-531.174	1.06E-05	-1972.96	-111.021	0.348725
-1997.2	-93.4972	9.72E-06	-1412.51	-621.558	0.085575	-1771.09	-400.208	3.02E-05
-1786.38	-159.672	3.4E-10	-1942.3	-24.4505	0	-1626.29	-531.352	0.556177
-1717.48	-389.966	0.000397	-1400.67	-693.81	0.000841	-1656.5	-441.897	0.007259
-1572.68	-521.111	0.00056	-1460.72	-610.105	0.138332	-1395.53	-625.956	0.139862
-1639.63	-397.248	0.594576	-1725.61	-311.552	0.005193	-1581.63	-523.516	9.41E-05
-1811.66	-102.311	0	-1803.09	-399.476	0.552344	-1677.86	-499.031	0.74403
-1967.18	-184.533	0.00232	-1430.88	-604.355	0.036262	-1737.9	-415.326	7.63E-09
-1765.32	-473.72	0.004542	-1885.8	-88.8664	0	-1864.9	-207.759	0
-1330.08	-687.966	6.28E-05	-1353.03	-611.637	0.003641	-1332.13	-730.53	1.09E-05
-1799.82	-174.563	3.3E-09	-1963.28	-176.79	0.003147	-1666.02	-571.283	0.003675
-1672.45	-477.336	1.53E-07	-1761.42	-465.977	0.443119	-1570.17	-500.562	0.003823
-1389.75	-699.468	0.00072	-1680.58	-398.922	0.870377	-1838.04	-276.345	7.1E-10
-1925.51	-251.034	0.737564	-1478.72	-688.108	0.000181	-1760.19	-283.628	4.5E-05
-1345.46	-596.425	0.000873	-1308.37	-603.801	0.000506	-1287.47	-722.694	8.83E-05
-1687.84	-385.796	0.907158	-1385.85	-691.725	0.001046	-1900.7	-362.184	7.77E-06
-1873.94	-283.356	0.004996	-1842.82	-439.406	5.68E-05	-1872.17	-72.3951	0
-1799.08	-364.976	8.59E-06	-1921.61	-243.291	0.693135	-1755.9	-493.329	0.007836
-1862.11	-355.608	0.001389	-1763.63	-533.991	0.000787	-1864.66	-131.681	0
-1971.1	-70.0384	0.001235	-1836.45	-189.203	0	-1924.7	-47.9765	0
-1848.03	-163.11	0	-1634.58	-478.389	0.000384	-1923.4	-332.015	1.26E-06
-1646.16	-452.297	0.007135	-1935.65	-239.054	0.198572	-1529.46	-574.966	0.130786
-1959.26	-142.29	0.884071	-1541.72	-482.006	0.106221	-1299.06	-574.364	0.003269
-1738.66	-543.886	0.000156	-1860.79	-320.673	0.070408	-1788.48	-497.339	0.000611
-1363.46	-674.428	1.37E-05	-1939.57	-124.559	3E-10	-1782.51	-348.665	2.35E-09
-1393.67	-584.973	0.001464	-1415.28	-595.947	0.00276	-1529.09	-670.173	0.000158
-1910.69	-248.949	0.295467	-1746.19	-362.363	4.73E-06	-1689.65	-352.281	0.381113
-1857.35	-70.31	0	-1831.88	-126.091	0	-1349.88	-732.454	5.98E-06
-1305.84	-705.49	0.000606	-1873.19	-154.796	0	-1960.7	-203.982	0.00337
-1462.11	-597.3	0.058202	-1950.67	-242.72	1.85E-05	-1804.8	-216.966	1.32E-08
-1727	-298.746	0.911194	-1748.81	-531.906	8.77E-05	-1665.97	-496.785	0.091484
-1793.95	-174.884	1.93E-08	-1578.46	-447.599	0.211415	-1383.27	-718.917	3.09E-05
-1721.13	-519.672	0.003608	-1768.48	-230.664	0.438434	-1919.02	-270.483	0.485867

X	Y	Attr	X	Y	Attr	X	Y	Attr
-1294.37	-682.536	9.94E-05	-1496.31	-664.582	0.001458	-1681.36	-405.245	0.514359
-1562.25	-458.319	0.179201	-1817.43	-28.7992	0	-1867.46	-302.805	0.008936
-1964.62	-89.4873	0.003719	-1855.62	-375.057	0.000549	-1792.59	-384.425	0.000904
-1841.54	-182.559	0	-1934.41	-178.943	0.209018			

130

X	Y	Attr	X	Y	Attr	X	Y	Attr
-1378.15	-633.16	0.618915	-1749.61	-299.721	0.000191	-1686.41	-504.243	0.889068
-1578.71	-628.012	0.002098	-1595.95	-577.454	0.006203	-1813.41	-296.676	0
-1881.08	-104.639	0	-1472.87	-670.526	0.001426	-1293.41	-558.362	0.01629
-1858.96	-41.1824	0	-1316.97	-683.511	7.49E-06	-1389.63	-533.877	0.04245
-1326.18	-563.953	0.018299	-1755.2	-543.601	0.000727	-1311.78	-541.159	0.023481
-1936.44	-129.106	4.6E-10	-1815.25	-459.897	0.000181	-1608.19	-606.731	0.001882
-1655.78	-614.407	0.000521	-1767.98	-282.517	3.74E-07	-1452.29	-619.715	0.1281
-1734.57	-418.293	6.89E-09	-1942.24	-252.33	0.004918	-1849.21	-451.101	5.46E-06
-1281.52	-556.117	0.014327	-1693.11	-364.137	0.038791	-1768.38	-384.046	2.59E-07
-1359	-644.041	0.941923	-1789.33	-339.651	1.37E-09	-1566.51	-673.232	0.000361
-1815.97	-391.722	0.834714	-1647.51	-545.133	0.007371	-1851.08	-73.437	0
-1756.86	-286.594	8.65E-05	-1439.28	-584.116	0.000281	-1318.31	-596.208	0.001226
-1741.1	-473.341	0.178218	-1334.94	-564.778	0.017922	-1744.7	-528.55	0.00039
-1566.47	-598.735	0.005824	-1819.14	-148.667	0	-1514.31	-527.947	0.001711
-1850.1	-187.771	0	-1807.3	-220.919	3.84E-09	-1444	-672.679	0.001033
-1762.46	-530.475	0.000846	-1665.48	-426.4	0.006739	-1273.65	-588.372	0.00145
-1822.5	-446.77	6.18E-05	-1742.96	-514.324	0.004247	-1890.04	-107.045	0
-1775.23	-269.391	4.12E-08	-1736.99	-365.65	5.44E-05	-1324.44	-549.727	0.018575
-1934.48	-235.538	0.524141	-1841.42	-16.9682	0	-1617.87	-540.962	0.732034
-1723.67	-301.713	0.910419	-1900.16	-217.302	0.000221	-1845.38	-99.2085	0
-1654.77	-532.006	0.351444	-1963.19	-207.934	0.002074	-1312.6	-621.979	0.006845
-1588.75	-467.037	0.516419	-1903.15	-291.639	0.518292	-1922.86	-187.132	0.011886
-1726.28	-471.256	0.953675	-1897.18	-142.965	0	-1720.99	-476.319	0.941461
-1291.04	-685.503	1.36E-05	-1620.45	-513.771	0.004655	-1640.16	-409.264	0.02737
-1883.86	-79.0275	0	-1448.79	-713.501	3.98E-06	-1438.29	-698.45	0.000189
-1294.96	-571.008	0.009351	-1873.5	-287.469	0.006031	-1922.49	-282.339	0.017011
-1886.47	-248.571	0.000611	-1300.36	-592.702	0.001531	-1739.36	-459.115	0.664955
-1747.64	-528.39	0.000132	-1596.77	-658.274	0.000527	-1345.43	-702.067	0.00071

121

X	Y	Attr	X	Y	Attr	X	Y	Attr
-1306.43	-593.962	0.001377	-1896.16	-60.5641	0	-1664.49	-540.735	0.004787
-1909.13	-21.6662	0	-1497.94	-513.217	0.159984	-1743.28	-344.62	0.001086
-1565.45	-516.334	0.002965	-1895.79	-155.77	0	-1956.61	-78.3885	1.62E-05
-1907.82	-305.704	0.004774	-1756.96	-435.589	0.081831	-1549.9	-582.424	0.392019
-1705.96	-594.891	0.000496	-1768.43	-458.544	0.494609	-1773.49	-255.165	2.94E-06
-1869.5	-130.731	0	-1585.3	-635.32	0.000845	-1676.9	-374.857	0.012726
-1355.47	-541.092	0.028457	-1844.23	-188.092	0	-1754.38	-462.781	0.529637
-1474.26	-657.721	0.000431	-1322.68	-657.739	0.004947	-1382.17	-667.66	3.83E-05
-1660.37	-555.281	0.000485	-1760.91	-517.83	9.68E-05	-1449.12	-543.798	0.017128
-1872.12	-300.274	0.020554	-1820.96	-434.125	0.001038	-1572.19	-450.726	0.224253
-1585.5	-636.901	0.000453	-1935.92	-297.229	3.76E-06	-1914.57	-240.096	0.319627
-1906.62	-1.11776	0	-1932.94	-222.892	0.809089	-1712.7	-529.282	0.003984
-1589.42	-522.406	8.02E-05	-1791.12	-428.374	0.787621	-1967.06	-18.9421	2.07E-09
-1848.44	-444.778	1.6E-05	-1822.63	-54.8805	0	-1289.49	-672.857	0.002324
-1678.09	-360.471	0.617524	-1870.84	-43.4279	0			
-1755.57	-448.395	0.211838	-1670.82	-495.835	0.297159			

150

X	Y	Attr	X	Y	Attr	X	Y	Attr
-1948.55	-266.638	2.65E-06	-1773.35	-485.657	0.003741	-1792.91	-233.462	3.14E-06
-1327.2	-583.324	0.001457	-1628.54	-616.802	0.000324	-1988.9	-165.202	2.6E-10
-1773.91	-392.031	6.64E-06	-1658.75	-527.346	0.678195	-1817.81	-271.307	0
-1404.68	-671.247	0.000219	-1535.68	-620.418	0.002975	-1438.33	-611.55	0.089093
-1919.65	-72.0548	0	-1721.78	-517.979	0.003397	-1643.17	-396.701	0.447918
-1982.68	-62.6873	2.06E-05	-1920.57	-301.87	3.49E-05	-1839.17	-328.441	0.000362
-1762.07	-464.283	0.527314	-1633.95	-638.496	0.000555	-1478.42	-556.274	0.002718
-1859.6	-155.759	0	-1977.63	-143.828	0.000161	-1333.62	-687.419	9.25E-05
-1464.36	-682.749	0.000773	-1775.77	-433.014	0.62829	-2003.68	-92.7895	8.36E-07
-1729.25	-384.195	1.99E-05	-1805.97	-343.559	1.13E-06	-1609	-526.154	0.033278
-1796.2	-260.333	2.57E-09	-1682.9	-436.631	0.000315	-1723.96	-389.258	3.85E-05
-1342.22	-586.989	0.001806	-1731.11	-425.178	2.18E-06	-1853.94	-256.028	2.54E-08
-1438.44	-562.504	0.002561	-1794.14	-415.811	0.768731	-1913.99	-172.324	6.49E-06
-1631.45	-419.906	0.044916	-1619.5	-541.205	0.756204	-1288.35	-698.711	0.000321
-1896.34	-121.352	0	-1903.13	-130.241	0	-1815.15	-27.2663	0
-1973.82	-209.276	7.07E-08	-1742.57	-448.133	0.253782	-1746.25	-257.56	0.931

122

-1771.96	-498.463	0.00043	-1828.26	-211.861	0	-1496.37	-559.779	0.000628
-1829.02	-340.421	0.000103	-1607.66	-613.457	0.002319	-1633.9	-563.999	0.004266
-1318.91	-636.287	0.298641	-1987.52	-178.007	1.47E-09	-1936.28	-40.6255	0
-1911.73	-29.8119	0	-1816.43	-284.113	0	-1325.65	-570.678	0.006466
-1989.21	-117.736	1.11E-05	-1284.59	-618.051	0.001556	-1577.77	-533.208	0.000214
-1787.35	-406.922	0.114316	-1741.56	-365.732	8.43E-06	-1828.59	-42.157	0
-1642.54	-538.067	0.500948	-1837.78	-341.246	0.007799	-1809.44	-53.0378	0
-1807.02	-105.68	0	-1626.96	-407.421	0.545986	-1849.17	-92.968	0
-1334.3	-544.746	0.022351	-1558.06	-637.715	0.001945	-1967.95	-209.597	1.44E-06
-1411.78	-632.67	0.876012	-1492.05	-572.745	0.002425	-1766.09	-498.783	0.001589
-1868.75	-380.351	3.81E-05	-1629.58	-576.965	0.0007	-1930.57	-66.397	0
-1805.31	-288.19	4E-11	-1931.95	-53.5915	0	-1457.84	-505.463	0.0931
-1789.56	-474.937	0.001101	-1321.33	-583.644	0.001377	-1572.06	-558.98	0.256602
-1862.38	-130.148	0	-1573.45	-546.174	0.025799	-1776.91	-344.131	3.22E-09
-1898.55	-189.367	5.96E-08	-1824.26	-55.123	0	-1431.18	-575.63	0.001585
-1961.58	-179.999	0.003838	-1808.1	-140.341	0	-1762.09	-342.046	3.43E-06
-1429.74	-513.938	0.0734	-1806.8	-424.379	0.248061	-1811.04	-140.18	0
-1781.64	-432.694	0.751995	-1368.57	-564.289	0.008878	-1966.57	-222.403	7.11E-07
-1811.84	-343.238	5.03E-06	-1524.1	-646.511	0.001339	-1764.7	-511.589	0.000133
-1853.15	-371.943	0.001673	-1710.2	-544.071	0.003524	-1619.9	-642.734	0.000619
-1736.98	-424.858	4.81E-06	-1773.23	-534.704	3.08E-05	-1922.28	-119.36	9.12E-09
-1800.01	-415.49	0.813529	-1889.5	-113.77	0	-1650.11	-553.278	0.003017
-1406.07	-658.442	6.68E-05	-1966.99	-201.694	0.000648	-1527.03	-646.35	0.001743
-1909	-129.921	3E-11	-1882.23	-249.134	0.000129	-1713.14	-543.911	0.002351
-1417.54	-681.396	0.001149	-1961.02	-53.0197	1.16E-06	-1911.92	-327.802	2.29E-05
-1748.44	-447.812	0.220389	-1807.36	-330.753	8.18E-08	-1968.99	-169.76	0.001309
-1834.13	-211.54	0	-1684.29	-423.825	0.001924	-1767.12	-458.946	0.591823
-1875.44	-240.245	2.03E-06	-1916.36	-45.1837	0	-1331.88	-673.193	0.000369
-1580.71	-533.048	0.002139	-1979.39	-35.8163	1.84E-07	-1797.33	-369.491	9.96E-06
-1785.56	-318.199	4.55E-07	-1758.78	-437.412	0.139286	-1674.25	-462.563	4.01E-06
-1439.82	-549.698	0.000439	-1989.28	-69.9955	7.32E-05	-1722.46	-451.11	2.69E-07
-1816.7	-39.9115	0	-1904.52	-117.436	0	-1785.49	-441.743	0.464793
-1819.68	-114.249	0	-1967.55	-108.068	0.923538	-1610.85	-567.137	0.006005
-1975.21	-196.471	1.17E-06	-1858.92	-298.432	0.000553	-1894.49	-156.173	0

123

Variogram Equation

Variogram Equations are specified in the format required by GSTAT. (Pebesma, 1999)

A Nug(0) + B Sph(C, D, E)

where A is the nugget, B is the partial sill (sill − nugget), C is the range, D is the anisotropy angle and E is the anisotropy ratio. Sph denotes a spherical variogram model.

<u>Standard</u>

30: 0.106487 Sph(160, 315,0.48)

50: 0.082778 Sph(265,315,0.39)

70: 0.076135 Sph(140,315,0.45)

90: 0.051811 Sph(160,315,0.44)

110: 0.03653 Nug(0) + 0.033597 Sph(365,315,0.43)

130: 0.068813 Sph (85,315,0.45)

150: 0.05112 Sph(150,315,0.25)

<u>Flowline</u>

30: 0.103582 Sph(240,90,0.35)

50: 0.000608 Nug(0) + 0.080303 Sph(260,90,0.34)

70: 0.011578 Nug(0) + 0.065994 Sph(235,90,0.39)

90: 0.052367 Sph(145,90,0.24)

110: 0.015603 Nug(0) + 0.04867 Sph(145,90,0.33)

130: 0.074783 Sph(115,90,0.34)

150: 0.054159 Sph(205,90,0.21)

Appendix D – Channel with Island Simulation Inputs

CH3D Channel Geometry (grid.inp)

Although the CH3D grid file describing the channel geometry is too large to include in an appendix, a brief description of the channel follows.

The two ends of the channel are 205 m wide and 250 m long. They are divided into a computational mesh with regular square cells $5m^2$. The island is placed in the exact centre of the channel. The channel is 1000 m long measured straight through the centre of the channel and the centre of the island. Measuring along the centreline, the island begins 5 m wide at the 250 m mark. It increases in width linearly to 200 m wide at the 500 m mark. It then constricts linearly to 5 m wide at the 750 m mark. At the 500 m mark, the channels flowing around the island are 100 m wide each, measured vertically. This creates 2 channels divided into 4 areas off each side of the island. The computational mesh for each of these areas is created by placing 20 equal length segments vertically along the width of each channel at the 250 m, 500 m and 750 m marks. Then 50 equal length segments are placed along the banks of each channel and the island. The mesh is created by connecting the endpoints of the segments across and along the channels.

CH3D Main Input File (main.inp)

```
TITLE(A80)
Jason Wintermute, Test run.
    IT1     IT2       DT  ISTART    ITEST   ITSALT    ISCOM  NTSED0NDTINDTS
      1    1500        1       0        0        0        1     300         1
  WPRCRD
      0
  WXCEL1  WXCEL2  WYCEL1  WYCEL2  WZCEL1  WZCEL2  WPRINT  WPRSTR  WPREND  WPRVAR
  SNPCRD
      1
  SXCEL1  SXCEL2  SYCEL1  SYCEL2  SZCEL1  SZCEL2  SNPINT  SNPSTR  SNPEND  SNPVAR
      1     200       1      41       1       2      10     300    1500CBUV
   NRANG
      0
  RANGDR   RPOS1   RPOS2   RPOS3  RRNAME
     IGI     IGH     IGT     IGS     IGU     IGW     IGC     IGQ     IGP
       0       1       0       0       0       0       0       0       0
    XREF    ZREF    UREF     COR      GR     RO0     ROR      T0      TR
     500     200      20     1.0   981.0    1.00   1.021      20      20
   THETA
     0.6
```

125

```
ITEMP   ISALT    ICC      IFI    ifitim    IFA      IFB      IFC      IFD
   0       0       0        0        0        0        0        0        1
 TWE     TWH     FKB
   0       0       0
IEXP    IAV     AVR      AV1      AV2      AVM     AVM1      AHR
   1       0       1       0.       0.    0.002    0.002    10000
 IVIS    IQW     IPT
   0       0       0
GAMAX   GBMAX
60000   60000
IWIND   TAUX    TAUY
   0     0.00    0.00
 ISPAC(I),I=1,10
   0       0       0        1        0        0        0        0        0        0
 JSPAC(I),I=1,10
   1       1      -1        0        0        0        0        0        0        0
 RSPAC(I),I=1,10
0.035000      0 0.00000  0.00000      0        0        0    0.000     0.00        0
 IBTM    HADD    HMIN      H1       H2      SSS0     HMAX
   4     0.0     0.0      0.0      0.0      1.0   999999.
ISMALL   ISF     ITB    ZREFBN     CTB      BZ1    ZREFTN      TZ1
   1       0       5        5     0.003    0.200       5      2.0
 XMAP   ALXREF  ALYREF
100.0      0       0
ITRAN   IBD(1)  IBD(2)   IBD(3)   IBD(4)
   2       4       4        4        4
ITBRK(1)   (2)     (3)      (4)      (5)      (6)      (7)      (8)      (9)     (10)
   0       0       0        0        0        0        0        0        0        0
 NSTA    NFREQ   NSTART       (CURRENT STATIONS)
   0       0       0
IST JST  STATID(K)    (2I4,A48)     ( ONE CARD FOR EACH STATION )
 NSTAS   NFREQS  NSTRTS     (TIDE STATIONS)
   0       0       0
IST JST  STATID(K)    (2I4,A48)     ( ONE CARD FOR EACH STATION )
 MSTA    MFREQ   MSTART     (SALINITY STATIONS)
   0       0       0
IST JST  STATID(K)    (2I4,A48)      ( ONE CARD FOR EACH STATION )here
 NRIVER
  -6
IJRDIR  IJRROW  IJRSTR   IJREND       ( ONE CARD FOR EACH RIVER )
   2      12      82       82
   2      21      46       46
   2      37      35       35
   2      20      46       46
   2      22      46       46
   2      24     136      136
   I       J    QRIVER              ( ONE CARD FOR EACH CELL )
  82      12       0
  46      21       0
  35      37       0
  46      20       0
  46      22       0
 136      24       0
 NBAR
   0
IJBDIR  IJBROW  IJBSTR   IJBEND     ( ONE CARD FOR EACH BAR )
TIDFNO  TIDBND
   2       2
TIDSTR     2       3        4        5        6        7        8        9       10
   1       1       1        1        1        1
IJTDIR  IJTROW  IJTSTR   IJTEND   TIDTYP   TIDFN1   TIDFN2
   1       1       1       41CONSTANT        1        0
   3     200       1       41CONSTANT        2        0
RESET HS(I,J) TO ZERO AT THE FOLLOWING CELLS
  51      21
  52      21
  53      21
  54      21
  55      21
  56      21
  57      21
```

126

```
 58    21
 59    21
 60    21
 61    21
 62    21
 63    21
 64    21
 65    21
 66    21
 67    21
 68    21
 69    21
 70    21
 71    21
 72    21
 73    21
 74    21
 75    21
 76    21
 77    21
 78    21
 79    21
 80    21
 81    21
 82    21
 83    21
 84    21
 85    21
 86    21
 87    21
 88    21
 89    21
 90    21
 91    21
 92    21
 93    21
 94    21
 95    21
 96    21
 97    21
 98    21
 99    21
100    21
101    21
102    21
103    21
104    21
105    21
106    21
107    21
108    21
109    21
110    21
111    21
112    21
113    21
114    21
115    21
116    21
117    21
118    21
119    21
120    21
121    21
122    21
123    21
124    21
125    21
126    21
127    21
128    21
```

```
129    21
130    21
131    21
132    21
133    21
134    21
135    21
136    21
137    21
138    21
139    21
140    21
141    21
142    21
143    21
144    21
145    21
146    21
147    21
148    21
149    21
150    21
RESET HU(I,J) TO ZERO AT THE FOLLOWING CELLS
RESET HV(I,J) TO ZERO AT THE FOLLOWING CELLS
RESET HS(I,J) TO THE FOLLOWING DEPTHS
     END OF DATA
     END OF FILE
```

CH3D Sediment Input File (sed.inp)

```
     99999    99999    99999    99999    99999    99999    99999    99999    99990    99999
     99999    99999    99999    99999    99999    99999    99999    99999    99999    99999
     99999    99999    99999    99999    99999    99999    99999    99999    99999    99999
     99999    99999    99999    99999    99999    99999    99999    99999    99999    99999
     99999    99999    99999    99999    99999    99999    99999    99999    99999    99999
     99999    99999    99999    99999    99999    99999    99999    99999    99999    99999
     99999    99999    99999    99999    99999    99999    99999    99999    99999    99999
     99999    99999    99999    99999    99999    99999    99999    99999    99999    99999
     99999    99999    99999    99999    99999    99999    99999    99999    99999    99999
     99999    99999    99999    99999    99999    99999    99999    99999    99999    99999
     99999    99999    99999    99999    99999    99999    99999    99999    99999    99999
     99999    99999    99999    99999    99999    99999    99999    99999    99999    99999
     99999    99999    99999    99999    99999    99999    99999    99999    99999    99999
     99999    99999    99999    99999    99999    99999    99999    99999    99999    99999
     99999    99999    99999    99999    99999    99999    99999    99999    99999    99999
     99999    99999    99999    99999    99999    99999    99999    99999    99999    99999
     99999    99999    99999    99999    99999    99999    99999    99999    99999    99999
     99999    99999    99999    99999    99999    99999    99999    99999    99999    99999
     99999    99999    99999    99999    99999    99999    99999    99999    99999    99999
     99999    99999    99999    99999    99999    99999    99999    99999    99999    99999
          1        1        1        0        0
0 0 0 0 0 0 0 0 0 1 0 0 1 0 0 0 0 0 0 0 0 0
1 1 1 1 1 1 1
          0        0
             1.00e-6             5.00e-5
          0.00000114
       2.65      0.4
       0.60      0.10     0.100    0.030    0.010
          0.0000001         0.00000001
        100
        0.01
          0
          0        0
          0        0
       1000.
          1
          1        1        1
```

```
0.100              100
    2       1        2
0.100              100
   -1      12       82       82
    2       1        2
0.100              100
   -1      21       46       46
    2       1        2
0.100              100
   -1      37       35       35
    2       1        2
0.100              100
   -1      22       46       46
    2       1        2
0.100              100
   -1      20       46       46
    2       1        2
0.100              100
   -1     -24      136      136
    1   1.000    0.000
   -2   0.000    1.000
    1       1        1        1        1
    1       2        1        1        1
    1       3        1        1        1
    1       4        1        1        1
    1       5        1        1        1
    1       6        1        1        1
    1       7        1        1        1
    1       8        1        1        1
    1       9        1        1        1
    1      10        1        1        1
    1      11        1        1        1
    1      12        1        1        1
    1      13        1        1        1
    1      14        1        1        1
    1      15        1        1        1
    1      16        1        1        1
    1      17        1        1        1
    1      18        1        1        1
    1      19        1        1        1
    1      20        1        1        1
    1      21        1        1        1
    1      22        1        1        1
    1      23        1        1        1
    1      24        1        1        1
    1      25        1        1        1
    1      26        1        1        1
    1      27        1        1        1
    1      28        1        1        1
    1      29        1        1        1
    1      30        1        1        1
    1      31        1        1        1
    1      32        1        1        1
    1      33        1        1        1
    1      34        1        1        1
    1      35        1        1        1
    1      36        1        1        1
    1      37        1        1        1
    1      38        1        1        1
    1      39        1        1        1
    1      40        1        1        1
    1      41        1        1        1
  200       1       -1
  200       2       -1
  200       3       -1
  200       4       -1
  200       5       -1
  200       6       -1
  200       7       -1
  200       8       -1
  200       9       -1
```

129

```
     200        10        -1
     200        11        -1
     200        12        -1
     200        13        -1
     200        14        -1
     200        15        -1
     200        16        -1
     200        17        -1
     200        18        -1
     200        19        -1
     200        20        -1
     200        21        -1
     200        22        -1
     200        23        -1
     200        24        -1
     200        25        -1
     200        26        -1
     200        27        -1
     200        28        -1
     200        29        -1
     200        30        -1
     200        31        -1
     200        32        -1
     200        33        -1
     200        34        -1
     200        35        -1
     200        36        -1
     200        37        -1
     200        38        -1
     200        39        -1
     200        40        -1
    -200        41        -1
      82        12         1         3         3
      46        21         1         2         2
      35        37         1         3         3
      46        22         1         2         2
      46        20         1         2         2
    -136        24         1         3         3
       0         0
                 1     1.000     0.000
                 2     1.000     0.000
                -3     1.000     0.000
                 1     0.000     0.000
                       0.000     0.000
                 2     0.000     0.333
                       0.000     0.333
                 3     0.000     0.100
                       0.000     0.100
       2         3
                 1     1.000     0.000
                 2     1.000     0.000
                -3     1.000     0.000
                 1     0.000     0.000
                       0.000     0.000
                 2     0.000     0.333
                       0.000     0.333
                 3     0.000     0.100
                       0.000     0.100
```

CH3D Boundary Conditions (tide.inp)

```
FORTRAN 16 FILE: TIDE TABLE DATA
1   1   98   0 0       1.00      1.00
1   1   98   0 1       1.20      0.80
8   2   98   3 0       1.20      0.80
```

Sample Points

30

X	Y	Attr	X	Y	Attr	X	Y	Attr
586.0774	244.8073	9.72E-06	358.8203	35.88452	0.010501	663.7345	50.40145	0.024008
479.1573	-53.2476	0.001506	80.82793	154.1416	0	787.9895	204.7509	1.12E-09
334.6565	-6.17971	2.75E-09	671.0669	183.7679	1.29E-07	378.5411	238.7272	0.236746
766.3862	8.956636	1.79E-05	945.0101	24.5942	1.1E-09	246.1878	2.544692	0
976.1772	158.15	7.83E-07	231.2389	86.79844	0.046258	113.1997	21.33056	0
924.6761	130.8633	0.37517	441.03	235.9918	0.003828	768.0062	1.038177	1.52E-07
539.7637	-48.9345	0.03201	389.5289	208.7051	0.001024	710.1531	37.03782	0.419508
65.26595	141.5071	0	4.616402	28.90727	0	945.3773	124.3587	0.510827
655.9203	23.58179	0.7015	419.2737	188.6192	0.256937	889.5861	109.4288	0.609209
720.0724	121.2148	0.410727	483.4258	286.2522	0.00839	555.5401	211.8861	0.00022

50

X	Y	Attr	X	Y	Attr	X	Y	Attr
161.6232	34.17332	0	300.0611	155.8023	0.004989	415.2989	22.27356	0.07673
935.4973	28.68551	2.69E-09	902.863	160.6266	1.57E-06	442.505	210.061	0.010602
120.628	83.41129	0	587.9247	-36.9618	0.007268	57.59253	30.26322	0
64.57432	67.6114	0	113.4269	153.4799	5.1E-10	521.7156	-33.2681	0.834563
420.0044	268.3652	0.048859	457.3442	-23.4843	0.884892	928.0121	43.74069	2.35E-08
960.4271	19.2164	1E-11	375.8573	22.58825	0.001536	846.5251	89.81326	0.000383
824.0246	148.1174	5.76E-05	4.230494	64.16834	0	424.6667	0.169948	0.251031
124.1738	176.7312	2.93E-06	223.8928	138.8547	7.41E-06	146.6744	118.4271	5.5E-10
798.9851	8.294877	1.7E-05	416.349	25.75364	0.092901	201.349	88.87205	0.001309
178.8484	147.1762	7.02E-09	405.0555	-53.3811	4E-11	94.42888	196.8171	1.5E-10
396.7378	-27.7974	9.1E-07	268.653	75.51989	0.047795	70.76854	102.3495	0
933.1113	88.13731	0.000591	321.2923	201.4349	0.020392	290.4308	177.0359	0.004272
612.351	5.972452	0.832597	253.091	62.88538	0.028867	166.1759	22.6865	0
437.2296	-24.632	0.427079	579.6734	29.62672	0.042082	820.9823	2.394123	7.77E-08
712.9456	65.85427	0.026062	301.6811	147.8839	0.190445	222.8427	135.3747	4.33E-05
606.0255	173.7993	0.000231	474.5262	-18.7683	0.880584	565.0303	223.0373	0.000156
868.4558	42.90769	3.9E-05	855.3895	120.113	0.871444			

131

70

X	Y	Attr	X	Y	Attr	X	Y	Attr
851.2275	155.4091	4.47E-06	576.2775	13.3895	0.384395	718.9839	68.51825	0.019895
973.2062	112.5019	0.41256	401.1561	-17.215	0.002015	4.074531	32.0942	0
335.7346	-10.9112	5.3E-10	358.3881	188.3631	0.000712	701.649	212.2238	2.4E-10
508.5797	228.4366	4.73E-05	304.1072	16.22311	9.74E-08	849.0609	107.4441	0.188921
782.5228	69.26296	0.000879	342.8261	175.7286	0.004042	938.6461	143.2046	0.011478
741.5276	118.5009	0.860098	832.3823	50.32474	0.000454	743.9136	59.04914	0.114292
916.649	149.1054	0.000995	263.112	65.46108	0.019758	752.012	140.8822	0.212563
942.9578	184.9912	2.7E-10	410.5239	-39.3186	7.96E-08	279.2871	174.9838	0.011687
583.4786	-56.6791	0.001525	500.1091	-3.55808	0.054201	612.9345	223.8245	2.18E-06
859.1946	33.80718	8.72E-06	367.7558	166.2594	0.440215	912.3108	2.778314	1.2E-10
752.2745	141.7522	0.121266	548.9186	-25.9764	0.78751	465.0192	-24.9925	0.875986
773.6585	38.96322	0.015476	74.42083	164.4653	0	396.8179	242.458	0.165555
655.2256	175.1903	6.8E-05	418.3381	-12.4989	0.485263	620.5294	-47.9391	0.000529
612.4575	-25.2317	0.008239	336.8512	33.57366	0.000435	317.1039	132.1905	0.720064
297.5192	183.18	0.013773	978.3719	197.9034	1E-11	526.8949	281.3838	0.000111
229.3179	44.63045	6.7E-07	873.2247	149.5084	0.002325	421.7477	232.9888	0.007191
147.831	90.70303	6.51E-09	190.7087	34.41662	1E-11	605.843	37.18466	0.036228
451.0156	-36.1532	0.034083	83.78859	142.3617	0	866.5005	62.63308	0.00013
566.0341	-62.2652	0.000821	110.0974	178.2475	7.17E-08	457.9277	194.3677	0.344539
497.8328	205.1853	0.201998	541.8271	193.3838	0.015146	992.5283	60.64243	1.59E-08
987.3891	79.78151	4.48E-05	778.8242	124.3647	0.911993	350.5306	53.2566	0.200829
627.9098	244.1112	1.09E-07	393.9118	-55.4332	0	734.3265	188.5695	4.66E-08
920.9607	190.892	3E-11	109.4843	81.35922	0			
460.3834	-58.2568	1.88E-06	12.4354	114.7973	0			

90

X	Y	Attr	X	Y	Attr	X	Y	Attr
334.6567	-23.5262	0	70.56318	6.997107	0	902.111	9.390726	2.68E-09
542.1715	-71.5894	1.92E-05	280.0917	155.3204	0.000134	940.8299	168.8962	7.3E-07
691.8597	20.88751	0.34902	429.7799	247.7974	0.009625	861.1158	58.62869	0.000321
289.6124	-15.2048	1E-11	114.8416	50.20902	0	27.13882	7.400077	0
117.2707	99.04401	0	641.3438	240.6507	9.12E-08	775.5797	63.78473	0.009027

132

X	Y	Attr	X	Y	Attr	X	Y	Attr
820.8866	56.33332	0.000693	985.2611	63.68648	9.09E-08	238.7028	0.253388	0
105.9773	19.90927	0	903.7742	109.7591	0.590635	877.1812	18.85984	2.71E-07
803.5517	200.0389	1.45E-09	747.7605	185.109	2.98E-08	867.9647	13.96724	9.14E-08
950.9636	95.25921	0.003014	704.9925	-15.313	5.39E-05	247.8279	152.8485	3.93E-05
39.54887	131.0197	0	252.7328	115.9546	0.72388	117.2475	166.326	1.21E-07
845.8163	46.86421	0.000253	167.1967	121.1106	4.17E-08	309.7037	53.2249	0.000289
853.9147	128.6973	0.65863	314.6086	16.33095	1.01E-07	204.5564	4.829898	0
381.1898	162.7989	0.664724	670.0386	217.0847	2.01E-09	952.9973	61.21455	5E-09
445.3419	260.4319	0.053245	957.9022	24.3206	2E-11	212.6548	86.66298	0.009905
180.3727	193.1969	0.014091	483.4045	214.7623	0.062036	822.4168	74.69202	0.000278
796.4603	13.39908	0.000113	872.3661	29.47664	7.75E-07	740.9299	120.7646	0.862302
648.545	170.5821	0.000485	652.2004	7.193607	0.554129	48.28025	79.30982	0
549.7232	-45.6398	0.02437	609.4323	212.7716	2.83E-06	373.0898	202.3912	0.000761
500.6297	-78.2349	9.15E-05	53.18513	42.41586	0	7.285065	128.5478	0
166.5836	24.22235	0	91.90401	201.9213	3E-11	174.3081	77.31917	4.53E-08
350.9415	235.2882	0.249066	12.18994	91.65383	0	526.3237	-17.812	0.915843
930.083	145.6449	0.008087	179.213	40.42521	0	710.6816	193.2539	3.2E-10
267.1782	84.10417	0.348867	927.6538	96.80987	0.004512	712.4544	36.91382	0.397462
924.6548	59.37341	8.8E-08	390.7769	33.27852	0.103664	626.9183	42.06986	0.017488
621.2292	239.503	2.37E-07	797.0734	110.2873	0.304468	283.3949	17.3391	8.97E-08
502.7963	-30.2699	0.932862	717.3593	0.019863	7.56E-05	980.9693	197.4687	0
858.2264	170.4838	9.41E-07	293.728	66.7166	0.091568	216.9665	128.4495	1.71E-05
671.5922	168.1614	0.00019	15.73567	184.9737	0	819.7684	133.2738	0.488225
261.2465	50.23607	7.75E-06	690.547	16.53742	0.195184	770.6748	100.6787	0.014991
797.62	166.1708	4.83E-05	70.41032	155.4187	0	30.33229	126.1271	0

110

X	Y	Attr	X	Y	Attr	X	Y	Attr
951.9142	24.2222	3.6E-10	271.3223	131.7942	0.373881	805.4859	91.47712	8.45E-05
15.06624	121.8552	0	735.4453	68.26285	0.032031	510.1587	-52.5602	0.071528
530.0557	-65.4211	0.007351	140.7418	145.2717	1.1E-10	379.5783	-39.0827	1E-11
252.0634	52.83601	5.34E-06	492.9768	-57.2762	0.001449	298.0914	6.989847	6.37E-09
534.1049	-24.5046	0.914837	133.4975	107.0535	2E-11	161.6889	135.8908	4E-11
85.04035	104.0646	0	28.35024	58.65846	0	146.1269	123.2563	1.1E-10
720.2356	30.22121	0.160939	409.2135	197.5397	0.012997	338.5831	10.15524	9.42E-08

133

X	Y	Attr	X	Y	Attr	X	Y	Attr
664.1819	14.42132	0.609097	341.0123	58.99023	0.228261	867.7555	196.1585	1.3E-10
621.4138	219.9993	2.05E-06	436.4196	-20.6728	0.773671	334.9277	173.5437	0.002861
572.3203	187.4042	0.003396	667.5947	25.73157	0.656799	869.5283	39.81848	1.6E-05
674.9287	37.67262	0.425628	562.4474	-22.6634	0.747999	249.3916	178.6998	0.08493
221.815	125.3253	0.00025	943.3107	116.2179	0.609755	80.09227	32.67179	0
394.6601	-41.3268	1.4E-10	310.7639	131.4795	0.730683	118.8112	192.1772	5.04E-07
775.5234	97.55444	0.008086	460.4521	223.9564	0.000613	39.09709	81.90976	0
668.6032	205.4995	6.59E-09	145.5138	26.36807	0	685.5426	-21.0857	8.72E-05
931.0336	74.60786	2.75E-06	812.4677	128.8253	0.761361	775.1279	14.67478	0.000157
571.5543	238.9376	0.000556	998.5985	183.5511	1E-09	642.7746	184.4923	6.2E-06
864.6052	185.7183	4.52E-09	827.4166	44.57155	0.000238	390.2155	240.877	0.189018
671.0307	-30.2401	0.000204	57.59169	90.9759	0	854.3385	177.3456	2.2E-07
446.0499	-41.9064	0.000388	16.59651	140.2139	0	197.2558	0.381403	0
789.9671	187.1294	7.8E-10	961.5428	124.414	0.432986	299.9739	-0.05859	1E-11
572.0777	-43.897	0.005262	752.6273	72.97889	0.010292	941.4946	164.2711	4.06E-07
556.5157	-56.5315	0.005558	797.1682	117.0608	0.813909	99.15679	30.3394	0
107.4512	72.03768	0	519.1759	235.3179	0.000233	608.3242	-41.5134	0.000873
103.402	31.12114	0	692.021	68.66582	0.000671	933.1338	81.56802	3.57E-05
706.2039	35.9454	0.447892	289.7737	32.57354	4.78E-08	777.1201	156.918	3.67E-05
391.2656	244.357	0.206661	931.2944	196.9032	4E-11	866.7054	192.6785	2.4E-10
917.7678	28.79871	3.18E-09	223.3453	143.684	2.11E-06	680.0712	190.356	1.13E-08
587.53	225.4459	3.97E-05	272.1547	121.2657	0.69342	288.8333	178.3851	0.026301
43.69291	178.7097	0	122.4665	28.78874	0	806.099	188.3654	7.2E-10
490.4811	258.8839	0.006184	658.84	144.7234	0.008016	675.4089	52.55124	0.069247
659.277	51.31527	0.003285	256.5927	108.6312	0.051692	595.6948	-57.7162	0.000383
748.8623	87.07577	0.000116	891.788	34.78775	2.92E-07	436.5724	236.9056	0.004863
554.1297	2.920268	0.632967	835.7343	18.98786	3.96E-05	566.6495	275.8315	2.43E-05
301.5706	59.30492	0.007659	540.4071	280.9505	5.76E-05	743.6102	191.1007	8.88E-08
216.0345	64.46096	2.1E-06	392.4918	32.13355	0.092516	567.1529	223.4282	0.000168
186.2896	84.54688	6.3E-06	191.9372	63.40156	1.52E-08			

130

X	Y	Attr	X	Y	Attr	X	Y	Attr
850.6203	39.53206	7.82E-05	946.3566	1.743883	0	566.4104	190.333	0.005237
623.4943	34.04424	0.087118	339.1333	211.8414	0.011334	422.5443	-17.5674	0.68103

134

809.6251	88.77002	6.94E-05	537.4116	-16.6832	0.916283	294.2402	193.1667	0.022014
753.5713	72.97013	0.00902	768.5867	29.7212	0.004745	463.036	-14.402	0.796482
143.5252	29.92767	0	663.4394	-18.6738	9.86E-05	631.8319	184.0293	1.97E-05
7.122658	158.8286	0	43.3027	120.2075	0	319.1699	183.6975	0.00095
370.6511	35.41548	0.041278	958.7666	125.3635	0.423186	988.116	22.39795	0
543.4961	274.7634	6.85E-05	105.1785	20.58386	0	367.9793	161.2792	0.61269
861.9802	159.6716	5.94E-06	194.7637	56.34436	3.84E-09	198.68	15.25126	0
527.9342	262.1288	0.003559	476.8052	-20.9962	0.893189	237.3989	174.7567	0.066681
16.49042	136.725	0	160.9697	35.51373	0	72.1487	69.64527	0
12.44125	95.80849	0	460.346	220.4676	0.003665	598.651	260.0869	5.86E-06
64.18328	69.82183	0	13.05436	192.6967	0	942.5682	83.12274	0.000103
731.1372	172.2791	1.89E-05	230.9438	17.72319	3.3E-10	861.0813	129.1953	0.62742
853.1159	129.3719	0.645471	164.5154	128.8336	3.2E-10	360.8879	-25.3606	2E-11
153.2651	157.9857	3.36E-06	767.3173	133.6579	0.670295	938.2565	41.33618	1.18E-09
388.4894	245.3066	0.202314	978.8812	126.5112	0.300039	660.2642	159.5933	0.014978
706.9734	130.2148	0.824145	384.1777	203.52	0.000185	212.9726	131.8225	1.45E-05
600.0533	238.1599	3.46E-06	24.71836	137.4185	0	430.862	-43.1511	5.5E-06
962.2027	69.3918	5.25E-07	325.8676	166.0323	0.012791	127.4365	136.9785	0
709.6435	125.7765	0.414861	561.0918	253.3532	0.000284	274.8483	32.19884	1.6E-06
172.7666	62.24511	9E-11	879.5759	138.2615	0.110838	912.3199	155.612	1.63E-05
476.1921	288.1155	0.008886	545.5299	240.7187	0.001448	832.6058	45.34453	0.000247
306.8928	142.0875	0.561301	34.08613	115.3149	0	747.0697	50.50057	0.157661
283.2325	47.61996	0.003741	167.3151	43.25563	0	117.4556	62.19386	0
835.1679	176.1892	1.14E-06	111.2614	27.45574	0	403.5463	25.76981	0.051643
912.3432	88.33003	0.000536	466.6914	228.2095	0.000259	247.5326	101.1197	0.168982
142.5183	134.7344	0	19.39977	200.4386	0	166.0457	147.1923	5.8E-10
486.4355	-42.2298	0.257466	870.7116	107.9617	0.571742	338.8907	-19.4598	0
404.9486	3.842752	0.013367	448.8531	18.3184	0.102507	719.754	119.4215	0.098689
268.5461	132.7437	0.271253	170.8608	136.5755	5E-10	612.8339	227.3665	2.19E-06
252.9841	120.1092	0.679323	343.7059	-30.0766	0	875.2642	96.4749	0.004791
445.4403	7.008142	0.036143	617.649	216.7497	1.59E-06	7.493173	24.41565	0
472.6464	194.7956	0.309783	376.9965	43.15738	0.201102	952.4394	8.615762	0
87.73395	14.9978	0	979.7984	47.98165	4E-11	306.8695	209.3695	0.346374
970.5203	43.80811	1.6E-10	190.3623	40.83496	1E-11	860.5779	181.5987	4.78E-08
350.3836	182.6894	0.001014	579.3239	261.5493	4.44E-05	526.5318	284.0559	7.07E-05
219.8032	196.1669	0.23554	359.1582	239.2663	0.212106	648.5105	241.1487	4.13E-08

135

608.7648	10.88122	0.786967	316.3901	38.84431	0.00091	226.652	151.5054	4.96E-08
503.6175	-37.5138	0.536882	369.0294	164.7593	0.564376	382.3816	21.14205	0.001749
884.4808	101.3675	0.01312	300.8282	26.2098	8.52E-08	215.3585	72.37066	7.92E-05
753.9003	114.845	0.407146	929.9389	66.91987	2.68E-08	211.3094	31.45412	2.1E-10
38.991	78.42092	0	160.114	113.3242	1.18E-08	751.732	188.3054	4.69E-08
765.0177	3.683278	1.55E-07						

150

X	Y	Attr	X	Y	Attr	X	Y	Attr
805.9721	78.6937	0.000129	856.0924	182.0509	6.19E-08	782.1356	199.9297	4.02E-09
491.0337	287.1053	0.005955	496.6132	-59.6194	0.001198	18.13274	130.9105	0
689.312	58.58073	0.018698	772.3292	30.86685	0.00502	368.3755	192.1194	0.000648
343.1184	38.28835	0.001071	255.0634	20.88655	3E-11	832.4986	128.5881	0.729732
920.4871	104.9851	0.221561	686.7931	36.02289	0.547115	62.67365	174.9925	0
580.1156	-30.7308	0.015934	896.5842	185.2163	7E-11	723.3021	39.27656	0.301345
815.3398	56.59008	0.000723	657.9454	208.0105	7.96E-09	958.5264	126.5975	0.402868
195.2031	195.4714	0.076424	476.4986	-60.7671	1.85E-05	512.132	250.7283	0.002428
584.1847	185.7545	0.000278	2.000841	129.6746	0	405.2118	-47.3267	7.3E-10
671.4936	24.25841	0.650793	90.53602	161.955	1E-11	364.2167	1.911295	1.37E-05
84.88844	183.1003	7E-11	650.5698	-33.6427	0.000399	531.2397	-49.3173	0.040341
5.174382	72.83282	0	607.8018	171.9353	0.000233	278.6806	7.067334	2E-11
539.775	-60.8924	0.014072	926.2859	56.84355	1.16E-07	805.1828	197.509	1.54E-09
920.6383	77.98886	1.53E-05	819.3657	164.7886	1.29E-05	164.2968	184.211	0.149142
16.18375	96.95415	0	722.3168	198.2267	9.8E-10	876.9298	23.37842	5.49E-07
790.0578	91.46633	2.72E-05	14.36769	145.0074	0	915.6487	182.8839	2.3E-10
649.3436	178.5808	9.59E-06	630.4552	-34.7904	0.000138	903.2386	59.26422	1.17E-06
238.998	60.6554	7.31E-05	562.254	232.6601	0.000664	543.7594	223.5939	3.53E-05
775.3715	176.5901	1.49E-06	917.4215	26.54381	2.85E-09	570.9654	5.381404	0.712305
48.31462	17.41644	0	981.5736	124.1768	0.324251	712.5553	16.02526	0.003879
759.8095	163.9556	0.000407	495.5631	-63.0995	0.000511	337.514	167.7205	0.026608
7.319431	66.65441	0	217.5708	55.15762	1.34E-06	572.7383	255.0414	2.38E-05
889.8865	202.8815	1E-11	765.4571	142.8103	0.001001	891.2224	139.9496	0.079809
535.2224	-49.4056	0.042235	685.743	32.54281	0.566128	279.2039	130.2327	0.62348
809.1655	197.4207	9E-10	895.5341	181.7362	1.28E-09	428.8921	222.7097	0.000443
152.0828	20.45652	0	790.3868	133.3412	0.552467	113.9538	25.12131	0

136

336.4407	231.5224	0.264787	643.3687	36.42586	0.167952	640.456	215.563	6.32E-07
915.5822	141.879	0.045642	468.2474	5.821399	0.075022	701.1937	17.31107	0.061045
252.6774	80.33834	0.016804	363.1001	-42.5736	0	277.5623	84.00781	0.172441
404.1385	16.47522	0.010927	743.9634	96.30768	0.002629	615.6576	22.46711	0.47699
5.940352	21.29949	0	637.0432	204.2527	6.35E-07	712.203	41.43239	0.410326
754.3812	77.68414	0.002033	81.6933	185.7986	7E-11	750.9219	200.9378	2.46E-09
713.6054	19.50534	0.03717	477.6151	-16.2822	0.710762	472.667	-87.6751	1E-11
118.9018	96.51415	0	833.0452	184.4715	3E-10	359.3118	38.80525	0.038058
839.6332	17.51469	1.82E-05	884.7872	158.4849	1.83E-06	569.1028	187.9986	0.004368
847.7316	99.34777	0.015109	144.4447	183.9333	0.000622	330.4641	210.7928	0.06461
437.3859	-18.5776	0.835635	672.7198	218.0349	6E-10	946.5517	30.99501	1.46E-09
540.8916	-16.4075	0.922662	674.4927	61.69487	0.001271	206.2091	56.44343	3.1E-08
750.6826	132.7858	0.887388	250.8614	128.3916	0.038702	640.8498	13.86802	0.764285
184.3233	90.21043	2.19E-05	145.7141	79.9966	1.1E-10	598.0818	219.446	2.5E-06
509.1329	213.2918	0.033449	526.5774	218.8779	8.33E-05	307.6794	214.0835	0.458933
872.6613	89.87865	0.000645	853.3791	78.20245	1.57E-06	284.0191	119.6159	0.383699
809.3849	90.00396	8.89E-05	177.1887	201.2838	5.39E-06	476.4753	6.51486	0.078297
924.4033	63.89199	1.36E-08	812.3839	127.4404	0.82101	371.328	-41.8801	0
793.8229	77.36945	0.000278	756.3302	111.6405	0.087	118.7689	14.50451	0
344.7584	205.9387	0.017845	659.2813	145.0786	0.009343	379.4264	39.95293	0.117096
923.8999	116.2953	0.694448	248.9357	27.15325	2.3E-10	785.7229	116.9617	0.72203
12.48516	152.0558	0	92.922	102.5032	0	907.7015	74.05456	1.27E-06
818.7526	67.90034	0.000558	324.0971	148.9075	0.522453	971.8536	171.6875	2.51E-07
497.9923	-14.2645	0.541225	84.56113	19.80009	0	939.1761	195.3418	2E-11

Variogram Equation

Variogram Equations are specified in the format required by GSTAT. (Pebesma, 1999)

A Nug(0) + B Sph(C, D, E)

where A is the nugget, B is the partial sill (sill − nugget), C is the range, D is the anisotropy angle and E is the anisotropy ratio. Sph denotes a spherical variogram model.

137

Standard

30: 0.0477 Sph(95, 90, 0.44)

50: 0.00103 Nug(0) + 0.0949 Sph(165, 90, 0.33)

70: 0.0624 Sph(90, 90, 0.29)

90: 0.00740 Nug(0) + 0.0674 Sph(305, 90, 0.48)

110: 0.0582 Sph(115, 90, 0.44)

130: 0.0236 Nug(0) + 0.0479 Sph(500, 90, 0.47)

150: 0.0606 Sph(110, 90, 0.45)

Flowline

30: 0.0453 Sph(105, 90, 0.48)

50: 0.0197 Nug(0) + 0.0772 Sph(500, 90, 0.17)

70: 0.0956 Sph(225, 90, 0.29)

90: 0.00948 Nug(0) + 0.0546 Sph(260, 90, 0.40)

110: 0.0677 Sph(210, 90, 0.29)

130: 0.0227 Nug(0) + 0.0415 Sph(355, 90, 0.43)

150: 0.0814 Sph(200, 90, 0.37)

138

Appendix E – Diverging Channel Simulation Inputs

CH3D Channel Geometry (grid.inp)

Although the CH3D grid file describing the channel geometry is too large to include in an appendix, a brief description of the channel follows.

The diverging channel is 400 m wide at the downstream end, 100 m wide at the upstream end and 1000 m long through its centre. The computational mesh is created by placing 40 equal length segments along the upstream end, 40 equal length segments along the downstream end and 200 equal length segments along each bank. The interior of the mesh is then created by connecting the endpoints of the segments across and along the channel.

CH3D Main Input File (main.inp)

```
TITLE(A80)
Jason Wintermute, Test run.
    IT1     IT2       DT  ISTART   ITEST  ITSALT    ISCOM  NTSEDONDTINDTS
      1    2000        1       0       0       0        1       300       1
  WPRCRD
      0
  WXCEL1  WXCEL2  WYCEL1  WYCEL2  WZCEL1  WZCEL2  WPRINT   WPRSTR  WPREND  WPRVAR
  SNPCRD
      1
  SXCEL1  SXCEL2  SYCEL1  SYCEL2  SZCEL1  SZCEL2  SNPINT   SNPSTR  SNPEND  SNPVAR
      1     200       1      40       1       2      10      300    2000CBUV
   NRANG
      0
  RANGDR   RPOS1   RPOS2   RPOS3  RRNAME
     IGI     IGH     IGT     IGS     IGU     IGW     IGC      IGQ     IGP
       0       1       0       0       0       0       0        0       0
    XREF    ZREF    UREF     COR      GR     RO0     ROR       T0      TR
     500     200      20     1.0   981.0    1.00   1.021       20      20
   THETA
     0.6
   ITEMP   ISALT     ICC     IFI  ifitim     IFA     IFB      IFC     IFD
       0       0       0       0       0       0       0        0       1
     TWE     TWH     FKB
       0       0       0
    IEXP     IAV     AVR     AV1     AV2     AVM    AVM1      AHR
       1       0       1      0.      0.   0.002   0.002    10000
    IVIS     IQW     IPT
       0       0       0
   GAMAX   GBMAX
   60000   60000
   IWIND    TAUX    TAUY
       0    0.00    0.00
    ISPAC(I),I=1,10
       0       0       0       1       0       0       0        0       0       0
    JSPAC(I),I=1,10
       1       1      -1       0       0       0       0        0       0       0
```

139

```
      RSPAC(I),I=1,10
  0.035000        0 0.00000 0.00000        0        0        0 0.000      0.00          0
     IBTM     HADD     HMIN       H1       H2     SSS0     HMAX
        4      0.0      0.0      0.0      0.0      1.0  999999.
   ISMALL      ISF      ITB    ZREFBN      CTB      BZ1   ZREFTN      TZ1
        1        0        5        5    0.003    0.200        5      2.0
     XMAP    ALXREF   ALYREF
    100.0        0        0
    ITRAN    IBD(1)   IBD(2)   IBD(3)   IBD(4)
        2        4        4        4        4
  ITBRK(1)      (2)      (3)      (4)      (5)      (6)      (7)      (8)      (9)     (10)
        0        0        0        0        0        0        0        0        0        0
     NSTA    NFREQ   NSTART    (CURRENT STATIONS)
        0        0        0
  IST JST  STATID(K)    (2I4,A48)      ( ONE CARD FOR EACH STATION )
    NSTAS   NFREQS   NSTRTS    (TIDE STATIONS)
        0        0        0
  IST JST  STATID(K)    (2I4,A48)      ( ONE CARD FOR EACH STATION )
     MSTA    MFREQ   MSTART    (SALINITY STATIONS)
        0        0        0
  IST JST  STATID(K)    (2I4,A48)      ( ONE CARD FOR EACH STATION )here
    NRIVER
       -6
   IJRDIR   IJRROW   IJRSTR   IJREND      ( ONE CARD FOR EACH RIVER )
        2       11       56       56
        2       17       98       98
        2       17      167      167
        2       20       20       20
        2       28      148      148
        2       29       77       77
        I        J   QRIVER             ( ONE CARD FOR EACH CELL )
       56       11        0
       98       17        0
      167       17        0
       20       20        0
      148       28        0
       77       29        0
     NBAR
        0
   IJBDIR   IJBROW   IJBSTR   IJBEND     ( ONE CARD FOR EACH BAR )
   TIDFNO   TIDBND
        2        2
   TIDSTR        2        3        4        5        6        7        8        9       10
        1        1        1        1        1        1
   IJTDIR   IJTROW   IJTSTR   IJTEND   TIDTYP   TIDFN1   TIDFN2
        1        1        1       40CONSTANT        1        0
        3      200        1       40CONSTANT        2        0
RESET HS(I,J)  TO ZERO AT THE FOLLOWING CELLS
RESET HU(I,J)  TO ZERO AT THE FOLLOWING CELLS
RESET HV(I,J)  TO ZERO AT THE FOLLOWING CELLS
RESET HS(I,J)  TO THE FOLLOWING DEPTHS
     END OF DATA
     END OF FILE
```

CH3D Sediment Input File (sed.inp)

```
     99999   99999   99999   99999   99999   99999   99999   99999   99990   99999
     99999   99999   99999   99999   99999   99999   99999   99999   99999   99999
     99999   99999   99999   99999   99999   99999   99999   99999   99999   99999
     99999   99999   99999   99999   99999   99999   99999   99999   99999   99999
     99999   99999   99999   99999   99999   99999   99999   99999   99999   99999
     99999   99999   99999   99999   99999   99999   99999   99999   99999   99999
     99999   99999   99999   99999   99999   99999   99999   99999   99999   99999
     99999   99999   99999   99999   99999   99999   99999   99999   99999   99999
     99999   99999   99999   99999   99999   99999   99999   99999   99999   99999
     99999   99999   99999   99999   99999   99999   99999   99999   99999   99999
     99999   99999   99999   99999   99999   99999   99999   99999   99999   99999
```

140

```
99999   99999   99999   99999   99999   99999   99999   99999   99999   99999
99999   99999   99999   99999   99999   99999   99999   99999   99999   99999
99999   99999   99999   99999   99999   99999   99999   99999   99999   99999
99999   99999   99999   99999   99999   99999   99999   99999   99999   99999
99999   99999   99999   99999   99999   99999   99999   99999   99999   99999
99999   99999   99999   99999   99999   99999   99999   99999   99999   99999
99999   99999   99999   99999   99999   99999   99999   99999   99999   99999
99999   99999   99999   99999   99999   99999   99999   99999   99999   99999
99999   99999   99999   99999   99999   99999   99999   99999   99999   99999
     1       1       1       0       0
0 0 0 0 0 0 0 0 0 1 0 0 1 0 0 0 0 0 0 0 0 0
1 1 1 1 1 1 1
       0         0
          1.00e-6            1.00e-5
        0.00000114
      2.65      0.4
      0.60      0.10     0.100     0.030     0.010
        0.0000001          0.00000001
       100
      0.02
         0
         0         0
         0         0
     1000.
         1
         1         1         1
     0.100               100
         2         1         2
     0.100               100
        -1        11        56        56
         2         1         2
     0.100               100
        -1        17        98        98
         2         1         2
     0.100               100
        -1        17       167       167
         2         1         2
     0.100               100
        -1        20        20        20
         2         1         2
     0.100               100
        -1        28       148       148
         2         1         2
     0.100               100
        -1       -29        77        77
         1     1.000     0.000
        -2     0.000     1.000
         1         1         1         1         1
         1         2         1         1         1
         1         3         1         1         1
         1         4         1         1         1
         1         5         1         1         1
         1         6         1         1         1
         1         7         1         1         1
         1         8         1         1         1
         1         9         1         1         1
         1        10         1         1         1
         1        11         1         1         1
         1        12         1         1         1
         1        13         1         1         1
         1        14         1         1         1
         1        15         1         1         1
         1        16         1         1         1
         1        17         1         1         1
         1        18         1         1         1
         1        19         1         1         1
         1        20         1         1         1
         1        21         1         1         1
         1        22         1         1         1
         1        23         1         1         1
         1        24         1         1         1
```

141

1	25	1	1	1
1	26	1	1	1
1	27	1	1	1
1	28	1	1	1
1	29	1	1	1
1	30	1	1	1
1	31	1	1	1
1	32	1	1	1
1	33	1	1	1
1	34	1	1	1
1	35	1	1	1
1	36	1	1	1
1	37	1	1	1
1	38	1	1	1
1	39	1	1	1
1	40	1	1	1
200	1	-1		
200	2	-1		
200	3	-1		
200	4	-1		
200	5	-1		
200	6	-1		
200	7	-1		
200	8	-1		
200	9	-1		
200	10	-1		
200	11	-1		
200	12	-1		
200	13	-1		
200	14	-1		
200	15	-1		
200	16	-1		
200	17	-1		
200	18	-1		
200	19	-1		
200	20	-1		
200	21	-1		
200	22	-1		
200	23	-1		
200	24	-1		
200	25	-1		
200	26	-1		
200	27	-1		
200	28	-1		
200	29	-1		
200	30	-1		
200	31	-1		
200	32	-1		
200	33	-1		
200	34	-1		
200	35	-1		
200	36	-1		
200	37	-1		
200	38	-1		
200	39	-1		
-200	40	-1		
56	11	1	2	2
98	17	1	2	2
167	17	1	2	2
20	20	1	2	2
148	28	1	2	2
-77	29	1	2	2
0	0			
	1	1.000	0.000	
	-2	1.000	0.000	
	1	0.000	0.000	
		0.000	0.000	
	2	0.000	5.000	
		0.000	5.000	
2	3			
	1	1.000	0.000	

142

```
-2   1.000    0.000
 1   0.000    0.000
     0.000    0.000
 2   0.000    5.000
     0.000    5.000
```

CH3D Boundary Conditions (tide.inp)

```
FORTRAN 16 FILE: TIDE TABLE DATA
1  1  98  0 0      1.00    1.00
1  1  98  0 1      1.20    0.80
8  2  98  3 0      1.20    0.80
```

Sample Points

30

X	Y	Attr	X	Y	Attr	X	Y	Attr
255.4257	-223.276	0.014637	401.8523	-169.773	0.878516	147.1265	-161.457	0.88414
310.9976	-102.436	0.066605	720.3363	-283.447	3.14E-07	148.8994	-315.872	1.25E-07
242.7963	-239.28	0.000983	613.4162	-176.832	0.776778	726.268	-249.996	0.000862
225.4615	-97.3439	0.0014	589.7559	-270.136	0.000127	621.1208	-297.795	9.78E-07
372.8733	-200.833	0.550023	140.6913	-143.15	0.014979	871.4036	-147.313	5.4E-10
462.4586	-165.513	0.890412	719.8329	-231.689	0.031293	156.4943	-183.288	0.536417
77.54616	-343.097	1.4E-09	809.4182	-196.369	0.193687	62.85981	-259.021	2.34E-06
930.6309	-187.849	0.000186	614.6856	-279.488	2.94E-05	90.06587	-73.5464	1.23E-05
506.9995	-121.974	0.908066	362.1265	-223.798	0.032467	706.1534	-251.13	0.001128
166.628	-256.019	6.46E-05	228.6134	-206.962	0.066399	575.573	-237.818	0.004969

50

X	Y	Attr	X	Y	Attr	X	Y	Attr
302.9879	-132.117	0.046141	445.6278	-118.167	0.83103	465.8089	-76.534	0.032948
24.99556	-15.3167	0	111.5818	-16.972	3.52E-09	16.74435	-350.548	1E-11
260.2198	-330.071	0	45.26303	-160.777	0.78019	714.3188	-172.637	0.125756
510.5027	-179.589	0.957135	622.6317	-94.9015	0.00192	951.316	-240.806	0
796.5933	-215.564	0.257539	134.4113	-33.1989	9.09E-09	553.1178	-236.041	0.003327
430.7886	-288.498	8.74E-07	452.8954	-146.873	0.88963	761.7492	-239.576	0.003486
535.4324	-188.941	0.31121	118.8493	-45.6778	1.35E-07	167.0456	-163.515	0.526383
282.8733	-133.251	0.007572	367.3593	-141.781	0.580606	23.1795	-368.855	0
543.5308	-108.116	0.652605	311.3056	-157.386	0.39076	24.95236	-122.27	0.004097
133.1851	-224.589	8.28E-05	604.3564	-209.95	0.042382	590.1735	-177.632	0.744054

143

X	Y	Attr	X	Y	Attr	X	Y	Attr
134.958	-379.004	0	206.1583	-205.185	0.042145	872.215	-254.021	1E-11
125.3709	-251.078	8.23E-06	157.0648	-237.379	0.000185	1.292029	-215.574	0.0322
360.5952	-164.833	0.774285	417.7222	-212.244	0.104835	47.75867	-72.0434	1.13E-06
679.0792	-278.507	6.81E-06	945.9974	-178.562	7.54E-07	924.5037	-224.492	3.91E-08
572.1591	-171.892	0.862303	9.149453	-82.1315	8.15E-07	185.934	-353.772	0
531.1639	-123.26	0.91457	308.5258	-300.455	4.57E-09	250.0861	-257.341	0.000298
475.1102	-138.865	0.928507	755.314	-221.269	0.123441			

70

X	Y	Attr	X	Y	Attr	X	Y	Attr
711.0855	-235.715	0.016338	37.32422	-65.9158	2.1E-09	471.5695	-189.826	0.88166
287.4542	-169.84	0.457413	672.5195	-138.85	0.939133	928.7323	-235.986	1E-11
182.3069	-217.639	0.006269	616.4658	-154.455	0.976084	366.4222	-237.625	0.001467
494.9689	-217.311	0.002977	586.9834	-133.757	0.956515	481.4407	-263.415	4.59E-05
415.2549	-326.22	3.66E-09	437.2952	-225.095	0.001254	347.9276	-246.579	0.000272
625.046	-178.864	0.687726	12.50414	-310.11	1.88E-09	330.5927	-104.644	0.189008
519.8987	-226.663	0.00306	288.2201	-220.738	0.032803	497.6158	-155.241	0.926145
267.3396	-170.973	0.345058	181.3	-114.123	0.003438	182.6774	-350.396	1E-11
52.33957	-108.632	5.1E-05	202.684	-215.646	0.015649	52.09697	-337.085	6.3E-10
415.868	-230.525	0.00149	84.25111	-81.0964	3.96E-05	34.76212	-195.149	0.362461
651.0923	-144.28	0.9784	439.6812	-283.815	1.5E-06	271.7593	-263.318	1.37E-05
862.6562	-151.339	4E-11	253.047	-286.109	4.62E-08	506.9835	-177.073	0.780482
635.5303	-156.759	0.978275	659.3435	-210.048	0.108973	718.5475	-184.131	0.003231
186.4658	-29.773	2.4E-06	421.8429	-90.1212	0.241894	308.2018	-300.604	4.52E-09
572.1442	-304.088	2.43E-07	143.8506	-374.32	0	677.5523	-135.5	0.879348
516.0904	-319.693	3.52E-09	81.84187	-356.923	8E-11	844.5753	-186.098	0.000374
562.5571	-176.163	0.767984	89.94022	-276.098	5.22E-06	592.0162	-130.407	0.938434
164.359	-171.398	0.909021	66.27988	-369.402	0	55.13925	-193.156	0.512422
115.2654	-203.592	0.0964	555.8361	-92.2617	0.075097	461.4357	-117.096	0.836346
375.9229	-178.457	0.851545	196.3569	-330.956	3.2E-10	379.9488	-71.5906	0.021913
904.198	-144.775	0	551.787	-132.674	0.958934	691.7352	-167.817	0.931962
266.7265	-266.368	0.111471	91.20963	-378.755	0	486.3887	-192.902	0.691358
501.9507	-180.423	0.963928	365.1528	-134.968	0.586434			
713.5147	-187.481	0.003133	627.5831	-264.248	0.000435			

144

90

X	Y	Attr	X	Y	Attr	X	Y	Attr
251.1426	-315.491	1E-11	362.1551	-274.741	9.51E-08	229.2967	-336.327	0
107.2765	-119.831	0.001343	622.8126	-249.606	0.003901	122.3766	-229.711	6.48E-05
470.8049	-241.724	0.000281	147.1551	-212.4	0.00152	98.71623	-323.015	6.6E-08
23.51326	-269.153	1.07E-06	148.928	-366.814	0	650.6517	-196.029	0.0234
917.5931	-162.537	7.1E-10	448.3043	-184.138	0.920457	19.00217	-30.9246	0
893.9328	-255.842	0	1.012681	-211.567	0.0322	228.7932	-284.569	3.98E-06
179.0235	-291.817	3.37E-06	418.4498	-311.753	4.26E-08	255.9993	-99.0938	0.001483
23.00982	-217.395	0.028426	604.5805	-257.701	0.000951	123.646	-332.368	7.95E-09
112.5951	-182.075	0.809445	500.8107	-140.774	0.947624	809.7076	-126.523	0
666.3034	-209.504	0.118699	471.3283	-120.076	0.883286	335.2099	-339.426	2E-11
926.9609	-184.369	6.8E-05	321.6401	-211.414	0.163213	741.5064	-263.366	1.58E-05
516.6153	-300.842	1.95E-07	622.7893	-183.152	0.41821	238.161	-306.4	1.24E-09
817.7645	-272.581	2E-10	237.8769	-360.736	0	130.0811	-350.675	1.8E-10
370.4728	-300.009	7.07E-09	592.9348	-310.767	1.58E-07	510.9444	-213.504	0.005714
263.5527	-193.394	0.299265	588.9953	-203.726	0.026342	380.3639	-200.192	0.571123
242.825	-290.222	1.6E-07	825.9924	-271.896	7E-11	363.0291	-58.2564	0.003534
466.5364	-176.043	0.946545	427.7943	-267.131	2.25E-06	572.8202	-311.9	6.01E-08
372.902	-251.776	2.68E-05	112.8559	-61.2858	2.29E-06	350.5094	-327.807	2.1E-10
462.4873	-216.456	0.004044	639.3582	-274.189	6.82E-05	429.72	-167.139	0.879799
267.7547	-299.575	1.09E-09	765.3861	-276.156	6.26E-08	395.0503	-284.268	6.51E-08
213.4739	-68.5948	0.000114	818.0253	-151.791	6.99E-08	281.1052	-321.493	3.3E-10
804.1282	-185.068	0.001234	300.7595	-161.649	0.433806	661.9685	-184.322	0.059317
166.6566	-306.961	4.36E-07	732.4892	-146.699	0.011934	531.388	-171.011	0.846467
339.5017	-70.5609	0.017662	296.7104	-202.061	0.301922	817.4787	-206.986	0.794439
613.4448	-227.774	0.030931	110.0762	-204.355	0.105836	451.6739	-279.92	3.5E-06
386.3189	-233.195	0.001272	516.3727	-128.295	0.937519	661.465	-132.564	0.885353
572.4497	-179.143	0.705969	375.4391	-337.159	3E-11	556.3178	-180.363	0.660373
516.3959	-194.748	0.107089	439.5912	-240.729	4.57E-05	303.7586	-124.673	0.039918
809.4468	-247.312	1.66E-05	219.4255	-262.737	0.000139	564.4161	-99.5382	0.229952
411.2487	-242.547	4.57E-05	176.6574	-59.6909	8.07E-05	235.5574	-261.516	0.000226

145

X	Y	Attr	X	Y	Attr	X	Y	Attr
825.2819	-194.386	0.181693	416.5762	-145.273	0.797404	688.1999	-203.267	0.136119
605.1162	-216.394	0.041628	314.3616	-196.597	0.461819	461.0739	-208.687	0.095651
327.1239	-99.5936	0.138659	61.80244	-140.906	0.221584	647.2047	-154.636	0.982477
499.9689	-264.193	6.83E-05	322.4599	-115.771	0.159987	591.1509	-170.241	0.881556
614.9874	-289.984	3.76E-06	491.2558	-320.784	1.75E-09	295.8238	-312.504	1.3E-09
484.4069	-276.672	1.02E-05	213.2635	-203.983	0.064743	165.2433	-299.193	1.86E-06
35.34242	-149.686	0.561578	766.9718	-231.412	0.019723	21.37716	-103.533	7.33E-05
614.484	-238.226	0.009127	660.0517	-124.796	0.49866	928.7427	-179.266	2.91E-06
845.6591	-192.393	0.00089	636.3914	-218.1	0.070901	124.2481	-250.561	7.54E-06
188.5763	-367.178	0	922.482	-254.076	0	417.299	-303.125	1.24E-07
107.0894	-321.673	8.14E-08	766.4684	-179.654	0.001357	957.7216	-148.206	0
108.8623	-75.0872	1.68E-05	856.0536	-144.334	0	230.6648	-305.419	5.38E-09
952.0757	-247.251	0	471.1412	-321.917	1.23E-09	636.9613	-229.358	0.034362
345.8594	-143.256	0.426865	669.4195	-146.628	0.979845	399.4607	-109.431	0.613879
855.0268	-214.224	0.142466	74.71593	-70.5671	6.34E-06	856.6236	-155.592	5.1E-10
396.965	-198.165	0.633104	259.0738	-263.101	0.2516	356.6926	-307.385	2.89E-09
828.6947	-183.215	0.000505	560.223	-234.839	0.004321	406.3993	-179.496	0.898187
37.48579	-35.8588	1E-11	112.9314	-262.268	1.09E-05	299.4792	-72.8806	0.005651
64.69186	-251.384	1.66E-05	6.011233	-155.652	0.561227	275.8188	-166.185	0.36121
206.2817	-240.871	0.000477	265.509	-281.408	1.53E-07	468.275	-277.893	6.78E-06
532.8641	-273.72	2.57E-05	261.4598	-321.82	0	495.4811	-92.4182	0.275778
109.2328	-207.845	0.030547	801.8824	-166.901	1.61E-05	363.1278	-325.692	2.4E-10
4.085509	-255.644	1.64E-05	74.82559	-324.114	2.46E-08	110.5687	-270.002	1.31E-05
384.9488	-118.473	0.670944	418.7429	-97.8989	0.422912	899.5013	-211.185	0.004237
215.6494	-262.703	0.000158	603.1007	-290.432	3.86E-06	477.6428	-299.724	1.69E-07
254.3683	-105.162	0.00187	904.2499	-262.171	0	199.6505	-182.924	0.094443
237.0335	-364.226	0	138.4742	-175.925	0.918839	753.3588	-210.353	0.358272
131.9959	-264.572	2.34E-05	456.9583	-289.6	1.09E-06	646.4387	-103.737	0.001754
159.2019	-79.0969	0.000465	350.0382	-182.984	0.775082	236.093	-220.21	0.020224
26.84861	-312.371	4.14E-09	60.53302	-38.2496	1.23E-08	45.40968	-262.916	9.53E-07
775.2895	-256.68	7.18E-06	309.043	-134.353	0.079651	878.8832	-160.561	3.96E-08
238.4126	-319.429	1E-11	252.9892	-149.958	0.028075	241.4116	-282.454	3.64E-06
582.3298	-93.2142	0.020276	546.0401	-202.522	0.027255	476.6359	-196.208	0.663098

146

X	Y	Attr	X	Y	Attr	X	Y	Attr
141.3636	-286.403	8.42E-06	147.842	-197.757	0.026404	247.7803	-341.261	0
864.3713	-169.602	1.8E-07	98.74845	-229.951	0.00033	286.4992	-183.72	0.489158
36.21638	-334.202	3.3E-10	359.4059	-204.816	0.384543	206.7851	-292.629	1.79E-06
417.0797	-197.031	0.68203	765.7024	-128.755	1.19E-09			

130

X	Y	Attr	X	Y	Attr	X	Y	Attr
357.4401	-233.487	0.003434	231.9356	-109.873	0.002445	246.0089	-289.643	1.55E-07
104.881	-177.797	0.860805	233.7085	-264.287	0.000158	455.8	-142.287	0.900754
569.004	-240.546	0.003586	811.0772	-198.412	0.514618	350.6527	-190.086	0.706177
975.3005	-164.486	0	705.9299	-246.211	0.002928	98.09357	-134.396	0.009506
256.342	-240.874	0.000933	85.79319	-109.04	0.000711	358.751	-109.261	0.443167
810.0504	-268.303	1.22E-08	303.6826	-281.859	7.09E-08	527.5469	-314.273	1.22E-08
679.4699	-254.991	0.001118	237.2542	-172.117	0.214664	249.5546	-197.473	0.184122
662.135	-113.055	0.011925	840.0561	-167.352	2.69E-06	800.3303	-221.377	0.104038
829.1581	-163.653	2.44E-06	50.62004	-174.411	0.8191	693.4102	-114.761	6.44E-05
446.0185	-94.6514	0.362686	456.9165	-98.3502	0.52	17.21976	-394.196	0
5.052309	-287.84	4.84E-09	281.7951	-128.578	0.005332	402.8982	-267.511	1.45E-07
728.06	-171.039	0.00093	176.6479	-176.377	0.076684	507.542	-167.954	0.546476
283.7009	-201.993	0.260798	291.6664	-202.167	0.279262	254.9829	-112.264	0.002628
176.7808	-95.3771	0.001332	184.7462	-95.5514	0.001337	515.6403	-87.1286	0.100343
215.4997	-338.836	0	161.0859	-188.856	0.093195	105.2947	-203.602	0.128274
439.2112	-224.657	0.001101	143.751	-46.9199	3.15E-06	107.0676	-358.016	1.2E-10
73.40642	-297.591	6.45E-07	353.5421	-300.564	6.16E-09	613.2592	-131.413	0.931199
283.1975	-150.235	0.087664	245.4622	-344.838	0	951.3544	-192.196	1.14E-06
178.0502	-198.034	0.027057	781.8357	-230.332	0.018064	168.2438	-365.015	0
926.4911	-142.343	0	845.9878	-133.901	0	101.8154	-255.272	2.84E-06
186.1486	-117.208	0.003797	144.3642	-352.225	8E-11	642.2381	-100.353	0.0015
776.8029	-233.682	0.008727	591.1524	-273.038	0.000104	655.5238	-282.701	7.71E-06
354.9445	-322.221	3.4E-10	118.4275	-239.356	6.29E-06	916.1812	-257.566	0
14.57293	-55.2654	3.2E-10	550.1572	-224.406	0.006336	443.4564	-223.885	0.001057
630.6605	-232.849	0.026319	654.801	-124.849	0.560809	21.59792	-312.424	2.8E-09
523.7404	-126.233	0.935401	402.2419	-69.1591	0.012803	744.6056	-195.623	0.063456
296.6144	-131.653	0.012538	334.0406	-206.002	0.326065	297.3139	-223.052	0.029667
786.1707	-255.513	4.82E-06	252.5537	-160.497	0.128327	190.3938	-116.436	0.003662

147

X	Y	Attr	X	Y	Attr	X	Y	Attr
482.7452	-77.6017	0.036719	254.3266	-314.912	1E-11	211.7778	-217.959	0.014906
364.3122	-344.052	1E-11	831.6952	-249.036	2.06E-06	93.3449	-83.4101	5.77E-05
69.09472	-338.863	1.2E-09	106.4112	-159.665	0.879783	448.775	-286.129	1.75E-06
20.00119	-371.056	0	38.21	-296.508	4.48E-08	1.483313	-313.557	3.6E-10
218.2794	-195.767	0.120438	168.287	-258.061	6.75E-05	9.691324	-85.2792	1.04E-06
624.5759	-119.706	0.681251	198.4257	-76.1109	0.000277	353.6086	-260.064	8.08E-06
873.0859	-215.809	0.015951	66.07237	-309.385	7.68E-08	178.4872	-290.292	5.92E-06
109.083	-283.978	7.38E-06	814.5132	-253.694	2.04E-06	73.33995	-338.091	1.76E-09
344.3073	-197.733	0.550052	277.6363	-316.443	4.5E-10	454.2032	-200.92	0.458249
555.8712	-204.791	0.015143	180.5874	-283.417	1.15E-05	284.9039	-345.149	1E-11
328.7453	-210.212	0.240892	903.5951	-166.616	1.36E-07	996.3988	-200.415	0
529.5391	-173.782	0.780312	75.44013	-331.216	7.32E-09	243.9087	-296.518	1.13E-08
473.4854	-189.387	0.883857	456.3034	-194.045	0.770766	128.4084	-165.493	0.923261
444.003	-168.689	0.907732	287.0041	-338.275	3E-11	85.64033	-363.446	4E-11
47.57776	-318.339	1E-08	325.7229	-180.734	0.717167	771.702	-157.601	7.96E-06
703.5007	-294.445	7.34E-08						

150

X	Y	Attr	X	Y	Attr	X	Y	Attr
452.8413	-276.282	5.01E-06	402.4352	-312.772	2.28E-08	259.2021	-249.01	0.000281
149.4158	-98.3703	0.001256	244.6487	-83.9351	0.000452	494.4264	-162.765	0.866018
296.8277	-201.86	0.304598	905.2771	-217.98	3.61E-06	92.17906	-198.413	0.294754
386.4129	-166.54	0.832078	139.5014	-131.734	0.001828	727.3743	-271.347	3.47E-06
1.500496	-344.123	0	254.5199	-157.525	0.087374	608.9414	-136.797	0.961276
619.4706	-127.668	0.866178	85.22054	-301.754	6.59E-07	579.459	-116.099	0.774378
537.9836	-82.1631	0.0209	123.9394	-144.213	0.111859	429.7708	-207.437	0.257945
592.5486	-258.807	0.000809	610.5631	-264.548	0.000417	7.912374	-295.977	2.15E-09
827.7729	-172.562	1.33E-05	41.29273	-249.598	6.1E-05	730.92	-179.176	0.002058
145.257	-286.236	8.7E-06	188.7046	-353.087	0	283.6284	-206.605	0.174318
38.33685	-179.62	0.737427	357.5005	-157.1	0.663969	176.7083	-99.9891	0.001591
14.67651	-272.925	6.22E-07	588.6756	-111.267	0.534712	198.0923	-201.512	0.05018
300.7672	-308.9	1.79E-09	44.63846	-157.427	0.763886	79.65935	-66.9628	5.45E-06
144.7535	-234.478	0.000111	483.5283	-159.066	0.881343	435.0894	-269.681	3.7E-06
234.3388	-199.158	0.132697	598.5468	-184.856	0.398427	248.4552	-271.975	2.69E-05
39.60626	-282.277	1.18E-07	491.6267	-78.2407	0.036049	654.7517	-195.915	0.023452

148

788.0471	-226.587	0.038236	81.28102	-194.714	0.483612	773.7978	-234.769	0.008085
575.9798	-167.77	0.917384	660.4226	-283.253	6.83E-06	837.9498	-138.339	0
173.7324	-203.418	0.016753	750.0078	-247.933	0.000585	414.3185	-72.4632	0.016172
492.2165	-317.092	3.1E-09	302.7162	-275.362	4.99E-07	136.3262	-356.662	6E-11
385.2964	-210.477	0.283963	172.1357	-262.05	6.78E-05	309.1713	-120.262	0.071136
92.85863	-62.2176	2.65E-06	90.64879	-216.545	0.008688	583.1144	-277.476	4.11E-05
341.3686	-158.321	0.59474	92.42165	-370.96	1E-11	293.6093	-132.741	0.009962
285.3149	-173.926	0.490587	391.798	-188.284	0.826527	542.1192	-228.844	0.003809
578.3657	-226.49	0.014091	948.439	-219.237	7.1E-09	423.6863	-94.2946	0.381486
180.1676	-221.725	0.003004	431.1732	-229.094	0.000839	380.9182	-292.248	1.69E-08
131.0741	-253.919	1.37E-05	9.314723	-317.634	4.2E-10	65.97989	-86.4033	3.77E-05
391.7315	-228.784	0.005414	98.9	-282.314	6.01E-06	592.4822	-299.307	8.22E-07
920.0067	-195.102	0.033956	178.1106	-121.646	0.005642	726.6084	-220.448	0.148453
282.5351	-316.995	5.9E-10	567.0722	-304.65	1.82E-07	316.2627	-336.921	5E-11
455.3802	-80.595	0.067629	81.0617	-88.6198	0.000104	685.6132	-171.816	0.893537
729.3233	-237.808	0.012137	38.29365	-286.574	8.38E-08	249.8343	-227.179	0.009258
502.1974	-243.229	0.000585	249.8576	-293.632	3.74E-09	63.20013	-229.473	0.001861
688.3281	-189.177	0.002803	208.8624	-245.001	0.000338	469.4966	-153.412	0.894153
632.2744	-204.782	0.059358	418.6535	-97.6446	0.41906	392.7152	-265.846	1.1E-07
925.3253	-257.346	0	375.8854	-295.598	1.25E-08	234.9286	-37.0095	2.06E-06
464.7479	-102.426	0.611639	60.94709	-89.7534	3.1E-05	380.1955	-134.396	0.680033
478.0336	-284.775	3.18E-06	321.6046	-64.6184	0.004583	889.3629	-205.364	0.569717
738.6911	-259.64	5.53E-05	993.7458	-226.597	0	416.638	-171.683	0.89913
72.81049	-22.8514	1.19E-09	490.4005	-269.631	2.72E-05	848.3677	-156.733	3.4E-09
257.1684	-215.385	0.04373	212.4081	-152.83	0.018558	57.15877	-9.37672	5E-11
558.3176	-187.123	0.367576	382.3206	-313.905	1.73E-09	700.562	-255.032	0.000475
173.4051	-364.707	0	632.6034	-163.423	0.959844	448.0029	-199.342	0.550171
4.105795	-107.937	0.00043	918.6941	-199.398	0.004011	912.126	-262.091	0
25.48982	-209.46	0.101125	825.0596	-275.131	3E-11	59.10776	-376.839	0
970.4361	-225.065	0	602.7488	-291.037	3.81E-06	916.2416	-181.179	7E-05
262.487	-277.629	3.24E-07	155.4572	-318.466	7.7E-08	278.77	-303.072	1.82E-09
802.9096	-122.709	0	416.1146	-293.331	3.14E-07	725.5583	-223.885	0.099651
75.85277	-279.923	2.21E-06	22.20495	-180.841	0.656977	252.8334	-190.203	0.277989
482.1492	-203.862	0.068937	599.5736	-114.966	0.734452	684.5631	-175.253	0.517966

Variogram Equation

Variogram Equations are specified in the format required by GSTAT. (Pebesma, 1999)

A Nug(0) + B Sph(C, D, E)

where A is the nugget, B is the partial sill (sill – nugget), C is the range, D is the anisotropy angle and E is the anisotropy ratio. Sph denotes a spherical variogram model.

Standard

30: 0.190 Sph(410, 90, 0.44)

50: 0.105 Sph(205, 90, 0.40)

70: 0.172 Sph(405, 90, 0.27)

90: 0.000925 Nug(0) + 0.125 Sph(455, 90, 0.39)

110: 0.0961 Sph(340, 90, 0.45)

130: 0.008 Nug(0) + 0.103 Sph(400, 90, 0.48)

150: 0.109 Sph(350, 90, 0.46)

Flowline

30: 0.185 Sph(440, 90, 0.40)

50: 0.121 Sph(220, 90, 0.45)

70: 0.174 Sph(285, 90, 0.47)

90: 0.000434 Nug(0) + 0.128 Sph(450, 90, 0.40)

110: 0.0945 Sph(350, 90, 0.42)

130: 0.006 Nug(0) + 0.100 Sph(375, 90, 0.45)

150: 0.112 Sph(375, 90, 0.45)

Appendix F – Detroit River Interpolation Inputs

Detroit River Sample Points

Upper Reach				Middle Reach		
Easting	Northing	% Fines		Easting	Northing	% Fines
340525	4689888	2.19		326039	4679972	43.92
340525	4689888	2.47		326039	4679972	43.07
340525	4689888	1.57		326039	4679972	41.81
334337	4689203	4.38		326013	4680015	16.1
334337	4689203	6.01		326138	4679956	16.13
334337	4689203	3.06		326040	4680172	2.54
334288	4689191	3.64		328443	4686261	1.250938
334437	4689203	4.18		327412	4684361	0
334322	4689004	4.28		327349	4683743	4.637282
342012	4690026	6.933858		327445	4684911	0.47142
341265	4689461	33.28028		327445	4684911	0.117578
339866	4690879	0.772532		327685	4684445	0
340689	4690485	3.565918		328058	4684919	27.43215
340689	4690485	4.007568		328241	4685513	12.749
339735	4689632	2.137953		326497	4683108	0
340044	4689750	2.052124		326489	4682294	18.93592
340044	4689750	1.995885		326790	4683131	2.712032
341644	4690534	2.182494		326623	4683930	2.571042
341872	4691693	2.880253		327281	4684542	0.090827
336514	4690570	10.55328		325815	4679726	7.647174
335902	4689866	15.97602		326039	4679972	52.9991
336014	4689650	14.48919		326316	4681402	0.453515
336329	4690145	30.1092		324946	4679870	0
333961	4688833	5.39559		325061	4680283	11.12903
334337	4689203	6.586022		325210	4680549	31.73847
338700	4688664	4.647436		325235	4679862	0
338700	4688664	3.883052		326235	4681835	11.03231
335245	4689617	20.90395		325052	4679247	1.415701
334666	4688232	14.72603		325165	4679073	41.33333
335206	4688656	25.23452		325165	4679073	7.650926
336336	4688387	8.5		325165	4679073	24.09488
336861	4688637	0		325461	4679714	0.559843
339064	4688929	6.058394		325887	4681100	7.344973
337834	4690914	8.97598		325887	4681100	7.924985
337664	4689184	59.41176		325927	4680541	0
337976	4689071	0.382803		323429	4678367	12.78415
332740	4688196	11.89221		330631	4687575	1.094891
330631	4687575	1.094891				
330915	4687127	0				
330915	4687127	0				
328443	4686261	1.250938				

151

Lower Reach

Easting	Northing	% Fines		Easting	Northing	% Fines
320376	4667135	1.63		323328	4662375	62.03704
320376	4667135	1.54		324623	4664772	50.98684
320376	4667135	1.95		325090	4667938	3.373313
320567	4668984	75.21		323535	4666909	31.57208
320407	4667096	2.76		320332	4667836	7.002999
320430	4667219	0.46		320376	4667135	4.22942
320459	4667317	0.41		322525	4663157	25.13795
320337	4659721	7.96		322525	4663157	26.27178
320769	4661772	16.41924		322525	4663157	21.13127
319633	4660188	2.969247		319823	4664009	1.818182
319797	4660314	2.814862		319964	4664402	0.479677
320017	4660195	1.017675		320011	4663255	33.1117
320017	4660195	1.086376		319825	4665335	0.151
326196	4673436	54.57986		324600	4656532	13.57312
325207	4668554	64.68657		322023	4661246	19.94671
325207	4668554	63.8864		323465	4660802	8.497921
324584	4669090	2.901655		323994	4661069	48.62288
324896	4669943	35.16414		324293	4660463	53.1052
324896	4669943	35.48185		323676	4661683	4.663981
324898	4668876	22.62537		320123	4661687	0.986085
324984	4668676	17.61594		320338	4662073	17.74801
325854	4673722	44.95413		319135	4659201	2.318159
325533	4668879	36.84871		319184	4658306	1.792468
325627	4671975	11.71024		319593	4658774	15.14903
324019	4670807	30.62404		319593	4658774	17.88751
324395	4670942	11.87648		320352	4661404	6.654457
324395	4670942	21.09441		319777	4658737	7.911344
324395	4670942	21.11136		321153	4660779	11.05528
324985	4672077	22.13801		320306	4659752	10.50035
325171	4671674	3.085106		319171	4662640	2.53895
322978	4671822	3.130831		319288	4661395	18.59756
323762	4671460	35.63974		319552	4662458	2.841705
324580	4672546	46.7128		325052	4679247	1.415701
322568	4673914	31.33854		325165	4679073	41.33333
323453	4668586	20.85354		325165	4679073	7.650926
323586	4674175	22.91667		325165	4679073	24.09488
321547	4671180	56.78012		323429	4678367	12.78415
323056	4672283	5.045409		320551	4669003	67.71
323268	4670552	8.975954		320536	4669019	61.71
324508	4668357	2.675585				
324508	4668357	2.768166				
324855	4662280	57.41379				
324855	4662280	57.26694				
322412	4662476	72.53976				
323328	4662375	62.53122				

Variogram Equations

Variogram Equations are specified in the format required by GSTAT. (Pebesma, 1999)

A Nug(0) + B Sph(C, D, E)

where A is the nugget, B is the partial sill (sill – nugget), C is the range, D is the anisotropy angle and E is the anisotropy ratio. Sph denotes a spherical variogram model.

Standard

Upper Reach: 174.27 Sph(3000, 40, 0.21)

Middle Reach: 212.07 Nug(0) + 271.31 Sph(7820, 20, 0.16)

Lower Reach: 256.63 Nug(0) + 345.72 Sph (9000, 0, 0.41)

Flowline

Upper Reach: 132.08 Sph(1530, 90, 0.21)

Middle Reach: 121.89 Nug(0) + 144.57 Sph(7920, 90, 0.11)

Lower Reach: 234.104 Nug(0) + 292.392 Sph(9120, 90, 0.44)

Vita Auctoris

Name: Jason Stanley Wintermute

Place of Birth: Leamington, Ontario, Canada

Year of Birth: 1973

Education: University of Guelph
                 Guelph, Ontario, Canada
                 1992-1996 B.Sc.(Eng.)

                 University of Windsor
                 Windsor, Ontario, Canada
                 1997-1999 B.C.S.

                 University of Windsor
                 Windsor, Ontario, Canada
                 2000-2004 M.A.Sc.

154